

# Phosphorus nutrition of poplar

Dissertation

zur Erlangung des mathematisch-naturwissenschaftlichen

Doktorgrades

"Doctor rerum naturalium"

der Georg-August-Universität Göttingen

im Promotionsprogramm Biologie

der Georg-August University School of Science (GAUSS)

vorgelegt von

Mareike Jana Kavka

aus Hamburg

Göttingen, 2016

### Betreuungsausschuss

Prof. Dr. Andrea Polle, Forstbotanik und Baumphysiologie, Büsgen-Institut, Universität Göttingen

Prof. Dr. Elvira Hörandl, Systematik, Biodiversität und Evolution der Pflanzen, Albrecht-von-Haller-Institut für Pflanzenwissenschaften, Universität Göttingen

### Mitglieder der Prüfungskommission

Referentin:

Prof. Dr. Andrea Polle, Forstbotanik und Baumphysiologie, Büsgen-Institut, Universität Göttingen

Korreferentin:

Prof. Dr. Elvira Hörandl, Systematik, Biodiversität und Evolution der Pflanzen, Albrecht-von-Haller-Institut für Pflanzenwissenschaften, Universität Göttingen

### Weitere Mitglieder der Prüfungskommission:

Prof. Dr. Ivo Feußner, Biochemie der Pflanze, Albrecht-von-Haller-Institut für Pflanzenwissenschaften, Universität Göttingen

PD Dr. Thomas Teichmann, Zellbiologie der Pflanze, Albrecht-von-Haller-Institut für Pflanzenwissenschaften, Universität Göttingen

Prof. Dr. Konstantin Krutovsky, Forstgenetik und Forstpflanzenzüchtung, Büsgen-Institut, Universität Göttingen

Prof. Dr. Christian Ammer, Waldbau und Waldökologie der gemäßigten Zonen, Burckhardt-Institut, Universität Göttingen

Tag der mündlichen Prüfung: 15.12.2016

## Table of contents

List of abbreviations .....	IV
List of tables.....	V
List of figures.....	VI
Summary.....	1
1 Introduction.....	4
1.1 Phosphorus as a plant nutrient.....	4
1.2 Plant adaptations to low P .....	4
1.3 Phosphate transporters .....	5
1.4 Purple acid phosphatases.....	6
1.5 Poplar, a model to study the P nutrition of trees .....	7
1.6 Objectives.....	8
1.7 References .....	9
2 Dissecting nutrient-related co-expression networks in phosphate starved poplar .....	14
2.1 Introduction .....	14
2.2 Materials and Methods.....	16
2.2.1 Plant material, growth conditions and harvest .....	16
2.2.2 Element concentrations .....	16
2.2.3 RNA-extraction and microarray .....	17
2.2.4 Statistical analyses of microarrays .....	17
2.2.5 Additional statistical analyses .....	18
2.3 Results .....	19
2.3.1 P deprivation affects nutrient element concentrations.....	19
2.3.2 P deprivation leads to massive transcriptional reprogramming.....	21
2.3.3 Co-expression modules are correlated with nutrient element concentrations and biomass .....	22
2.3.4 Network analysis reveals a hierarchy of modules .....	24
2.3.5 Functional characterization of P-related and highly connected modules.....	26
2.4 Discussion .....	30
2.4.1 Regulation of P responses .....	30
2.4.2 Transcriptional regulation of P acquisition and P uptake.....	31

## Table of contents

---

2.4.3 Metabolism of mineral nutrients, sulfur, nitrogen and carbon upon P starvation .....	33
2.4.4 Conclusions .....	35
2.5 References .....	36
2.6 Supporting information .....	41
2.7 Declaration .....	46
3 Phosphate uptake kinetics and tissue-specific transporter expression profiles in poplar ( <i>Populus × canescens</i> ) at different phosphorus availabilities.....	47
3.1 Introduction .....	47
3.2 Methods.....	49
3.2.1 Plant material and growth conditions .....	49
3.2.2 Labeling of the poplars with <sup>33</sup> P and harvest.....	50
3.2.3 Phosphorus distribution at the whole-plant level .....	50
3.2.4 Determination of net <sup>33</sup> P and total P uptake .....	50
3.2.5 Determination of total P contents .....	51
3.2.6 Phosphate uptake after glucose supply and determination of carbohydrates .	52
3.2.7 Kinetic measurements .....	53
3.2.8 RNA extraction and microarray analysis .....	55
3.2.9 Quantitative Real Time PCR of P transporter genes .....	57
3.2.10 Statistical analyses.....	58
3.3 Results .....	58
3.3.1 Plant performance, P uptake and allocation in response to P deficiency .....	58
3.3.2 P uptake is not energy limited .....	62
3.3.3 Low P concentrations in the nutrient solution limit P uptake .....	63
3.3.4 Low P availabilities lead to differential regulation of P transporters.....	65
3.4 Discussion .....	67
3.4.1 P uptake and allocation.....	67
3.4.2 Regulation of the poplar PHT families in response to P starvation .....	70
3.4.3 Conclusions .....	72
3.5 Acknowledgements .....	73
3.6 References .....	74
3.7 Supporting information .....	82
3.8 Authors' contributions .....	91

## Table of contents

---

3.9 Declaration .....	91
4 Phosphate acquisition by poplar: Phylogeny, tissue-specific expression, and activity of root secreted purple acid phosphatases .....	92
4.1 Introduction .....	92
4.2 Materials and Methods .....	93
4.2.1 Measurement of root-associated acid phosphatase activity <i>in vivo</i> .....	93
4.2.2 Purple acid phosphatases in apoplastic washing fluid (AWF) .....	95
4.2.3 Gene expression analysis .....	98
4.2.4 Quantitative Realtime PCR .....	98
4.2.5 Assessment of root morphological parameters .....	101
4.2.6 Phylogeny of PAPs in poplar compared with <i>Arabidopsis</i> , rice and maize. ....	101
4.2.7 Statistical analyses .....	102
4.3 Results .....	102
4.3.1 Phylogeny of PAPs .....	102
4.3.2 Expression of poplar PAPs is enhanced under phosphate deprivation in roots and leaves .....	106
4.3.3 Roots of P deprived poplar have altered root morphology and higher acid phosphatase activity .....	109
4.3.4 Roots of P deprived poplar secrete additionally PtPAP1 .....	112
4.4 Discussion .....	113
4.5 References .....	116
4.6 Supporting information .....	120
4.7 Declaration .....	146
5 Discussion .....	147
5.1 Discussion .....	147
5.2 Outlook .....	150
5.3 References .....	152
Acknowledgements .....	155
Eidesstattliche Erklärung .....	157
Curriculum vitae .....	158

## List of abbreviations

Al	Aluminum
AWF	Apoplastic washing fluid
BCIP	5-bromo-4-chloro-3-indolyl phosphate disodium salt
BM	Biomass
C	Carbon
Ca	Calcium
DEG	Differentially expressed gene
FC	Fold change
Fe	Iron
HP	High phosphate
ICP-OES	Inductively coupled plasma optical emission spectrometer
K	Potassium
LC-ESI-MS	Liquid-chromatography electrospray-ionization mass spectrometer
LP	Low phosphate
Mg	Magnesium
Mn	Manganese
MP	Medium phosphate
N	Nitrogen
P	Phosphorus
PAP	Purple acid phosphatase
PHT	Phosphate transporters
Pi	Inorganic phosphate
pNPP	4-nitrophenyl phosphate disodium salt
PUE	P use efficiency
qRT PCR	Quantitative Real Time PCR
S	Sulfur
WGCNA	Weighted gene co-expression network analysis
Zn	Zinc

## List of tables

**Table 2.1:** ANOVA results for the main factors “treatment” and “tissue”.

**Table 2.2:** Correlation analysis of element concentrations with P concentrations or biomass.

**Table S2.1:** Information about differentially expressed genes. (data CD)

**Table S2.2:** Overview about enriched GO terms in all modules. (data CD)

**Table S2.3:** Gene name abbreviations for Figure 2.6.

**Table 3.1:** In planta P and P uptake characteristics of P deficient poplar.

**Table 3.2:** Kinetic parameters for P uptake of P deficient poplar.

**Table S3.1:** In silico analyses of putative poplar phosphate transporters.

**Table S3.2:** Primers used for qRT PCR of putative P transporter genes.

**Table S3.3:** Transcript abundances of phosphate transporter genes.

**Table 4.1:** Primers used for qRT PCR.

**Table 4.2:** Summary of in silico analyses for poplar purple acid phosphatases.

**Table S4.1:** Proteins in the AWF of P starved poplar. (data CD)

## List of figures

**Figure 2.1.** Element concentrations in leaves, stem, coarse roots and fine roots of poplars.

**Figure 2.2.** Venn-diagram of differentially regulated genes.

**Figure 2.3.** Correlation matrix between eigengenes of co-expression modules and element concentrations and biomass.

**Figure 2.4.** Co-expression within and between modules of DEGs.

**Figure 2.5.** Hierarchy of enriched GO-terms in modules “Green”, “Blue” and “Brown”.

**Figure 2.6.** Relationship of P-responsive genes in roots and leaves.

**Figure S2.1.** Hierarchy of enriched GO-terms in modules “Green”, “Blue” and “Brown”. (data CD)

**Figure 3.1.** Growth characteristics of P deficient poplar.

**Figure 3.2.**  $^{33}\text{P}$  allocation in P deficient poplar.

**Figure 3.3.**  $^{33}\text{P}$  uptake and carbohydrate concentrations in P deficient poplar supplied with glucose in the nutrient solution.

**Figure 3.4.** Model of kinetic parameters for P uptake of P deficient poplars at different P concentrations.

**Figure 3.5.** Expression of phosphate transporters in P deficient poplars.

**Figure S3.1.** Biomass and performance of poplar grown with five different P concentrations.

**Figure S3.2.** Neighbor-Joining tree (Jones-Taylor-Thornton model, 500 bootstraps) of the amino acid sequences for inorganic phosphate transporters in poplar.

**Figure S3.3.** Correlations of absolute microarray expression data ( $\log_2$ -value) and qRT PCR relative expression values ( $\log_2$ ) for PtPHTs.

**Figure 4.1:** Experimental setup for measurement of root-associated acid phosphatase activity *in vivo*.

**Figure 4.2.** Neighbor-Joining tree (Jones-Taylor-Thornton model, 500 bootstraps) of the amino acid sequences for purple acid phosphatases in poplar.

**Figure 4.3.** Verification of array data by qRT PCR.



**Figure 4.4.** Expression of purple acid phosphatases in P deficient poplars.

**Figure 4.5.** Poplar roots grown with or without Pi stained for acid phosphatase activity.

**Figure 4.6.** Length of roots in different root diameter classes in percent of total root length.

**Figure 4.7.** Roots hairs of poplars grown with different P availabilities.

**Figure 4.8.** Root associated acid phosphatase activity of poplar.

**Figure 4.9.** In gel-assay of acid phosphatase activity from poplar root AWF.

**Figure 5.1.** Model for the possible contributions of PAPs and PHTs in P acquisition and P uptake in poplar (*P. × canescens*).

## Summary

Phosphorus (P) is a major plant nutrient required for the biosynthesis of nucleic acids, nucleotides, membrane lipids and metabolites such as organic esters. P further plays a role in enzyme regulation by phosphorylation. Plants take up P in its inorganic form  $\text{H}_2\text{PO}_4^-$  (Pi). Pi is present only in low concentrations in the soil solution and therefore has to be replenished all the time to ensure sufficient plant nutrition.

In plants different strategies can be distinguished in response to P starvation: (i) P conservation by re-use of P from P containing compounds e.g. membrane lipids and avoidance of P requiring metabolic pathways. This results in growth reduction. (ii) Enhanced acquisition of P from the soil. For this purpose plants secrete purple acid phosphatases (PAPs) to mobilize Pi from organic sources and increase the activity of phosphate transporters (PHTs) for enhanced uptake capacity. Only little is known for woody plants about the molecular responses to low P availability because to date most of our knowledge stems from the model plant *Arabidopsis*.

The main aims of this thesis were to characterize molecular changes at the whole-transcriptome level in leaves and roots of *Populus × canescens* in response to P deprivation and to relate these changes to poplar growth, Pi acquisition and Pi uptake. The following questions were addressed: (a) How does P deficiency affect the nutrient states of the plant and which genes are involved in the response to P limitation in poplar? (b) How is the poplar Pi uptake kinetics affected by decreasing P availabilities and how are PHTs transcriptionally regulated by P deficiency? (c) How does low P availability affect the expression profile of PAPs and which members of the large PAP family are released into the medium upon P starvation?

To address these questions transcriptome analyses for poplars (*Populus × canescens*) grown under reduced phosphorus availabilities were conducted using microarray technology. Plant nutrient concentrations were determined by inductively coupled plasma optical emission spectrometry and uptake by use of radioactive P. The secreted proteins were determined by proteome analyses using liquid-chromatography electrospray-ionization mass spectrometry.

(a) Poplars exhibited strong growth reduction and increased P use efficiency in response to lower P availabilities. P starvation resulted also in changes of most other elements (S,

N, K, Mg, Ca, Fe, Zn, Mn, Al) studied. A high number of genes (12068 in total) was differently expressed upon P starvation. These genes were clustered in eleven co-expression modules of which seven were correlated with distinct elements in the plant tissues. One module with 565 genes (4.7 % of all differentially expressed genes) was correlated with changes in the P concentration in the plant tissues and with the biomass. In this module, PAPs but no PHTs were identified among the highly upregulated P-related genes. The functional category “galactolipid synthesis” was enriched among the P-related genes. Galactolipids substitute phospholipids in membranes under P limitation. Two modules, one correlated with C and N and the other with biomass, S and Mg, were connected with the P-related module by co-expression. In these modules GO terms indicating DNA modification and cell division as well as defense (ethylene, respiratory burst) and RNA modification and signaling were enriched. In conclusion, most differentially expressed genes were not directly related to the tissue P concentrations and were, therefore, most likely regulated by downstream events of P starvation.

(b) Whole-plant P uptake kinetics and expression profiles of members of the phosphate transporter families were studied under high, intermediate and low P availability in relation to plant performance. The maximum P uptake rate was more than 13-times higher in P-starved than in well-supplied poplars. The  $K_m$ -values ranged between 20  $\mu\text{M}$  and 26  $\mu\text{M}$  for P starved poplars. The minimum concentration for net P uptake from the nutrient solution was 1  $\mu\text{M}$  P. Among the PHT subfamilies, all PHTs of family 1 (PHT1) studied showed significant up-regulation upon P starvation and were higher expressed in roots than leaves, with the exception of *PtPHT1;3*. The transcript abundance of *PtPHT1;3* was high in leaves under high P supply and increased further under P starvation. *PtPHT1;1* and *PtPHT1;2* showed root- and P-starvation specific expression. Expression profiles of distinct members of the PHT subfamilies, especially those of PHT1 were linked with changes in P uptake and allocation at whole-plant level. The regulation was tissue-specific with lower P-responsiveness in leaves than in roots. Because the  $K_m$  for P uptake was higher than typical soil concentrations of  $\text{P}_i$ , non-mycorrhizal poplars are expected to suffer from P limitations in most environments.

(c) To study the purple acid phosphatases, transcriptome and proteome analyses were combined with phosphatase activity assays. The family of PAPs was annotated showing 33 poplar PAPs that formed three main subfamilies. Among these PAPs, 23 had a probe

set on the microarray and showed significant transcript abundances. Ten PAPs were transcriptionally upregulated in roots and leaves of P-starved poplars. The P-starved poplars further showed higher phosphatase activity on the roots than the well P-supplied plants. The protein PtaPAP4 was secreted by poplar roots under high and low P conditions, whereas PtaPAP1 was secreted only under low P conditions. These results suggest that increased P acquisition from organic P sources under low P conditions is mediated in roots by a specific PAP enzyme.

Overall, the results of this thesis support that enhanced phosphate transporter and phosphatase activity can improve P uptake efficiency. Since poplar plantations for biomass production are often established on marginal sites where nutrients are limited, the present findings suggest that the selection of natural genotypes or molecular breeding can be used to improve tree P nutrition.

# 1 Introduction

## 1.1 Phosphorus as a plant nutrient

Phosphorus (P) is an essential element for plant nutrition. Plants take up P as inorganic phosphate (Pi), mainly in the form of  $\text{H}_2\text{PO}_4^-$  (Schachtman *et al.*, 1998). In most soils, P is the least available nutrient for plants (Holford, 1997) because of the formation of precipitates with cations (calcium, iron, aluminum) and absorption to soil particles (Attiwill and Adams, 1993; Holford, 1997). The concentration of Pi in the soil solution is below 10  $\mu\text{M}$  under most conditions, and thus, three magnitudes lower than the concentration in the plant with 5 to 20 mM (Bieleski, 1973). The concentration of total P can be up to 1% of the plant's dry weight (Bieleski, 1973). P is a constituent of nucleic acids, nucleotides, membrane lipids, proteins and organic esters as well as of ATP, an energy-rich compound. It is required for enzyme regulation by phosphorylation.

In natural ecosystems, recycling and re-use is an important basis for P availability to plants (Attiwill and Adams, 1993), i.e., P recycling in the plant from e.g. senescing leaves, and P storage during winter in buds and stem as phospholipids, P esters and nucleic acids (Chapin and Kedrowski, 1983). At the level of the ecosystem, P recycling by different organisms is an important property especially in P poor soils as recently reviewed by Lang *et al.* (2016). Up to now, only little is known about many aspects of this P dynamics in woody plants (Rennenberg and Herschbach, 2013), while P limitations increase in European forests (Braun *et al.*, 2010; Talkner *et al.*, 2015).

## 1.2 Plant adaptations to low P

Plants are able to sense the P availability locally at the root tips and systemically in the whole plant but a P receptor is not known until now (Baker *et al.*, 2015; Chiou and Lin, 2011; López-Arredondo *et al.*, 2014). Through a signaling system, plants are able to react when the P availability in the growth medium or the plant P concentration is not sufficient to maintain metabolism and growth (P starvation, P deprivation). Plants' responses to low P availability can be broadly divided into two categories: enhanced uptake capacity and acquisition of P, and conservation and efficient use of P (Lajtha

and Harrison, 1995; Vance *et al.*, 2003). To conserve the use of P, plants decrease their growth, re-use P from membrane lipids (Nakamura, 2013; Siebers *et al.*, 2015) and bypass P requiring metabolism pathways (Hammond and White, 2008; Plaxton and Carswell, 1999; Vance *et al.*, 2003). Enhanced uptake and acquisition includes a remodeling of the root system as shown e.g. for *Arabidopsis* (Gruber *et al.*, 2013). Increased activity of phosphate transporters and secretion of organic acids and phosphatases for mobilization of mineral and organic P under low P availability, respectively, are universal for plants (Vance *et al.*, 2003). To achieve these adaptations, massive transcriptional reprogramming is required (Lan *et al.*, 2015). For example, in long-term P starved *Arabidopsis*, Misson *et al.* (2005) found more than 700 genes with more than twofold changed transcript abundance. *Arabidopsis* shows a requirement of different genes during the adaptation process as only 48 regulated genes overlap with earlier time points during the starvation time (Misson *et al.*, 2005). Across four *Arabidopsis* transcriptome studies with similar conditions (Lan *et al.*, 2012; Misson *et al.*, 2005; Morcuende *et al.*, 2007; Woo *et al.*, 2012) only 95 genes were commonly upregulated upon P starvation. Among these genes, four phosphate transporters (*AtPHT1;2*, *AtPHT1;4*, *AtPHT1;8*, *AtPHT1;9*) and five purple acid phosphatases (*AtPAP1*, *AtPAP7*, *AtPAP12*, *AtPAP17*, *AtPAP22*) were detected (Lan *et al.*, 2015), emphasizing the importance of these enzymes in the P starvation response.

### 1.3 Phosphate transporters

To maintain a high P concentration in the plant against the concentration gradient to the soil and the negative membrane potential of plant cells, a high-affinity, active transport across the plasma membrane is needed (Rausch and Bucher, 2002; Smith, 2002). Kinetic measurements revealed two different P uptake systems for plants: a high-affinity system that responds to the P status of the plant and a low-affinity system that is expressed constitutively (Schachtman *et al.*, 1998). Whole-plant P uptake that was mainly studied in agricultural crops was up to five times higher in P starved than in P sufficient plants (Bhadoria *et al.*, 2004; Cogliatti and Clarkson, 1983; Jungk *et al.*, 1990; Lee, 1982).

The active P transport across membranes is performed by phosphate transporters (PHTs). In *Arabidopsis* the PHTs are divided into four families (Guo *et al.*, 2008; Rausch and Bucher, 2002). The subcellular localization of many members of the PHT family has been studied in *Arabidopsis*: The members of the first family, PHT1, are located in the plasma membrane (Nussaume *et al.*, 2011). These are responsible for the uptake of Pi from the soil, but also for the distribution and re-distribution inside the plant (Baker *et al.*, 2015; Młodzińska and Zboińska, 2016; Nussaume *et al.*, 2011). PHT1s have 12 transmembrane spanning domains in a '6+6' configuration (Smith, 2002). They transport  $\text{H}_2\text{PO}_4^-$  ions together with protons, energized by an electrochemical gradient due to an  $\text{H}^+$ -ATPase (Smith, 2002). PHT2s are located in the chloroplast envelope (Versaw and Harrison, 2002) and function as low-affinity transporters (Daram *et al.*, 1999). Members of the third family (PHT3) have been found in mitochondria (Rausch and Bucher, 2002). The members of PHT4 are distributed in chloroplasts, heterotrophic plastids and the Golgi apparatus (Guo *et al.*, 2008). All together, these phosphate transporters take up Pi from the soil into the plant cells, and distribute it inside the plant and between different organelles.

### 1.4 Purple acid phosphatases

Organically bound phosphate makes up 20 to 80 % of the soil's P reserves, mainly as phytate and its derivatives (Schachtman *et al.*, 1998). As PHTs transport only Pi, organic P has to be converted into inorganic P before uptake. Enzymes that cleave Pi from organic phosphate esters are ribonucleases and phosphatases. There are many different kinds of phosphatases in plants, but for most of them no specific role in the metabolism is known (Olczak *et al.*, 2003). Purple acid phosphatases (PAPs), the largest group of phosphatases (Olczak *et al.*, 2003), have their pH optimum in acidic conditions present in most soils. They are named after their purple color when concentrated in water, due to a ferric ligand in the active center of the enzyme (Vincent and Averill, 1990). Secreted acid phosphatases, associated with or bound to the root surface or released into the soil, are believed to play a role in the acquisition of phosphorus, whereas intracellular acid phosphatases are thought to recycle phosphorus from intracellular organic P reserves (Duff *et al.*, 1994). In *Arabidopsis*, three out of 29

known PAPs are responsible for about 70 % of phosphatase activity in the growth medium and root-associated acid phosphatase activity under low P conditions: AtPAP12 and AtPAP26 are mainly secreted by roots into the growth medium and AtPAP10 is bound to the cell-wall (*Wang et al.*, 2014).

### **1.5 Poplar, a model to study the P nutrition of trees**

Poplar (*Populus* spp.) is the model tree for forest biotechnology due to its fast growth, easy propagation and sequenced genome (*Bradshaw et al.*, 2000; *Brunner et al.*, 2004; *Taylor*, 2002; *Tuskan et al.*, 2006). Furthermore, poplar species are important woody crops that may be suitable for growth on marginal lands, where nutrient supply is low (*Polle et al.*, 2013; *Polle and Chen*, 2015).

Poplars can colonize a wide range of different environmental conditions (*Polle and Chen*, 2015) with riparian ecosystems being the main habitat of many poplar species. In these ecosystems flooding, sedimentation and dry periods lead to strong fluctuations in the availability of Pi (*Steiger and Gurnell*, 2002; *Trémolières et al.*, 1999). Thus, these species are obviously able to cope with differences in P availability, but the molecular basis for P uptake and allocation is not yet well understood (*Rennenberg and Herschbach*, 2013).

The expression of selected members of poplar PHTs and PAPs under P deprivation were studied before: Similar to *Arabidopsis*, members of the PHT1 family are up-regulated in poplar under low or the absence of P in the growth medium (*Gan et al.*, 2016; *Loth-Pereda et al.*, 2011; *Zhang et al.*, 2016). *Gan et al.* (2016) demonstrated an up-regulation of one member of the poplar PAPs under P deprivation and an enhanced phosphatase activity on roots. But which PHTs and PAPs are related to increased uptake and phosphatase activity remained open. Overall, how poplars respond to low P at the transcriptional level is currently unknown.



### 1.6 Objectives

The main goals of this thesis were to characterize transcriptomic changes in *Populus × canescens* in response to phosphate deprivation and to relate these changes to poplar P uptake and growth.

To address these goals, the poplar transcriptome in response to phosphate deprivation was studied (**chapter 2**). Nutrient-related co-expression networks were dissected in phosphate-starved poplars. To identify gene clusters and genes involved in the response to phosphorus limitation in poplar and to differentiate between P-related changes and relations to co-occurring changes in the concentration of other nutrients, co-expression gene modules were correlated with element concentrations in poplar roots and leaves.

Because increased phosphate uptake capacity is known to be a major response to phosphorus starvation in plants, **chapter 3** focuses on phosphate transporters. The phosphate uptake kinetics of poplar were characterized at different phosphorus availabilities. Putative phosphate transporters were annotated, their expression profiles measured under different P availabilities and P uptake kinetic parameters determined.

Because of the low concentration of inorganic phosphate in soil solutions, plants need mechanisms for enhanced phosphate acquisition from organic sources. Therefore, purple acid phosphatases of poplar were studied in **chapter 4**. The family of poplar PAPs was annotated and their expression profile under different P availabilities measured. Upregulated and secreted purple acid phosphatases and changes in root morphology to increase the soil volume access were studied.

## 1.7 References

- Attiwill, P.M., Adams, M.A. (1993): Nutrient cycling in forests. *New Phytol.* 124, 561–582.
- Baker, A., Ceasar, S.A., Palmer, A.J., Paterson, J.B., Qi, W., Muench, S.P., Baldwin, S.A. (2015): Replace, reuse, recycle: improving the sustainable use of phosphorus by plants. *J. Exp. Bot.* 66, 3523–3540.
- Bhadoria, P.S., Dessougi, H.E., Liebersbach, H., Claassen, N. (2004): Phosphorus uptake kinetics, size of root system and growth of maize and groundnut in solution culture. *Plant Soil* 262, 327–336.
- Bieleski, R.L. (1973): Phosphate pools, phosphate transport, and phosphate availability. *Annu. Rev. Plant Physiol.* 24, 225–252.
- Bradshaw, H.D., Ceulemans, R., Davis, J., Stettler, R. (2000): Emerging model systems in plant biology: Poplar (*Populus*) as a model forest tree. *J. Plant Growth Regul.* 19, 306–313.
- Braun, S., Thomas, V.F.D., Quiring, R., Flückiger, W. (2010): Does nitrogen deposition increase forest production? The role of phosphorus. *Environ. Pollut.* 158, 2043–2052.
- Brunner, A.M., Busov, V.B., Strauss, S.H. (2004): Poplar genome sequence: functional genomics in an ecologically dominant plant species. *Trends Plant Sci.* 9, 49–56.
- Chapin, F.S., Kedrowski, R.A. (1983): Seasonal changes in nitrogen and phosphorus fractions and autumn retranslocation in evergreen and deciduous Taiga trees. *Ecology* 64, 376–391.
- Chiou, T.-J., Lin, S.-I. (2011): Signaling network in sensing phosphate availability in plants. *Annu. Rev. Plant Biol.* 62, 185–206.
- Cogliatti, D.H., Clarkson, D.T. (1983): Physiological changes in, and phosphate uptake by potato plants during development of, and recovery from phosphate deficiency. *Physiol. Plant.* 58, 287–294.
- Daram, P., Brunner, S., Rausch, C., Steiner, C., Amrhein, N., Bucher, M. (1999): *Pht2;1* encodes a low-affinity phosphate transporter from *Arabidopsis*. *Plant Cell Online* 11, 2153–2166.
- Duff, S.M., Sarath, G., Plaxton, W.C. (1994): The role of acid phosphatases in plant phosphorus metabolism. *Physiol. Plant.* 90, 791–800.

Gan, H., Jiao, Y., Jia, J., Wang, X., Li, H., Shi, W., Peng, C., Polle, A., Luo, Z.-B. (2016): Phosphorus and nitrogen physiology of two contrasting poplar genotypes when exposed to phosphorus and/or nitrogen starvation. *Tree Physiol.* 36, 22–38.

Gruber, B.D., Giehl, R.F.H., Friedel, S., Wirén, N. von (2013): Plasticity of the *Arabidopsis* root system under nutrient deficiencies. *Plant Physiol.* 163, 161–179.

Guo, B., Jin, Y., Wussler, C., Blancaflor, E.B., Motes, C.M., Versaw, W.K. (2008): Functional analysis of the *Arabidopsis* PHT4 family of intracellular phosphate transporters. *New Phytol.* 177, 889–898.

Hammond, J.P., White, P.J. (2008): Sucrose transport in the phloem: integrating root responses to phosphorus starvation. *J. Exp. Bot.* 59, 93–109.

Holford, I.C.R. (1997): Soil phosphorus: its measurement, and its uptake by plants. *Soil Res.* 35, 227–240.

Jungk, A., Asher, C.J., Edwards, D.G., Meyer, D. (1990): Influence of phosphate status on phosphate uptake kinetics of maize (*Zea mays*) and soybean (*Glycine max*). *Plant Soil* 124, 175–182.

Lajtha, K., Harrison, A.F. (1995): Strategies of phosphorus acquisition and conservation by plant species and communities, in: Tiessen, H. (ed.): Phosphorus in the global environment. John Wiley Sons Ltd, Chichester, UK, pp. 140–147.

Lan, P., Li, W., Schmidt, W. (2012): Complementary proteome and transcriptome profiling in phosphate-deficient *Arabidopsis* roots reveals multiple levels of gene regulation. *Mol. Cell. Proteomics* 11, 1156–1166.

Lan, P., Li, W., Schmidt, W. (2015): “Omics” approaches towards understanding plant phosphorus acquisition and use, in: Plaxton, W.C., Lambers, H. (eds.): Annual Plant Reviews Volume 48. John Wiley & Sons, Inc., Hoboken, NJ, USA, pp. 65–97.

Lang, F., Bauhus, J., Frossard, E., George, E., Kaiser, K., Kaupenjohann, M., Krüger, J., Matzner, E., Polle, A., Prietzel, J., Rennenberg, H., Wellbrock, N. (2016): Phosphorus in forest ecosystems: New insights from an ecosystem nutrition perspective. *J. Plant Nutr. Soil Sci.* 179, 129–135.

Lee, R.B. (1982): Selectivity and kinetics of ion uptake by barley plants following nutrient deficiency. *Ann. Bot.* 50, 429–449.

López-Arredondo, D.L., Leyva-González, M.A., González-Morales, S.I., López-Bucio, J., Herrera-Estrella, L. (2014): Phosphate nutrition: Improving low-phosphate tolerance in crops. *Annu. Rev. Plant Biol.* 65, 95–123.

Loth-Pereda, V., Orsini, E., Courty, P.-E., Lota, F., Kohler, A., Diss, L., Blaudez, D., Chalot, M., Nehls, U., Bucher, M., Martin, F. (2011): Structure and expression profile

of the phosphate Pht1 transporter gene family in mycorrhizal *Populus trichocarpa*. *Plant Physiol.* 156, 2141–2154.

Misson, J., Raghothama, K.G., Jain, A., Jouhet, J., Block, M.A., Bligny, R., Ortet, P., Creff, A., Somerville, S., Rolland, N., Doumas, P., Nacry, P., Herrera-Estrella, L., Nussaume, L., Thibaud, M.-C. (2005): A genome-wide transcriptional analysis using *Arabidopsis thaliana* Affymetrix gene chips determined plant responses to phosphate deprivation. *Proc. Natl. Acad. Sci. U. S. A.* 102, 11934–11939.

Młodzińska, E., Zboińska, M. (2016): Phosphate uptake and allocation – A closer look at *Arabidopsis thaliana* L. and *Oryza sativa* L. *Plant Traffic Transp.* 7, 1198.

Morcuende, R., Bari, R., Gibon, Y., Zheng, W., Pant, B.D., Bläsing, O., Usadel, B., Czechowski, T., Udvardi, M.K., Stitt, M., Scheible, W.-R. (2007): Genome-wide reprogramming of metabolism and regulatory networks of *Arabidopsis* in response to phosphorus. *Plant Cell Environ.* 30, 85–112.

Nakamura, Y. (2013): Phosphate starvation and membrane lipid remodeling in seed plants. *Prog. Lipid Res.* 52, 43–50.

Nussaume, L., Kanno, S., Javot, H., Marin, E., Pochon, N., Ayadi, A., Nakanishi, T.M., Thibaud, M.-C. (2011): Phosphate import in plants: Focus on the PHT1 transporters. *Front. Plant Sci.* 2, 83.

Olczak, M., Morawiecka, B., Watorek, W. (2003): Plant purple acid phosphatases - genes, structures and biological function. *Acta Biochim. Pol.* 50, 1245–1256.

Plaxton, W.C., Carswell, M.C. (1999): Metabolic aspects of the phosphate starvation response in plants, in: Lerner, H.R. (ed.): *Plant responses to environmental stresses: From phytohormones to genome reorganization*. Marcel Dekker, Inc., New York, NY, USA, pp. 350 – 372.

Polle, A., Chen, S. (2015): On the salty side of life: molecular, physiological and anatomical adaptation and acclimation of trees to extreme habitats. *Plant Cell Environ.* 38, 1794–1816.

Polle, A., Janz, D., Teichmann, T., Lipka, V. (2013): Poplar genetic engineering: promoting desirable wood characteristics and pest resistance. *Appl. Microbiol. Biotechnol.* 97, 5669–5679.

Rausch, C., Bucher, M. (2002): Molecular mechanisms of phosphate transport in plants. *Planta* 216, 23–37.

Rennenberg, H., Herschbach, C. (2013): Phosphorus nutrition of woody plants: many questions - few answers. *Plant Biol.* 15, 785–788.

Schachtman, D.P., Reid, R.J., Ayling, S.M. (1998): Phosphorus uptake by plants: from soil to cell. *Plant Physiol.* 116, 447–453.

Siebers, M., Dörmann, P., Hözl, G. (2015): Membrane remodelling in phosphorus-deficient plants, in: Plaxton, W.C., Lambers, H. (eds.): *Annual Plant Reviews Volume 48*. John Wiley & Sons, Inc., Hoboken, NJ, USA, pp. 237–263.

Smith, F.W. (2002): The phosphate uptake mechanism. *Plant Soil* 245, 105–114.

Steiger, J., Gurnell, A.M. (2002): Spatial hydrogeomorphological influences on sediment and nutrient deposition in riparian zones: observations from the Garonne River, France. *Geomorphology* 49, 1–23.

Talkner, U., Meiwes, K.J., Potočić, N., Seletković, I., Cools, N., De Vos, B., Rautio, P. (2015): Phosphorus nutrition of beech (*Fagus sylvatica* L.) is decreasing in Europe. *Ann. For. Sci.* 72, 919–928.

Taylor, G. (2002): *Populus: Arabidopsis* for forestry. Do we need a model tree? *Ann. Bot.* 90, 681–689.

Trémolières, M., Schnitzler, A., Sánchez-Pérez, J.-M., Schmitt, D. (1999): Changes in foliar nutrient content and resorption in *Fraxinus excelsior* L., *Ulmus minor* Mill. and *Clematis vitalba* L. after prevention of floods. *Ann. For. Sci.* 56, 641–650.

Tuskan, G.A., DiFazio, S., Jansson, S., Bohlmann, J., Grigoriev, I., Hellsten, U., Putnam, N., Ralph, S., Rombauts, S., Salamov, A., Schein, J., Sterck, L., Aerts, A., Bhalerao, R.R., Bhalerao, R.P., Blaudez, D., Boerjan, W., Brun, A., Brunner, A., Busov, V., Campbell, M., Carlson, J., Chalot, M., Chapman, J., Chen, G.-L., Cooper, D., Coutinho, P.M., Couturier, J., Covert, S., Cronk, Q., Cunningham, R., Davis, J., Degroeve, S., Déjardin, A., dePamphilis, C., Detter, J., Dirks, B., Dubchak, I., Duplessis, S., Ehrling, J., Ellis, B., Gendler, K., Goodstein, D., Gribskov, M., Grimwood, J., Groover, A., Gunter, L., Hamberger, B., Heinze, B., Helariutta, Y., Henrissat, B., Holligan, D., Holt, R., Huang, W., Islam-Faridi, N., Jones, S., Jones-Rhoades, M., Jorgensen, R., Joshi, C., Kangasjärvi, J., Karlsson, J., Kelleher, C., Kirkpatrick, R., Kirst, M., Kohler, A., Kalluri, U., Larimer, F., Leebens-Mack, J., Leplé, J.-C., Locascio, P., Lou, Y., Lucas, S., Martin, F., Montanini, B., Napoli, C., Nelson, D.R., Nelson, C., Nieminen, K., Nilsson, O., Pereda, V., Peter, G., Philippe, R., Pilate, G., Poliakov, A., Razumovskaya, J., Richardson, P., Rinaldi, C., Ritland, K., Rouzé, P., Ryaboy, D., Schmutz, J., Schrader, J., Segerman, B., Shin, H., Siddiqui, A., Sterky, F., Terry, A., Tsai, C.-J., Uberbacher, E., Unneberg, P., Vahala, J., Wall, K., Wessler, S., Yang, G., Yin, T., Douglas, C., Marra, M., Sandberg, G., Peer, Y.V. de, Rokhsar, D. (2006): The genome of black cottonwood, *Populus trichocarpa* (Torr. & Gray). *Science* 313, 1596–1604.

Vance, C.P., Uhde-Stone, C., Allan, D.L. (2003): Phosphorus acquisition and use: critical adaptations by plants for securing a nonrenewable resource. *New Phytol.* 157, 423–447.

Versaw, W.K., Harrison, M.J. (2002): A chloroplast phosphate transporter, PHT2;1, influences allocation of phosphate within the plant and phosphate-starvation responses. *Plant Cell Online* 14, 1751–1766.

Vincent, J.B., Averill, B.A. (1990): An enzyme with a double identity: purple acid phosphatase and tartrate-resistant acid phosphatase. *FASEB J.* 4, 3009–3014.

Wang, L., Lu, S., Zhang, Y., Li, Z., Du, X., Liu, D. (2014): Comparative genetic analysis of *Arabidopsis* purple acid phosphatases AtPAP10, AtPAP12, and AtPAP26 provides new insights into their roles in plant adaptation to phosphate deprivation: Comparative analysis of three *Arabidopsis* APases. *J. Integr. Plant Biol.* 56, 299–314.

Woo, J., MacPherson, C.R., Liu, J., Wang, H., Kiba, T., Hannah, M.A., Wang, X.-J., Bajic, V.B., Chua, N.-H. (2012): The response and recovery of the *Arabidopsis thaliana* transcriptome to phosphate starvation. *BMC Plant Biol.* 12, 62.

Zhang, C., Meng, S., Li, M., Zhao, Z. (2016): Genomic identification and expression analysis of the phosphate transporter gene family in poplar. *Front. Plant Sci.* 7, 1398.

## Chapter 2

# Dissecting nutrient-related co-expression networks in phosphate starved poplar

Published in similar form as open access article distributed under the terms of the Creative Commons Attribution License (<http://creativecommons.org/licenses/by/4.0/>). © 2017 Kavka, Polle.

Mareike Kavka and Andrea Polle  
PLoS One (2017) 12(2):e0171958  
DOI 10.1371/journal.pone.0171958

## 2.1 Introduction

Phosphorus (P) is an important plant nutrient and essential for plant growth and metabolism. But P is also one of the least available nutrients in soil (*Holford, 1997*). Plants take up P only in its inorganic form, phosphate (*Schachtman et al., 1998*). Phosphate is present in very low concentrations in the soil solution ( $< 10 \mu\text{M}$ , *Bieleski, 1973*) due to its binding to soil particles, in organic forms, and precipitation with other soil elements like iron (Fe), aluminum (Al) and calcium (Ca) (*Holford, 1997*).

Responses of plants to P limitation have often been addressed although most studies focused on the model species *Arabidopsis* and only little is known for woody plants (*Rennenberg and Herschbach, 2013*). In poplar, the model for tree species (*Bradshaw et al., 2000; Brunner et al., 2004; Taylor, 2002*), most members of the plasma membrane located phosphate transporter family 1 (PHT1), responsible for the P uptake into the root (*Baker et al., 2015; Nussaume et al., 2011*), are upregulated upon P starvation (*Gan et al., 2016; Kavka and Polle, 2016; Loth-Pereda et al., 2011*). Also the expression of distinct purple acid phosphatases, that make organic P forms plant available, is enhanced (*Gan et al., 2016*). The resulting higher transport efficiency, secretion of phosphatases and, additionally, production and secretion of organic acids (*Desai et al., 2014; Gan et al., 2016*) lead to an enhanced P acquisition, uptake and accumulation capacity (*Desai et al., 2014; Kavka and Polle, 2016*). Poplars grown with low P have

reduced growth with a higher P use efficiency (Gan *et al.*, 2016; Kavka and Polle, 2016).

The genes highly regulated in four P deprivation studies in *Arabidopsis* (Lan *et al.*, 2012; Misson *et al.*, 2005; Morcuende *et al.*, 2007; Woo *et al.*, 2012) are however not only related to P, but are also linked with other elements (e.g. *SULTR1;3*: sulphate transport; *NASI*: iron chelating by nicotianamin (von Wirén *et al.*, 1999)) (Lan *et al.*, 2015). Therefore, it is to be expected that P limitation influences not only the P transport system (Kavka and Polle, 2016) and other P deficiency related acclimation responses inside the plant but also downstream processes caused by secondary deficiencies or changes of other nutrients. These effects got only little attention until now. Gan *et al.* (2016) showed that reduced P availability leads to higher nitrogen (N) concentrations in roots and lower N concentrations in leaves of poplar with higher free amino acid concentrations and reduced activity of N-related enzymes (NR, GOGAT, GDH). Wang *et al.* (2002) found rapid and overlapping gene regulation in response to P, potassium (K) and Fe deprivation in tomato, including transporters for these nutrients. In *Arabidopsis* tissues, not only the P concentration but also other nutrient concentrations are affected by P starvation (Kellermeier *et al.*, 2014; Misson *et al.*, 2005; Ward *et al.*, 2008). Conserved effects across all three studies with different amounts of P in the growth medium were a reduced concentration of K and an enhanced concentration of Fe in leaves of *Arabidopsis* plants (Kellermeier *et al.*, 2014; Misson *et al.*, 2005; Ward *et al.*, 2008). Further concentration changes were a reduction of Ca, magnesium (Mg) and manganese (Mn) (Kellermeier *et al.*, 2014; Ward *et al.*, 2008), thought to be an adjustment of the ionic charge (Kellermeier *et al.*, 2014) or a result of reduced P availability in P requiring steps of metabolism and transport (Misson *et al.*, 2005). While P-nutrient relations have been studied in *Arabidopsis*, only little is known for poplar.

The main goal of this study was to characterize changes in nutrient and other element concentrations (P, S, C, N, K, Mg, Ca, Fe, Zn, Mn, Al) in response to P starvation in poplar (*Populus × canescens*). A further aim was to differentiate between transcriptomic changes directly correlated with the plant P concentration and transcriptomic changes linked to downstream changes of other nutrient concentrations. For this purpose, we studied poplar transcriptomes under high, intermediate and low P availabilities, identified the weighted gene co-expression network and related gene modules to



element concentrations. Regulated gene modules and genes and their putative functions in the poplar P starvation response are discussed.

## 2.2 Materials and Methods

### 2.2.1 Plant material, growth conditions and harvest

*Populus × canescens* (INRA717 1-B4) plants were grown as previously described with three different P availabilities (Kavka and Polle, 2016). The plants were grown in sand culture and irrigated with one of three nutrient solutions. Long Ashton nutrient solution (Hewitt and Smith, 1974) with 641 μM P was used for control plants (high phosphate – HP). For intermediate phosphate (MP) availability, the phosphate concentration was reduced to 6.41 μM and potassium added as KCl (675.8 μM), for low phosphate (LP) availability to 0.0641 μM (additional 682.5 μM KCl).

After two months of growth with different P supplies, the poplars were harvested. Aliquots of the plant tissues (leaves, stem, coarse roots, fine roots < 2 mm diameter) were dried at 60°C for seven days for determination of biomass (n=10 per treatment):

$$\text{tissue biomass [g]} = \frac{\text{dry mass of aliquot [g]} \times \text{total tissue fresh mass [g]}}{\text{fresh mass of aliquot}}$$

The first three leaves from the top (> 2 cm length) and aliquots of fine roots (< 2 mm diameter) were immediately shock frozen in liquid nitrogen and stored at -80°C for RNA-extraction.

### 2.2.2 Element concentrations

Dry tissues of 2-months-old HP-, MP- and LP-poplars (n=4 per treatment) were milled (Retsch, type MM2, Haan, Germany) and 10 to 45 mg of plant powder was pressure-extracted in HNO<sub>3</sub> (Heinrichs et al., 1986). Element concentrations were measured using an inductively coupled plasma optical emission spectrometer (ICP-OES; Optima 5300 DV, PerkinElmer Life and Analytical Sciences, Rodgau, Germany). For determination of carbon and nitrogen concentrations, 0.7 to 0.9 mg dry plant powder (2-month-old HP-, MP- and LP-poplars, n=5 per treatment) was weighed into tin capsules (Hekatech, Wegberg, Germany) and analyzed in duplicates in an Elemental Analyzer

EA1108 (Carlo Erba Strumentazione, Rodano, Italy). Acetanilide (71.09 % C, 10.36 % N; Carlo Erba Strumentazione) was used as the standard.

### 2.2.3 RNA-extraction and microarray

RNA-extraction and microarray procedures at the Microarray Facility (MFT Services, Tübingen, Germany) were described in Kavka and Polle (2016). Three biological replicates (each consisting of two pooled tissue samples) were analyzed per treatment and tissue (fine roots and uppermost leaves). Raw and normalized data were uploaded into the EMBL-EBI ArrayExpress database (<http://www.ebi.ac.uk/arrayexpress/>) under E-MTAB-3934.

### 2.2.4 Statistical analyses of microarrays

Microarray raw data were analyzed using the free statistic software R (version 2.14.2, *R Development Core Team*, 2012) after the protocol described by Janz et al. (2010). The R package “affy” (*Gautier et al.*, 2004) was used for normalization of the array probes (“rma” function) using Bioconductor (*Kauffmann et al.*, 2009). The  $\log_2$  expression value of transcripts that were present (“mas5calls” function) on all replicate chips of at least one condition was used for further analyses. For the annotation of the microarrays, the best gene model for each Affymetrix ID (AffyID) in the annotation file of the Aspen Database was used (*Tsai et al.*, 2011).

Differentially expressed genes (DEGs) were identified by two methods: (a) Significance Analysis of Microarrays (SAM) was performed with R package “siggenes” (*Schwender*, 2011) ( $FDR \leq 0.05$ ) and (b) the data were analyzed using linear models with R package “limma” (*Smyth*, 2005) (adjusted p-value  $\leq 0.05$ ). Overlapping DEGs identified by both approaches were used for further analyses. Venn diagrams of DEGs were drawn using the online tool InteractiVenn (<http://www.interactivenn.net>, *Heberle et al.*, 2015). Log-fold change ratios (logFCs) were calculated with the mean  $\log_2$  expression values for MP/HP and LP/HP for roots and leaves.

A weighted correlation network analysis with all DEGs was conducted using R package “WGCNA” (Weighted Gene Co-expression Network Analysis; *Langfelder and*

*Horvath, 2008*). Block-wise clustering with a power of 24 was calculated and modules in the resulting dendrogram were merged at a height cut of 0.2. Pearson's correlations of eigengenes, which represent the expression profile of all genes in a given co-expression module, and mean values of element concentrations and biomass in fine roots and leaves of HP, MP and LP plants were calculated. Because the large number of DEGs did not allow a visualization of the co-expression network with the usual tools, gene numbers were reduced by using a p-value (limma) cut-off of 0.00001. Topology was recalculated for these genes by using the same power of 24 (command "TOMsimilarityFromExpr"). Nodes (DEGs) and edges (co-expression connections between nodes, based on expression pattern) were displayed in Cytoscape (version 3.3.0, *Shannon et al., 2003*) in group attributes layout to show DEGs belonging to one module.

GO term enrichment analyses were conducted using Ontologizer (version 2.1, *Bauer et al., 2008*) with Term-for-term approach and Benjamini-Hochberg-corrections. Enrichment in poplar gene lists were tested with  $p \leq 0.01$  against a "population" data set consisting of all genes present on the array as described above. Enriched GO terms were displayed using GOPathDrawer (version 6.0, [http://coxpresdb.jp/top\\_draw.shtml](http://coxpresdb.jp/top_draw.shtml)).

### **2.2.5 Additional statistical analyses**

ANOVA and Tukey's HSD were performed in R (version 2.14.2, *R Development Core Team, 2012*) to test for differences between treatments in biomass and element concentrations with  $p \leq 0.05$ . Residuals were tested visually for normal distribution and homogeneity of variance and data transformed logarithmically ( $\log_2$ ), by square root or by the exponent "2" if needed. Differences between treatments at  $p \leq 0.05$  are shown with different letters in figures. Correlations of mean values were calculated using Pearson's test in R.

## 2.3 Results

### 2.3.1 P deprivation affects nutrient element concentrations

P starvation resulted in strong decreases in P concentrations of MP and LP poplar tissues compared with well supplied plants and caused massive growth decline (Figure 2.1; *Kavka and Polle, 2016*).

The concentrations of sulfur, nitrogen, potassium, magnesium, calcium, iron, zinc, manganese and aluminum were influenced by P starvation (Table 2.1), but the differences were generally smaller than those for P (Figure 2.1). Sulfur, magnesium and calcium concentrations declined in all tissues except the stem in response to MP or LP treatments. Potassium was slightly reduced in all tissues except fine roots, whereas iron, manganese, zinc and aluminum concentrations increased in most tissues in response to P deficiency. Nitrogen concentrations were higher in MP than in HP poplars in all tissues. The carbon concentration did not change markedly under low P availability.

**Table 2.1: ANOVA results for the main factors “treatment” and “tissue”.**

parameter	treatment	tissue	interaction
P	<b>&lt;0.001</b>	0.225	<b>0.003</b>
S	<b>&lt;0.001</b>	<b>&lt;0.001</b>	0.116
C	0.641	<b>&lt;0.001</b>	<b>&lt;0.001</b>
N	<b>&lt;0.001</b>	<b>&lt;0.001</b>	<b>&lt;0.001</b>
K	<b>&lt;0.001</b>	<b>&lt;0.001</b>	<b>0.002</b>
Mg	<b>0.007</b>	<b>&lt;0.001</b>	<b>0.007</b>
Ca	<b>&lt;0.001</b>	<b>&lt;0.001</b>	<b>&lt;0.001</b>
Fe	<b>0.001</b>	<b>&lt;0.001</b>	<b>&lt;0.001</b>
Zn	<b>0.026</b>	<b>&lt;0.001</b>	0.094
Mn	<b>0.020</b>	<b>&lt;0.001</b>	0.593
Al	<b>0.001</b>	<b>&lt;0.001</b>	0.074
BM	<b>&lt;0.001</b>	<b>&lt;0.001</b>	<b>&lt;0.001</b>

P-values of linear models (Two-Way-ANOVA) were calculated for element concentrations and biomass (BM) (see Figure 2.1) with the factors treatment (HP, MP, LP) and tissue (leaves, stem, coarse, fine roots) and a factor of interaction. Correlations with  $p \leq 0.05$  are indicated in bold.

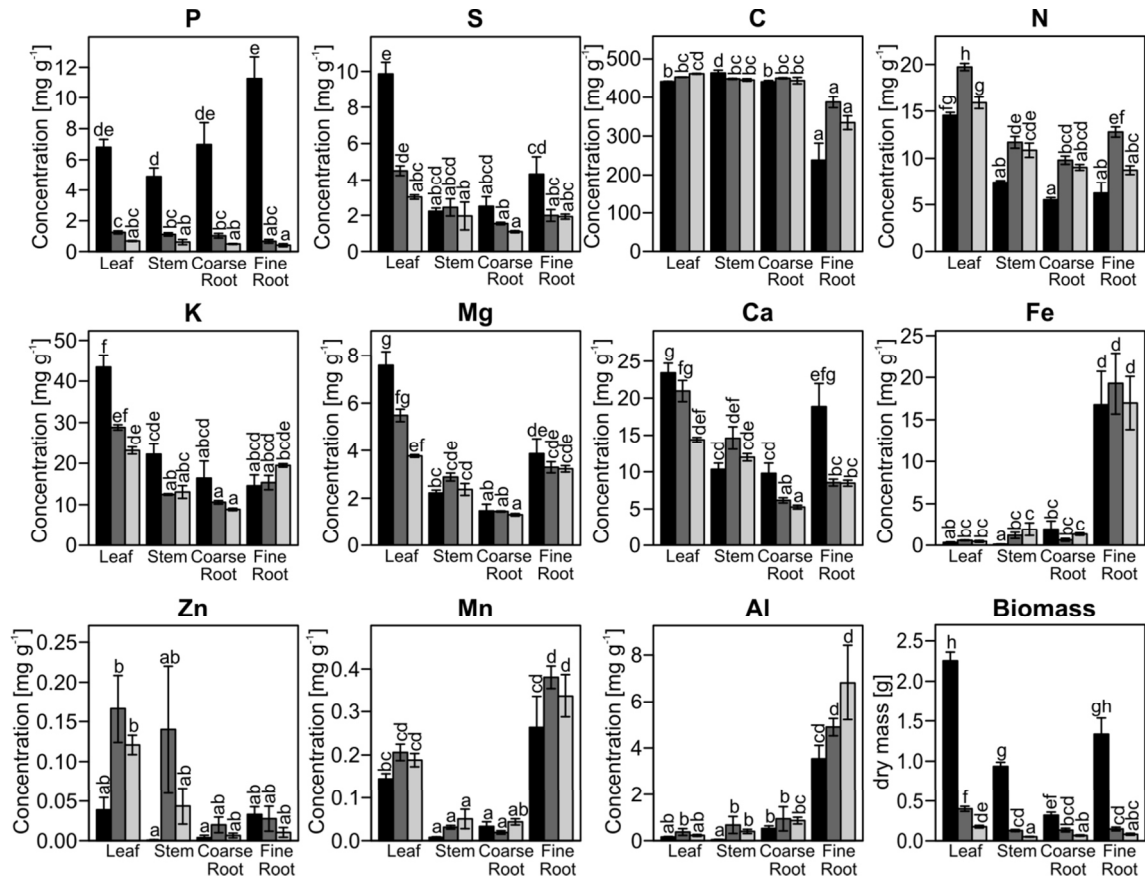


**Figure 2.1. Element concentrations in leaves, stem, coarse roots and fine roots of poplars.** *P. × canescens* was grown with high (HP, 641 μM, black), intermediate (MP, 6.4 μM, dark grey) or low (LP, 0.064 μM, light grey) P supply. Different letters indicate significant differences ( $p \leq 0.05$ , Two-Way-ANOVA and Tukey's honest significance test, mean $\pm$ SE,  $n=4-10$ ). P concentration and biomass from Kavka and Polle (2016). S: sulfur, C: carbon, N: nitrogen, K: potassium, Mg: magnesium, Ca: calcium, Fe: iron, Zn: zinc, Mn: manganese, Al: aluminum.

Although the changes in element tissue concentrations were caused by differences in P availability in the growth medium, they did not correlate with the P concentration across all tissues and treatments (Table 2.2). However, changes in biomass were correlated with P ( $p=0.005$ ,  $r=0.748$ ). Also sulfur, potassium, magnesium and calcium concentrations were correlated with biomass (S:  $p<0.001$ ,  $r=0.884$ ; K:  $p=0.007$ ,  $r=0.731$ ; Mg:  $p=0.010$ ,  $r=0.706$ ; Ca:  $p=0.011$ ,  $r=0.700$ ). We also tested whether the plant contents of elements were related to the P content. The contents of all studied elements except iron and aluminum were significantly correlated with P content. However, these relationships were results of changes in biomass.

**Table 2.2: Correlation analysis of element concentrations with P concentrations or biomass.**

element	P concentration		biomass	
	p	r	p	r
P	n.a.	n.a.	<b>0.005</b>	<b>0.748</b>
S	0.094	0.505	<b>0.000</b>	<b>0.884</b>
C	0.095	-0.504	0.488	-0.222
N	0.150	-0.443	0.950	0.020
K	0.404	0.266	<b>0.007</b>	<b>0.731</b>
Mg	0.420	0.257	<b>0.010</b>	<b>0.706</b>
Ca	0.128	0.465	<b>0.011</b>	<b>0.700</b>
Fe	0.648	0.147	0.908	-0.037
Zn	0.361	-0.29	0.677	-0.135
Mn	0.979	-0.008	0.876	0.050
Al	0.866	-0.055	0.610	-0.164

Data for concentrations in leaves, stem, coarse and fine roots (see Figure 2.1) were used and p-value and the Pearson's correlation coefficient (r) of correlation is shown. Correlations with  $p \leq 0.05$  are indicated in bold. n.a.: not applicable.

### 2.3.2 P deprivation leads to massive transcriptional reprogramming

A total number of 12068 genes were differentially expressed in response to MP or LP treatment compared with HP (Figure 2.2). Common to all P treatments were 766 DEGs. In general, roots contained less DEGs than leaves although the decline in P was more pronounced in roots than in leaves (Figures 2.1, 2.2). There were 1017 root-specific and 3347 leaf-specific DEGs in response to both MP and LP treatments (Figure 2.2).

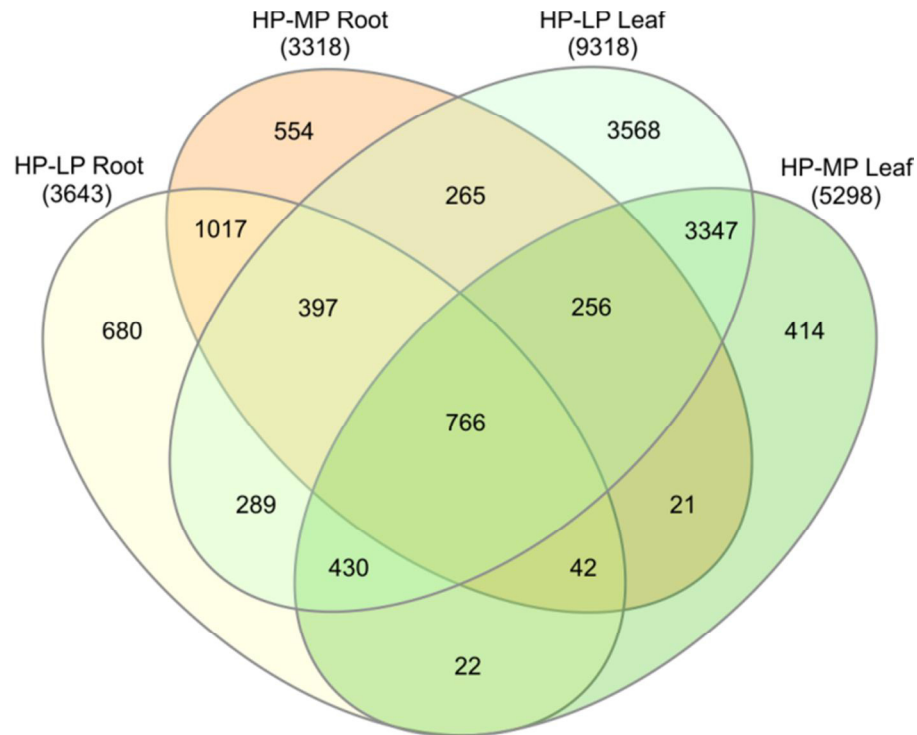


**Figure 2.2. Venn-diagram of differentially regulated genes.** *P. × canescens* was grown with high (HP, 641  $\mu\text{M}$ ), intermediate (MP, 6.4  $\mu\text{M}$ ) or low (LP, 0.064  $\mu\text{M}$ ) P supply. DEGs between HP and LP and HP and MP in roots and leaves are shown.

### 2.3.3 Co-expression modules are correlated with nutrient element concentrations and biomass

To identify genes linked to P nutrition, co-expression modules were calculated and the eigengenes were related to the element concentrations in roots and leaves and the biomass of these tissues. The co-expression analysis resulted in eleven modules (named after colors), which contained 5 to 3632 DEGs (Figure 2.3). The eigengenes of four modules (“Purple”, “Pink”, “Red”, “Grey”) were unrelated to any one of the examined elements or biomass (Figure 2.3) and, therefore, not considered furthermore. Eigengenes of module “Green” were strongly correlated with tissue P concentrations (p-value: 0.0004,  $r=0.98$ ). Module “Green” was weakly correlated with biomass (p-value=0.04,  $r=0.83$ , Figure 2.3). Module “Brown” was positively related to sulfur (p=0.0005,  $r=0.94$ ), magnesium (p=0.03,  $r=0.85$ ) and biomass (p=0.0006,  $r=0.98$ ). Eigengenes of module “Blue” were negatively correlated to carbon and nitrogen concentrations (Figure 2.3). The largest module “Turquoise” (3632 genes) showed

positive correlations with sulfur, potassium, magnesium and calcium and negative correlations with iron, manganese and aluminum concentrations (Figure 2.3). Modules “Black” showed negative correlations to potassium, manganese and sulfur concentration and “Magenta” positive correlations to manganese and aluminum and negative correlation to calcium (Figure 2.3). Module “Yellow” was negatively correlated with iron and aluminum, and positively correlated with zinc concentrations.

Green (565)	0.98 (4x10 <sup>-4</sup> )	0.62 (0.2)	-0.48 (0.3)	-0.36 (0.5)	0.2 (0.7)	0.44 (0.4)	0.72 (0.1)	-0.042 (0.9)	-0.17 (0.7)	-0.41 (0.4)	-0.27 (0.6)	0.83 (0.04)
Brown (1958)	0.71 (0.1)	0.94 (0.005)	-0.035 (0.9)	-0.046 (0.9)	0.71 (0.1)	0.85 (0.03)	0.77 (0.07)	-0.3 (0.6)	-0.22 (0.7)	-0.55 (0.3)	-0.39 (0.4)	0.98 (6x10 <sup>-4</sup> )
Turquoise (3632)	0.22 (0.7)	0.84 (0.04)	0.6 (0.2)	0.63 (0.2)	0.89 (0.02)	0.9 (0.01)	0.88 (0.02)	-0.92 (0.009)	0.54 (0.3)	-0.96 (0.003)	-0.91 (0.01)	0.62 (0.2)
Black (389)	0.016 (1)	-0.82 (0.04)	-0.73 (0.1)	-0.7 (0.1)	-0.96 (0.002)	-0.94 (0.006)	-0.68 (0.1)	0.78 (0.07)	-0.35 (0.5)	0.71 (0.1)	0.72 (0.1)	-0.56 (0.3)
Magenta (250)	-0.43 (0.4)	-0.62 (0.2)	-0.36 (0.5)	-0.48 (0.3)	-0.51 (0.3)	-0.62 (0.2)	-0.87 (0.02)	0.77 (0.07)	-0.63 (0.2)	0.87 (0.02)	0.93 (0.006)	-0.53 (0.3)
Yellow (1730)	-0.29 (0.6)	0.2 (0.7)	0.75 (0.09)	0.79 (0.06)	0.45 (0.4)	0.34 (0.5)	0.44 (0.4)	-0.91 (0.01)	0.88 (0.02)	-0.75 (0.08)	-0.84 (0.04)	-0.073 (0.9)
Blue (2562)	0.73 (0.1)	0.02 (1)	-0.92 (0.01)	-0.87 (0.02)	-0.4 (0.4)	-0.19 (0.7)	-0.054 (0.9)	0.74 (0.09)	-0.75 (0.08)	0.43 (0.4)	0.56 (0.2)	0.37 (0.5)
Purple (237)	0.16 (0.8)	0.78 (0.06)	0.31 (0.5)	0.1 (0.8)	0.81 (0.05)	0.76 (0.08)	0.35 (0.5)	-0.3 (0.6)	-0.36 (0.5)	-0.37 (0.5)	-0.2 (0.7)	0.69 (0.1)
Pink (294)	0.6 (0.2)	-0.15 (0.8)	-0.55 (0.3)	-0.36 (0.5)	-0.47 (0.3)	-0.29 (0.6)	0.25 (0.6)	0.11 (0.8)	0.18 (0.7)	-0.13 (0.8)	-0.12 (0.8)	0.07 (0.9)
Red (446)	-0.24 (0.6)	-0.54 (0.3)	0.08 (0.9)	0.13 (0.8)	-0.44 (0.4)	-0.53 (0.3)	-0.18 (0.7)	-0.19 (0.7)	0.54 (0.3)	-0.11 (0.8)	-0.2 (0.7)	-0.56 (0.3)
Grey (5)	0.16 (0.8)	0.17 (0.8)	0.048 (0.9)	-0.26 (0.6)	0.095 (0.9)	-0.024 (1)	-0.11 (0.8)	-0.088 (0.9)	-0.36 (0.5)	-0.22 (0.7)	-0.12 (0.8)	0.25 (0.6)
Module	P	S	C	N	K	Mg	Ca	Fe	Zn	Mn	Al	BM

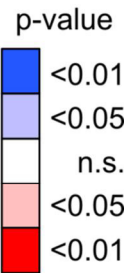


**Figure 2.3. Correlation matrix between eigengenes of co-expression modules and element concentrations and biomass.** Modules were composed of genes differentially expressed between poplars (*P. × canescens*) grown with high P availability and plants grown with intermediate or low P availability in fine roots or leaves. Correlation coefficient and p-value (in brackets) are given. Significant p-values ( $\leq 0.05$ ) of correlation are color coded (red: negative correlation, blue: positive correlation). Numbers of DEGs in modules are shown below module’s name.



### **2.3.4 Network analysis reveals a hierarchy of modules**

Network analysis showed that module “Green”, which was strongly correlated with P concentrations, was mainly connected with “Brown” and “Blue” (Figure 2.4). Links of “Green” with other modules were rare (“Magenta”, “Pink” and “Turquoise”) or did not exist (“Red”, “Black”, “Purple” and “Yellow”). Strong co-expressions were found between genes in module “Blue” with those in modules “Yellow”, “Pink” and “Brown” (Figure 2.4). Module “Brown” was further strongly connected to module “Turquoise”, whose genes were co-expressed with genes in modules “Purple”, “Magenta” and “Black”. The network structure thus indicated co-expression of P-related genes with the C- and N-related genes (“Blue”) on the one hand and the S-, Mg- and biomass-related genes on the other hand (“Brown”, Figures 2.3, 2.4). As all other modules were apparently not strongly connected with the P-related module, also elements correlated with these genes were not strongly connected with changes in P concentrations.

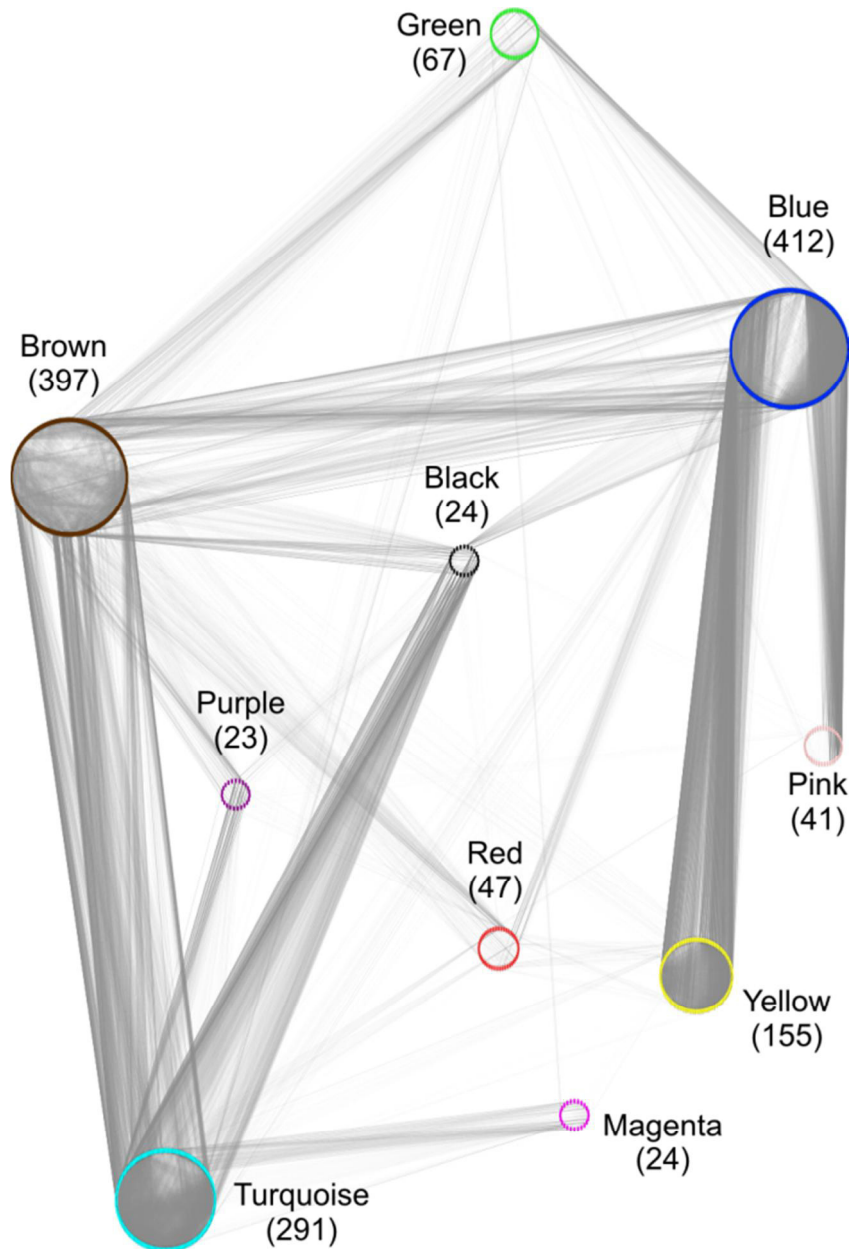


**Figure 2.4. Co-expression within and between modules of DEGs.** Due to computing power (about 12,000 nodes (= DEGs); about 45,000 edges (= co-expression between two DEGs) merely for module “Green”), only DEGs with  $p \leq 0.00001$  (limma) were drawn. Using a fold-change cut-off resulted in a similar network picture (not shown). Nodes (= DEGs of modules) are shown by their colors. Co-expression (Weighted Gene Co-expression Network Analysis) between two nodes, is represented by grey line (edge). Higher adjacency between two DEGs is indicated by darker line color (adjacency threshold for edge drawing: 0.25). The reduced number of DEGs used to draw the network is indicated below module’s name.

### 2.3.5 Functional characterization of P-related and highly connected modules

To characterize the modules functionally, GO term enrichment analysis was performed for all modules (Supplementary Table S2.2) and presented here for module “Green” and its two most connected modules “Blue” and “Brown” (Figure 2.5). GO terms enriched in module “Green” were related to protein catabolism with terms “protein catabolic process”, “proteasome assembly” and “response to misfolded protein”. Further enriched GO terms in module “Green” were related to energy metabolism with “protein localization to mitochondrion”, “purine nucleotide synthesis” and “photorespiration” as well as to “galactolipid synthesis” and “cellular response to phosphate starvation”. The latter GO term encompassed two phosphoenolpyruvate-carboxylase kinases (Potri.013G046100, Potri.019G018100), a sulfolipid synthase (Potri.016G112600), an SPX gene (Potri.006G069500), an inorganic pyrophosphatase (Potri.003G034600) and a purple acid phosphatase (Potri.005G233400).

The genes in this GO term belonged to the genes with the strongest up-regulation under low P availability in the module “Green” in both roots and leaves (Figure 2.6a). Other highly upregulated genes in roots and leaves in module “Green” were glycerol-3-P transporters (Potri.003G109300, Potri.001G124200), the purple acid phosphatase Potri.010G158200, a phosphoenolpyruvate-carboxylase kinase (Potri.013G046100), a phosphoenolpyruvate-carboxylase (Potri.008G114200), a serine/threonine-protein kinase (Potri.006G109600) and a glycerophosphodiester phosphodiesterase (Potri.001G325200). Strongly downregulated in roots and leaves upon P starvation in module “Green” were an asparaginase (Potri.014G022900) and a choline/ethanolamine kinase (Potri.005G197500). CBL-interacting serine/threonine-protein kinases (Potri.006G062800, Potri.019G128100) and WRKY-transcription factors (Potri.001G044500, Potri.018G019800) were downregulated only in roots of the P-starved plants. Wall-associated receptor kinase (Potri.002G075900) and a 50S ribosomal protein (Potri.005G154300) were downregulated in leaves but upregulated in roots (Figure 2.6a).

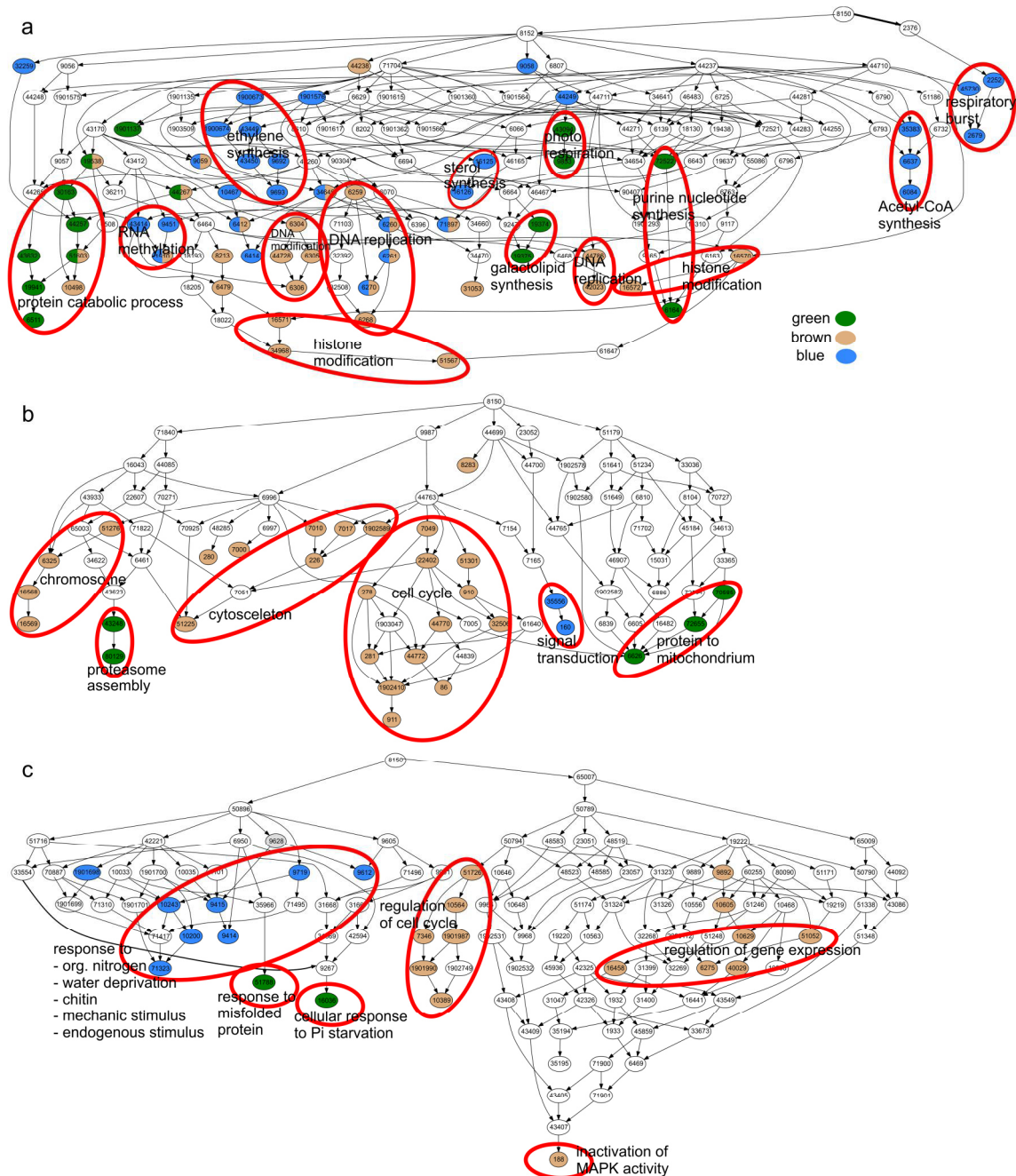


**Figure 2.5. Hierarchy of enriched GO-terms in modules “Green”, “Blue” and “Brown”.** Enriched GO terms are colored with module color, white: GO terms not enriched in modules. GO term hierarchy was drawn with GOPathDrawer. Some connections were omitted to display the figure in a page fitting format as three separated parts (a, b, c). They can be found in supplementary materials Figure S2.1.

In addition to “Biological Process” we analyzed the enrichment of GO terms for “Molecular Function” and “Cellular Component” in the co-expression modules. In agreement with “Biological Process” we found GO terms related to the respiratory chain and mitochondrion were enriched in module “Green” (Additional Table S2.2).

The P-related module “Green” was connected by 17268 edges with the biomass/S/Mg related module “Brown” (1958 DEGs) (cf. Figure 2.4). GO terms enriched for genes in module “Brown” were related to growth (“DNA replication”, “cytoskeleton”, “cell cycle” and “regulation of cell cycle”), and to the regulation of gene expression (“DNA-“ and “histone modification”, “chromosome” and “regulation of gene expression”). Genes encoding an SPX-domain containing protein (Potri.014G061200), the phosphate transporter PtPHT1;12 (Potri.001G318500), a chitinase (Potri.004G182000) and an NADH-dehydrogenase (Potri.011G044600) were especially highly upregulated in module “Brown” (Figure 2.6b). Genes encoding bark storage proteins (Potri.013G101000, Potri.013G100700) were highest upregulated in leaves. Phosphoethanolamine N-methyltransferases (Potri.015G039000, Potri.012G047400) were highly downregulated in both roots and leaves in module “Brown”.

Genes of module “Blue” (2562 DEGs and 5330 edges with module “Green”) (cf. Figure 2.4) were enriched in GO terms related to regulation and signaling (“RNA methylation”, “signal transduction”, “ethylene synthesis”), and to general stress responses (“respiratory burst”, response to some stresses and stimuli e.g. “response to endogenous stimulus”) (Figure 2.5). Further GO terms enriched in genes of module “Blue” might be related to membrane lipid degradation (“sterol-“ and “Acetyl-CoA synthesis”). Notably, among the genes of module “Blue” (Figure 2.6c) purple acid phosphatases (Potri.003G030700, Potri.005G233400, Potri.010G158200, Potri.015G031400, Potri.012G042200) were highly upregulated and the ethylene-responsive transcription factors were mostly upregulated in leaves and downregulated in roots.

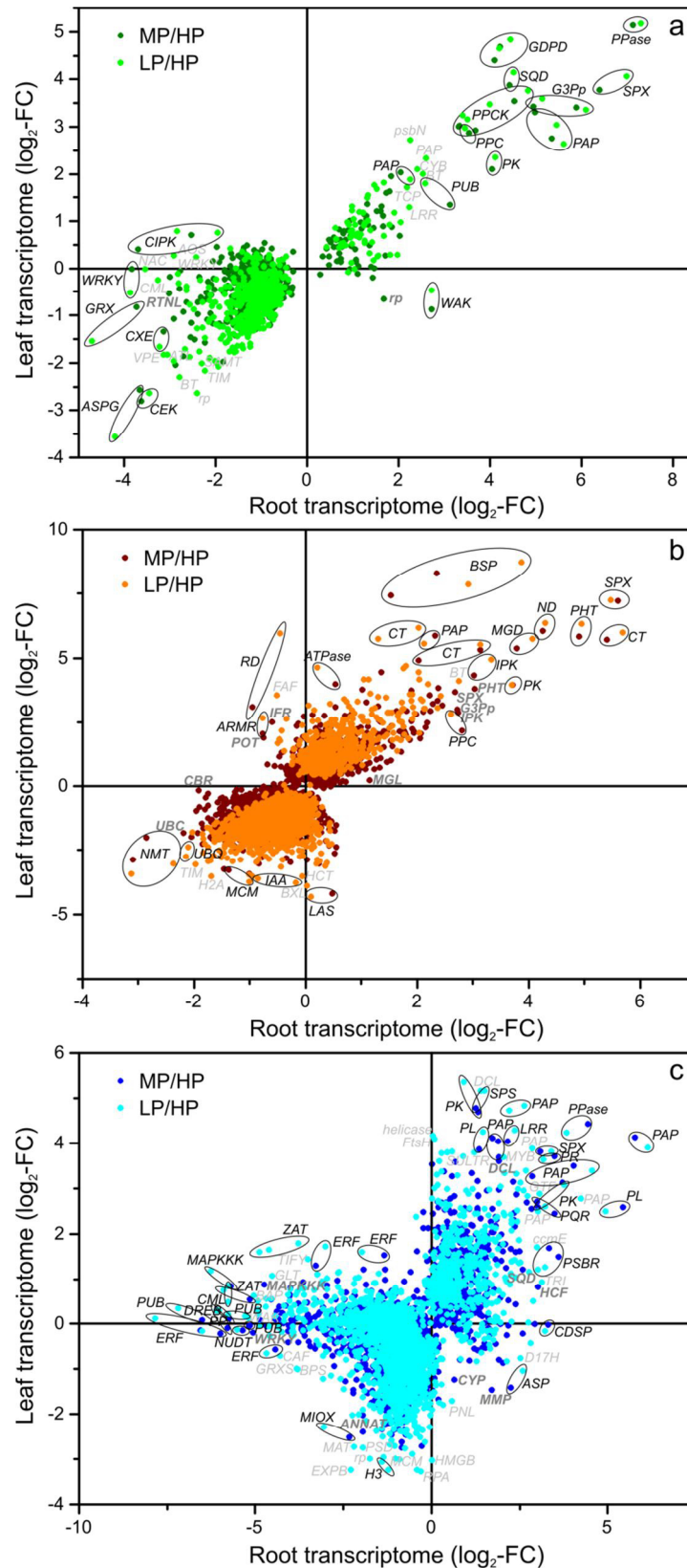


**Figure 2.6. Relationship of P-responsive genes in roots and leaves.** Log<sub>2</sub>-fold change of MP/HP and LP/HP DEGs in roots were plotted to the corresponding log<sub>2</sub>-fold changes in leaves for module “Green” (a), “Brown” (b) and “Blue” (c). Gene abbreviations were listed in supplementary materials Table S2.3.

## 2.4 Discussion

### 2.4.1 Regulation of P responses

Here, we present the transcriptional profiles of poplar roots and leaves in response to phosphate starvation. Leaves of P-starved poplars showed more DEGs than roots. This finding agrees with the P starvation response in *Arabidopsis* (Wu *et al.*, 2003) and suggests that the response in leaves is more complex than in roots. Among 12068 DEGs, we identified one gene cluster (module “Green”) with 565 genes, which was correlated with the tissue P concentrations. Whether cause-effect-relationships exist between DEGs in module “Green” and the tissue P concentration is unknown, but the module contains homologs of *Arabidopsis* transcription factors known to regulate P sensing and signaling (Chiou and Lin, 2011; Scheible and Rojas-Triana, 2015). It is therefore likely that this module is involved in the surveillance of the P status of the cell and in crucial metabolic adjustments because it was also enriched in functions indicating enhanced degradation activities, which may be required to achieve higher P recycling.

Among the DEGs in roots and leaves were several members of the SPX transcription factor family (highly expressed: Potri.006G069500, Potri.006G253400, moderately enhanced: Potri.014G061200, Potri.018G028200, Potri.006G069500), which are key regulatory factors of P homeostasis in plants (Chiou and Lin, 2011; Scheible and Rojas-Triana, 2015). The SPX protein interacts with PHR1 (Puga *et al.*, 2014). PHR1 enables the transcription of P responsive genes by binding to the P1BS element in the upstream region of those genes (Puga *et al.*, 2014). Under high P conditions, SPX proteins bind PHR1 and thereby prevent the activation of phosphate responsive genes in a P dependent manner (Puga *et al.*, 2014). Up-regulation of the expression of SPX genes under low P conditions further allows plants to react rapidly to P resupply because the binding of PHR1 stops the enhanced expression of PHR1 target genes (Puga *et al.*, 2014). Because the poplar SPX genes in module “Green” showed P concentration related transcript abundances, it is likely that they fulfill similar functions as their homologs in *Arabidopsis* and rice (Puga *et al.*, 2014; Z. Wang *et al.*, 2014), where they link P perception and signaling.

Further differentially expressed transcription factors known to respond to P starvation were found in other co-expression modules. For example, *AtWRKY75* is upregulated

during P starvation and regulates P starvation induced genes, whereas AtWRKY6 and AtWRKY42 bind to *PHO1* promoter in P sufficient conditions, inhibiting the transcription of PHO1 (PHOSPHATE1, involved in Pi xylem loading) (*Chiou and Lin, 2011*). Here, the poplar WRKY homolog Potri.001G097200 (module “Brown”) is upregulated upon P starvation in both roots and leaves, whereas others (e.g. Potri.003G138600, Potri.006G263600, Potri.016G128300 from module “Blue”, Potri.001G044500 from module “Green”, Potri.003G169100, Potri.003G182200, Potri.014G096200, Potri.014G096200 from module “Pink”) were downregulated especially in roots upon P starvation. This different expression pattern for different members of the large WRKY family emphasizes the different possible functions of distinct members. Ethylene-responsive element binding factors (ERFs) were especially abundant in the N- and C-related co-expression module with a down-regulation in roots and no or slight up-regulation in leaves upon P deprivation indicating an influence of ethylene signaling on root responses to low P conditions as for example root hair formation and primary root growth arrest (*Scheible and Rojas-Triana, 2015*). In *Arabidopsis* Zinc finger proteins (ZATs) such as AtZAT6 have functions in root development and P acquisition (*Baker et al., 2015; Scheible and Rojas-Triana, 2015*). Here poplar homologs from module “Blue” (Potri.009G027700, Potri.001G235800, Potri.014G017300, Potri.001G295500, Potri.008G051200, Potri.002G119300) were responsive to P deprivation with a strong down-regulation in roots upon P starvation suggesting a conserved function in poplar.

An important result of our study is that these transcription factors were assigned to different hierarchic levels of the transcriptional network: those being involved in perception and signaling were present in top level (module “Green”), while others, which control long distance transport and morphological adjustments were found in secondary positions (modules “Brown” and “Blue”).

## **2.4.2 Transcriptional regulation of P acquisition and P uptake**

Under P deficiency the expression of genes for phosphate transporters (PHTs) and purple acid phosphatases (PAPs) is upregulated increasing the P efficiency of poplar (*Gan et al., 2016; Kavka and Polle, 2016; Loth-Pereda et al., 2011*). Here, upregulated PAPs were present in the P-related module “Green” (Potri.005G233400,



Potri.010G158200) but also in the secondary modules “Blue” (Potri.012G042200, Potri.015G031400, Potri.010G158200, Potri.005G233400, Potri.003G030700) and “Brown” (Potri.008G139100). In *Arabidopsis*, *AtPAP10* and *AtPAP12*, which are the orthologs of the strongly P-responsive PAP Potri.005G233400 in module “Green”, are secreted and root cell-wall localized phosphatases (L. Wang *et al.*, 2014). These *Arabidopsis* PAPs are up-regulated under P deprivation and, thus, responsible for the P acquisition from organic P sources under low P conditions (L. Wang *et al.*, 2014; Wang *et al.*, 2011; Wang and Liu, 2012). It is therefore likely that the poplar orthologous PAP Potri.005G233400 also plays a central role in P acquisition. Since organic P source were not added to nutrient solution used in the present study, it seems that the activation of PAPs is a general response to P deprivation or that plants themselves release organic P compounds into their root surrounding, which they try to recapture or that they can even prey on bacterial debris. These suggestions are currently speculative and should be further studied. Here, other PAPs with intracellular localization might be more important because they can contribute to increase the internal P reuse of the plant. Many of those PAPs were activated in module “Blue”, in which stress responses and DNA/RNA remodeling clustered as major GO terms. These results are in agreement with those found for *Arabidopsis* (Del Pozo *et al.*, 1999). *AtPAP17*, the ortholog of the poplar PAPs Potri.012G042200 and Potri.015G031400, is highly expressed under P starvation in roots and leaves as well as in senescent leaves (Del Pozo *et al.*, 1999). *AtPAP17* has a dual function in P hydrolysis and peroxide formation (Del Pozo *et al.*, 1999). These findings correspond to present data showing association with stress response in poplar.

An unexpected result was that none of the PHTs was assigned to module “Green”, although various PHTs respond strongly to P deficiency (Kavka and Polle, 2016). Here, *PtPHT1;12* and *PtPHT1;9* (Potri.001G318500, Potri.002G005500) were detected in module “Brown”, whose eigengenes were strongly correlated with biomass, Mg and S and in which GO terms for cell cycle, chromosome organization and DNA were enriched. The orthologs of *PtPHT1;9* (*AtPHT1;8* and *AtPHT1;9*) maintain high-affinity P uptake into the roots of *Arabidopsis* under P starvation (Remy *et al.*, 2012) suggesting that *PtPHT1;9* is also crucial for P uptake in poplar. The orthologs of *PtPHT1;12* in *P. trichocarpa* and *Arabidopsis* (*AtPHT1;5*) show enhanced expression under P deficiency as well as in senescing leaves (Loth-Pereda *et al.*, 2011; Mudge *et al.*, 2002). Therefore,

PtPHT1;12 may function in the redistribution of P inside the plant. Furthermore, in the module “Turquoise”, which forms a tertiary level in the co-expression network, further PHTs were upregulated. Module “Turquoise” was strongly negatively correlated with Fe and Mn, which suggests links between the latter elements and P translocation. Earlier studies support this suggestion because enhanced P uptake prevented over-accumulation and toxicity of Mn (*Dučić and Polle, 2007*).

P release from plasma membranes by replacing phospholipids by galactolipids is a common adaptation to P starvation (*Andersson et al., 2003; Härtel and Benning, 2000*). In our study this response was evident at the transcriptome level. GO term enrichment indicated a correlation between membrane lipid remodeling and P concentrations in module “Green”. These results agree with studies in *Arabidopsis*, where at least parts of membrane lipid remodeling depend on P signaling and auxin/cytokinin crosstalk (*Kobayashi et al., 2006*). For example, the *Arabidopsis SQD1 (SULFOQUINOVOSYLDIACYLGLYCEROLI)* is involved in sulfolipid synthesis and regulated by the phosphate content in plant tissues (*Rouached et al., 2011*). Here, a putative *SQD* (Potri.016G112600) was one of the most strongly upregulated genes in module “Green” and correlated with the P concentration supporting similar functions in the poplar and *Arabidopsis* P starvation response.

### **2.4.3 Metabolism of mineral nutrients, sulfur, nitrogen and carbon upon P starvation**

The concentrations of basic cations declined 1.5 to 2-fold (Ca, Mg, K) upon P starvation in poplar leaves, but did not fall below threshold values reported for sufficient nutrition in leaves of young *P. × canescens* (Ca: 15.9 mg g<sup>-1</sup>, Mg: 2 mg g<sup>-1</sup>, K: 7.6 mg g<sup>-1</sup>; *Burg, 1985*). This was also true for sulfur, whose foliar concentrations declined 3-fold under P deficiency (threshold: 3 mg g<sup>-1</sup>; *Burg, 1985*). Together these elements were positively correlated with the co-expression module “Turquoise” in which GO terms for sulfur metabolism and organic acid biosynthesis were enriched. Production and exudation of organic acids is a known response to P deficiency because those metabolites can exchange anions such as Pi from soil particles, thereby increase Pi availability (*Vance et al., 2003*). The present data imply that the production of organic acids is not a direct

response to declining cellular P concentrations but a down-stream consequence that may perhaps also require the perception of general changes in the cellular ion balance.

Cross talk exists between the P sensing and Zn as well as Fe nutrition involving the PHR1 gene regulation (*Bournier et al.*, 2013; *Khan et al.*, 2014). In our study the concentration of Zn and Fe were increased or relatively stable and significantly correlated with the eigengenes of module “Turquoise” (negative for Fe) and “Yellow” (positive for Zn, negative for Fe). In contrast to poplar, in *Arabidopsis* and rice the Zn concentrations are reduced or unaffected during P starvation, whereas the Fe concentrations increase considerably upon P starvation (*Gruber et al.*, 2013; *Hirsch et al.*, 2006; *Kellermeier et al.*, 2014; *Rai et al.*, 2015; *Saenchai et al.*, 2016; *Zheng et al.*, 2009). In *Arabidopsis*, Fe as well as P homeostasis is regulated via PHR1 that induces the iron storage protein FERRITIN1 (*Bournier et al.*, 2013). Upon P starvation, iron is stored with ferritin in chloroplasts, which prevents precipitation with Pi (*Hirsch et al.*, 2006). But in our study, ferritin was not induced in leaves. Still, our data indicate that chloroplastic metabolism must have been massively affected because module “Yellow” was enriched in term photosynthesis, pigment biosynthesis, starch and carbohydrate metabolism. In poplar, carbohydrates accumulated in roots upon P starvation (*Kavka and Polle*, 2016) in agreement with other studies (*Hammond and White*, 2008) but the total tissue carbon concentrations were not significantly affected. One reason for this observation is a shift in metabolic use of carbon-bearing compounds. For example, in P starved poplars, we found a very high up-regulation of PPC (phosphoenolpyruvatcarboxylase) and the PPC activating kinase PPCK. PPC catalyzes the production of oxaloacetate from phosphoenolpyruvate and bicarbonate releasing Pi. Oxaloacetate can then be secreted or further metabolized into other organic acids and used for energy production.

Furthermore, P starvation has consequences for N nutrition. Both carbon and nitrogen clustered with module “Blue”, which is characterized by defense responses including respiratory burst (ethylene, phosphorelay signal transduction system) and histone modification suggesting massive transcriptional reprogramming. Unlike most of the mineral nutrients, tissue N concentrations increased, which may happen when growth is inhibited but N uptake continues. Here we noted a strong induction of BSP (Bark Storage Protein) gene expression. In poplar, *BSP* expression increases in fall resulting in BSP protein accumulation and N storage during winter (*Coleman et al.*, 1991;

*Wildhagen et al.*, 2010). Our result suggest that the strong growth reduction imposed by P deficiency led to N accumulation and as a further consequence induced the formation of BSPs to store N. This speculation is supported by earlier results showing that shoot growth influenced BSP promoter activity (*Zhu and Coleman*, 2001). Seasonal N cycling in perennial species also involves protein degradation (*Rennenberg et al.*, 2010). BSP induction may, thus, be related to protein degradation, which was found here among the directly P correlated transcriptional responses.

#### **2.4.4 Conclusions**

Surprisingly few regulated gene expression patterns were directly correlated with the total tissue P concentrations. Whether these genes are regulated by the P concentration is not known, but homologs of some of them are known to regulate P sensing and signaling in *Arabidopsis*. All other P starvation responsive genes were most likely regulated by downstream events of P starvation, by free phosphate concentrations or by co-occurring changes in e.g. other nutrient concentrations and not directly by the P concentration. Cross talk between the signaling pathways of different elements are beginning to be unraveled, but further research is needed.

## 2.5 References

- Andersson, M.X., Stridh, M.H., Larsson, K.E., Liljenberg, C., Sandelius, A.S. (2003): Phosphate-deficient oat replaces a major portion of the plasma membrane phospholipids with the galactolipid digalactosyldiacylglycerol. *FEBS Lett.* 537, 128–132.
- Baker, A., Ceasar, S.A., Palmer, A.J., Paterson, J.B., Qi, W., Muench, S.P., Baldwin, S.A. (2015): Replace, reuse, recycle: improving the sustainable use of phosphorus by plants. *J. Exp. Bot.* 66, 3523–3540.
- Bauer, S., Grossmann, S., Vingron, M., Robinson, P.N. (2008): Ontologizer 2.0--a multifunctional tool for GO term enrichment analysis and data exploration. *Bioinformatics* 24, 1650–1651.
- Bialeski, R.L. (1973): Phosphate pools, phosphate transport, and phosphate availability. *Annu. Rev. Plant Physiol.* 24, 225–252.
- Bournier, M., Tissot, N., Mari, S., Boucherez, J., Lacombe, E., Briat, J.-F., Gaymard, F. (2013): *Arabidopsis* Ferritin 1 (AtFer1) Gene regulation by the Phosphate Starvation Response 1 (AtPHR1) transcription factor reveals a direct molecular link between iron and phosphate homeostasis. *J. Biol. Chem.* 288, 22670–22680.
- Bradshaw, H.D., Ceulemans, R., Davis, J., Stettler, R. (2000): Emerging model systems in plant biology: Poplar (*Populus*) as a model forest tree. *J. Plant Growth Regul.* 19, 306–313.
- Brunner, A.M., Busov, V.B., Strauss, S.H. (2004): Poplar genome sequence: functional genomics in an ecologically dominant plant species. *Trends Plant Sci.* 9, 49–56.
- Burg, J. van den (1985): Foliar analysis for determination of tree nutrient status- a compilation of literature data. *Rapp. Rijksinst. Voor Onderz. Bos- En Landschapsbouw Dorschkamp Neth.*
- Chiou, T.-J., Lin, S.-I. (2011): Signaling network in sensing phosphate availability in plants. *Annu. Rev. Plant Biol.* 62, 185–206.
- Coleman, G.D., Chen, T.H.H., Ernst, S.G., Fuchigami, L. (1991): Photoperiod control of poplar Bark Storage Protein accumulation. *Plant Physiol.* 96, 686–692.
- Del Pozo, J.C., Allona, I., Rubio, V., Leyva, A., De La Peña, A., Aragoncillo, C., Paz-Ares, J. (1999): A type 5 acid phosphatase gene from *Arabidopsis thaliana* is induced by phosphate starvation and by some other types of phosphate mobilising/oxidative stress conditions. *Plant J.* 19, 579–589.
- Desai, S., Naik, D., Cumming, J.R. (2014): The influence of phosphorus availability and *Laccaria bicolor* symbiosis on phosphate acquisition, antioxidant enzyme activity, and rhizospheric carbon flux in *Populus tremuloides*. *Mycorrhiza* 24, 369–382.
- Dučić, T., Polle, A. (2007): Manganese toxicity in two varieties of Douglas fir (*Pseudotsuga menziesii* var. *viridis* and *glauca*) seedlings as affected by phosphorus supply. *Funct. Plant Biol.* 34, 31–40.

- Gan, H., Jiao, Y., Jia, J., Wang, X., Li, H., Shi, W., Peng, C., Polle, A., Luo, Z.-B. (2016): Phosphorus and nitrogen physiology of two contrasting poplar genotypes when exposed to phosphorus and/or nitrogen starvation. *Tree Physiol.* 36, 22–38.
- Gautier, L., Cope, L., Bolstad, B.M., Irizarry, R.A. (2004): affy—analysis of Affymetrix GeneChip data at the probe level. *Bioinformatics* 20, 307–315.
- Gruber, B.D., Giehl, R.F.H., Friedel, S., Wirén, N. von (2013): Plasticity of the *Arabidopsis* root system under nutrient deficiencies. *Plant Physiol.* 163, 161–179.
- Hammond, J.P., White, P.J. (2008): Sucrose transport in the phloem: integrating root responses to phosphorus starvation. *J. Exp. Bot.* 59, 93–109.
- Härtel, H., Benning, C. (2000): Can digalactosyldiacylglycerol substitute for phosphatidylcholine upon phosphate deprivation in leaves and roots of *Arabidopsis*? *Biochem. Soc. Trans.* 28, 729–732.
- Heberle, H., Meirelles, G.V., da Silva, F.R., Telles, G.P., Minghim, R. (2015): InteractiVenn: a web-based tool for the analysis of sets through Venn diagrams. *BMC Bioinformatics* 16.
- Heinrichs, H., Brumsack, H.-J., Loftfield, N., König, N. (1986): Verbessertes Druckaufschlußsystem für biologische und anorganische Materialien. *Z. Für Pflanzenernähr. Bodenkd.* 149, 350–353.
- Hewitt, E.J., Smith, T.A. (1974): Plant mineral nutrition. English University Press, London, 298 pp.
- Hirsch, J., Marin, E., Floriani, M., Chiarenza, S., Richaud, P., Nussaume, L., Thibaud, M.C. (2006): Phosphate deficiency promotes modification of iron distribution in *Arabidopsis* plants. *Biochimie* 88, 1767–1771.
- Holford, I.C.R. (1997): Soil phosphorus: its measurement, and its uptake by plants. *Soil Res.* 35, 227–240.
- Janz, D., Behnke, K., Schnitzler, J.-P., Kanawati, B., Schmitt-Kopplin, P., Polle, A. (2010): Pathway analysis of the transcriptome and metabolome of salt sensitive and tolerant poplar species reveals evolutionary adaption of stress tolerance mechanisms. *BMC Plant Biol.* 10, 150.
- Kauffmann, A., Rayner, T.F., Parkinson, H., Kapushesky, M., Lukk, M., Brazma, A., Huber, W. (2009): Importing ArrayExpress datasets into R/Bioconductor. *Bioinformatics* 25, 2092–2094.
- Kavka, M., Polle, A. (2016): Phosphate uptake kinetics and tissue-specific transporter expression profiles in poplar (*Populus × canescens*) at different phosphorus availabilities. *BMC Plant Biol.* 16, 206.
- Kellermeier, F., Armengaud, P., Seditas, T.J., Danku, J., Salt, D.E., Amtmann, A. (2014): Analysis of the root system architecture of *Arabidopsis* provides a quantitative readout of crosstalk between nutritional signals. *Plant Cell* 26, 1480–1496.

Khan, G.A., Bouraine, S., Wege, S., Li, Y., de Carbonnel, M., Berthomieu, P., Poirier, Y., Rouached, H. (2014): Coordination between zinc and phosphate homeostasis involves the transcription factor PHR1, the phosphate exporter PHO1, and its homologue PHO1;H3 in *Arabidopsis*. *J. Exp. Bot.* 65, 871–884.

Kobayashi, K., Masuda, T., Takamiya, K., Ohta, H. (2006): Membrane lipid alteration during phosphate starvation is regulated by phosphate signaling and auxin/cytokinin cross-talk. *Plant J.* 47, 238–248.

Lan, P., Li, W., Schmidt, W. (2012): Complementary proteome and transcriptome profiling in phosphate-deficient *Arabidopsis* roots reveals multiple levels of gene regulation. *Mol. Cell. Proteomics* 11, 1156–1166.

Lan, P., Li, W., Schmidt, W. (2015): “Omics” approaches towards understanding plant phosphorus acquisition and use, in: Plaxton, W.C., Lambers, H. (eds.): Annual Plant Reviews Volume 48. John Wiley & Sons, Inc., Hoboken, NJ, USA, pp. 65–97.

Langfelder, P., Horvath, S. (2008): WGCNA: an R package for weighted correlation network analysis. *BMC Bioinformatics* 9, 1–13.

Loth-Pereda, V., Orsini, E., Courty, P.-E., Lota, F., Kohler, A., Diss, L., Blaudez, D., Chalot, M., Nehls, U., Bucher, M., Martin, F. (2011): Structure and expression profile of the phosphate Pht1 transporter gene family in mycorrhizal *Populus trichocarpa*. *Plant Physiol.* 156, 2141–2154.

Misson, J., Raghothama, K.G., Jain, A., Jouhet, J., Block, M.A., Bligny, R., Ortet, P., Creff, A., Somerville, S., Rolland, N., Doumas, P., Nacry, P., Herrerra-Estrella, L., Nussaume, L., Thibaud, M.-C. (2005): A genome-wide transcriptional analysis using *Arabidopsis thaliana* Affymetrix gene chips determined plant responses to phosphate deprivation. *Proc. Natl. Acad. Sci. U. S. A.* 102, 11934–11939.

Morcuende, R., Bari, R., Gibon, Y., Zheng, W., Pant, B.D., Bläsing, O., Usadel, B., Czechowski, T., Udvardi, M.K., Stitt, M., Scheible, W.-R. (2007): Genome-wide reprogramming of metabolism and regulatory networks of *Arabidopsis* in response to phosphorus. *Plant Cell Environ.* 30, 85–112.

Mudge, S.R., Rae, A.L., Diatloff, E., Smith, F.W. (2002): Expression analysis suggests novel roles for members of the Pht1 family of phosphate transporters in *Arabidopsis*. *Plant J.* 31, 341–353.

Nussaume, L., Kanno, S., Javot, H., Marin, E., Pochon, N., Ayadi, A., Nakanishi, T.M., Thibaud, M.-C. (2011): Phosphate import in plants: Focus on the PHT1 transporters. *Front. Plant Sci.* 2, 83.

Puga, M.I., Mateos, I., Charukesi, R., Wang, Z., Franco-Zorrilla, J.M., de Lorenzo, L., Irigoyen, M.L., Masiero, S., Bustos, R., Rodriguez, J., Leyva, A., Rubio, V., Sommer, H., Paz-Ares, J. (2014): SPX1 is a phosphate-dependent inhibitor of PHOSPHATE STARVATION RESPONSE 1 in *Arabidopsis*. *Proc. Natl. Acad. Sci.* 111, 14947–14952.

R Development Core Team (2012): R: a language and environment for statistical computing. R Foundation for Statistical Computing, Vienna, Austria.

- Rai, V., Sanagala, R., Sinilal, B., Yadav, S., Sarkar, A.K., Dantu, P.K., Jain, A. (2015): Iron availability affects phosphate deficiency-mediated responses, and evidence of cross-talk with auxin and zinc in *Arabidopsis*. *Plant Cell Physiol.* 56, 1107–1123.
- Rennenberg, H., Herschbach, C. (2013): Phosphorus nutrition of woody plants: many questions - few answers. *Plant Biol.* 15, 785–788.
- Rennenberg, H., Wildhagen, H., Ehling, B. (2010): Nitrogen nutrition of poplar trees. *Plant Biol.* 12, 275–291.
- Rouached, H., Secco, D., Arpat, B., Poirier, Y. (2011): The transcription factor PHR1 plays a key role in the regulation of sulfate shoot-to-root flux upon phosphate starvation in *Arabidopsis*. *BMC Plant Biol.* 11, 19.
- Saenchai, C., Bouain, N., Kisko, M., Prom-u-thai, C., Doumas, P., Rouached, H. (2016): The involvement of OsPHO1;1 in the regulation of iron transport through integration of phosphate and zinc deficiency signaling. *Front. Plant Sci.* 7, 396.
- Schachtman, D.P., Reid, R.J., Ayling, S.M. (1998): Phosphorus uptake by plants: from soil to cell. *Plant Physiol.* 116, 447–453.
- Scheible, W.-R., Rojas-Triana, M. (2015): Sensing, signalling, and control of phosphate starvation in plants: molecular players and applications, in: Plaxton, W.C., Lambers, H. (eds.): Annual Plant Reviews Volume 48. John Wiley & Sons, Inc., Hoboken, NJ, USA, pp. 23–63.
- Schwender, H. (2011): siggenes: Multiple testing using SAM and Efron's empirical Bayes approaches. R package version 1.28.0.
- Shannon, P., Markiel, A., Ozier, O., Baliga, N.S., Wang, J.T., Ramage, D., Amin, N., Schwikowski, B., Ideker, T. (2003): Cytoscape: a software environment for integrated models of biomolecular interaction networks. *Genome Res.* 13, 2498–2504.
- Smyth, G.K. (2005): limma: Linear Models for Microarray Data, in: Gentleman, R., Carey, V.J., Huber, W., Irizarry, R.A., Dudoit, S. (eds.): Bioinformatics and computational biology solutions using R and Bioconductor. Springer New York, pp. 397–420.
- Taylor, G. (2002): *Populus: Arabidopsis* for forestry. Do we need a model tree? *Ann. Bot.* 90, 681–689.
- Tsai, C.-J., Ranjan, P., DiFazio, S., Tuskan, G., Johnson, V. (2011): Poplar genome microarrays, in: Joshi, C., DiFazio, S., Kole, C. (eds.): Genetics, genomics and breeding of poplars. Science Publishers, Enfield, NH, pp. 112–127.
- Vance, C.P., Uhde-Stone, C., Allan, D.L. (2003): Phosphorus acquisition and use: critical adaptations by plants for securing a nonrenewable resource. *New Phytol.* 157, 423–447.
- von Wirén, N., Klair, S., Bansal, S., Briat, J.-F., Khodr, H., Shioiri, T., Leigh, R.A., Hider, R.C. (1999): Nicotianamine chelates both FeIII and FeII. Implications for metal transport in plants. *Plant Physiol.* 119, 1107–1114.



Wang, L., Li, Z., Qian, W., Guo, W., Gao, X., Huang, L., Wang, H., Zhu, H., Wu, J.-W., Wang, D., Liu, D. (2011): The *Arabidopsis* purple acid phosphatase AtPAP10 is predominantly associated with the root surface and plays an important role in plant tolerance to phosphate limitation. *Plant Physiol.* 157, 1283–1299.

Wang, L., Liu, D. (2012): *Arabidopsis* purple acid phosphatase 10 is a component of plant adaptive mechanism to phosphate limitation. *Plant Signal. Behav.* 7, 306–310.

Wang, L., Lu, S., Zhang, Y., Li, Z., Du, X., Liu, D. (2014): Comparative genetic analysis of *Arabidopsis* purple acid phosphatases AtPAP10, AtPAP12, and AtPAP26 provides new insights into their roles in plant adaptation to phosphate deprivation: Comparative analysis of three *Arabidopsis* APases. *J. Integr. Plant Biol.* 56, 299–314.

Wang, Y.-H., Garvin, D.F., Kochian, L.V. (2002): Rapid induction of regulatory and transporter genes in response to phosphorus, potassium, and iron deficiencies in tomato roots. Evidence for cross talk and root/rhizosphere-mediated signals. *Plant Physiol.* 130, 1361–1370.

Wang, Z., Ruan, W., Shi, J., Zhang, L., Xiang, D., Yang, C., Li, C., Wu, Z., Liu, Y., Yu, Y., Shou, H., Mo, X., Mao, C., Wu, P. (2014): Rice SPX1 and SPX2 inhibit phosphate starvation responses through interacting with PHR2 in a phosphate-dependent manner. *Proc. Natl. Acad. Sci.* 111, 14953–14958.

Ward, J.T., Lahner, B., Yakubova, E., Salt, D.E., Raghothama, K.G. (2008): The effect of iron on the primary root elongation of *Arabidopsis* during phosphate deficiency. *PLANT Physiol.* 147, 1181–1191.

Wildhagen, H., Dürr, J., Ehlting, B., Rennenberg, H. (2010): Seasonal nitrogen cycling in the bark of field-grown Grey poplar is correlated with meteorological factors and gene expression of bark storage proteins. *Tree Physiol.* 30, 1096–1110.

Woo, J., MacPherson, C.R., Liu, J., Wang, H., Kiba, T., Hannah, M.A., Wang, X.-J., Bajic, V.B., Chua, N.-H. (2012): The response and recovery of the *Arabidopsis thaliana* transcriptome to phosphate starvation. *BMC Plant Biol.* 12, 62.

Wu, P., Ma, L., Hou, X., Wang, M., Wu, Y., Liu, F., Deng, X.W. (2003): Phosphate starvation triggers distinct alterations of genome expression in *Arabidopsis* roots and leaves. *Plant Physiol.* 132, 1260–1271.

Zheng, L., Huang, F., Narsai, R., Wu, J., Giraud, E., He, F., Cheng, L., Wang, F., Wu, P., Whelan, J., Shou, H. (2009): Physiological and transcriptome analysis of iron and phosphorus interaction in rice seedlings. *Plant Physiol.* 151, 262–274.

Zhu, B., Coleman, G.D. (2001): Phytochrome-mediated photoperiod perception, shoot growth, glutamine, calcium, and protein phosphorylation influence the activity of the poplar Bark Storage Protein gene promoter (bspA). *Plant Physiol.* 126, 342–351.

## 2.6 Supporting information

**Table S2.1:** Information about differentially expressed genes. (data CD)

**Table S2.2:** Overview about enriched GO terms in all modules. (data CD)

**Table S2.3:** Gene name abbreviations for Figure 2.6.

**Figure S2.1.** Hierarchy of enriched GO-terms in modules “Green”, “Blue” and “Brown”. (data CD)

**Table S2.3: Gene name abbreviations for Figure 2.6.**

Gene abbreviations	gene name	Potri.IDs (labeled in figure)
<b>(a)</b>		
AOS	allene oxide synthase	Potri.014G038700
ASPG	asparaginase	Potri.014G022900
ATL	RING-H2 zinc finger protein	Potri.001G162000
BT	BTB/POZ domain-containing protein	Potri.001G468700 Potri.007G140400
CEK	choline/ethanolamine kinase	Potri.005G197500
CIPK	CBL-interacting protein kinase	Potri.006G062800 Potri.019G128100
CML	calcium-binding protein	Potri.016G142000
CXE	carboxylesterase	Potri.009G104400
CYB	cytochrome b	Potri.013G136800
G3Pp	Glycerol-3-phosphate transporter	Potri.001G124200 Potri.003G109300
GDPD	glycerophosphodiester phosphodiesterase	Potri.001G325200
GRX	glutaredoxin	Potri.017G017300
LRR	leucine rich repeat protein	Potri.001G425500
NAC	NAC-domain containing protein	Potri.007G099400
PAP	purple acid phosphatase	Potri.002G243900 Potri.010G158200 Potri.005G233400
PK	serine/threonine-protein kinase	Potri.006G109600
PPase	pyrophosphatase	Potri.003G034600
PPC	phosphoenolpyruvatcarboxylase	Potri.008G114200
PPCK	phosphoenolpyruvatcarboxylase kinase	Potri.013G046100 Potri.019G018100
psbN	photosystem II reaction centre N protein	Potri.019G028300
PUB	U-box domain containing protein	Potri.014G084900
rp	ribosomal protein	Potri.009G064100 Potri.005G154300
RTNL	reticulon-like protein	Potri.015G027300
SAMT	S-adenosyl-L-methionine-dependent methyltransferase	Potri.007G021400
SPX	SPX domain containing protein	Potri.006G069500
SQD	sulfoquinovosyldiacylglycerol / UDP-sulfoquinovose synthase	Potri.016G112600
TCP	TCP transcription factor	Potri.002G152200

**Table S2.3** (continued)

Gene abbreviations	gene name	Potri.IDs (labeled in figure)
TIM	mitochondrial import inner membrane translocase	Potri.015G102000
VPE	vacuolar processing enzyme	Potri.006G232900
WAK	wall-associated kinase	Potri.002G075900
WRKY	WRKY transcription factor	Potri.001G044500 Potri.018G019800
<b>(b)</b>		
ARMR	Armadillo repeat-containing protein	Potri.002G118800
ATPase	ATP synthase	Potri.014G168000
BSP	bark storage protein	Potri.013G100700 Potri.013G101000
BT	s. (a)	Potri.001G468700
BXL	beta-D-xylosidase-related	Potri.014G122200
CBR	NADH-cytochrome B5 reductase	Potri.013G067300
CT	chitinase	Potri.009G142200 Potri.004G182000
FAF	Fantastic Four meristem regulator	Potri.001G216000
G3Pp	s. (a)	Potri.003G109300
H2A	histone H2A	Potri.005G040700
HCT	shikimate O-hydroxycinnamoyltransferase	Potri.005G028000
IAA	auxin responsive protein	Potri.001G177500
IFR	isoflavone reductase	Potri.005G228700
IPK	inositol-tetrakis/trisphosphate kinase	Potri.009G084600
LAS	ribosome biogenesis factor	Potri.009G067800
MCM	DNA replication licensing factor	Potri.018G112800
MGD	monogalactosyldiacylglycerol synthase	Potri.006G063300
MGL	methionine gamma-lyase	Potri.003G190600
ND	NADH:ubiquinone reductase (none-electrogenic)	Potri.011G044600
NMT	phosphoethanolamine N-methyltransferase	Potri.015G039000 Potri.012G047400
PAP	s. (a)	Potri.008G139100
PHT	phosphate transporter	Potri.001G318500 Potri.002G005500
PK	s. (a)	Potri.008G166500
POT	proton-dependent oligopeptide transporter	Potri.006G096800

**Table S2.3** (continued)

Gene abbreviations	gene name	Potri.IDs (labeled in figure)
PPC	s. (a)	Potri.011G110700
RD	dehydration-responsive protein	Potri.004G136000
SPX	s. (a)	Potri.014G061200
TIM	s. (a)	Potri.012G039100
UBC	ubiquitin-conjugating enzyme	Potri.001G254500
UBQ	ubiquitin extension protein	Potri.016G077200 Potri.015G007100
<b>(c)</b>		
ANNAT	annexin	Potri.001G024900
ASP	aspartyl protease	Potri.018G014800
BAP	BON association protein	Potri.002G155300
BPS	bypass1-related protein-related	Potri.010G171000
CAF	CCR4-associated factor	Potri.009G161500
ccmE	heme-binding protein-related	Potri.001G379000
CDSP	thioredoxin-like protein	Potri.005G245700
CML	calmodulin like / EF-hand calcium-binding domain containing protein	Potri.002G001400 Potri.005G259900
CYP	cytochrome P450 CYP2	Potri.004G106600
D17H	desacetyoxyvindoline-17-hydroxylase	Potri.005G222300
DCL	endoribonuclease dicer homolog	Potri.002G181400
DREB	dehydration-responsive element-binding protein	Potri.001G110800
ERF	ethylene responsive factor	Potri.006G138800 Potri.006G138700 Potri.009G101900 Potri.001G154200 Potri.007G138100
EXPB	beta-expansin precursor	Potri.014G066300
FtsH	FtsH protease	Potri.017G084000
GLT	glycosyltransferase domain-containing protein	Potri.008G192600
GRXS	monothiol glutaredoxin	Potri.007G134800
GTF	glycosyltransferase	Potri.006G097600
H3	histone H3	Potri.014G096900 Potri.002G028800
HCF	photosystem II stability/assembly factor	Potri.007G071300
helicase	DNA helicase	Potri.012G114100
HMGB	HMG-box-containing protein	Potri.007G000900
LRR	s. (a)	Potri.017G152500

**Table S2.3** (continued)

Gene abbreviations	gene name	Potri.IDs (labeled in figure)
MAPKKK	mitogen-activated protein kinase kinase kinase	Potri.005G139300 Potri.007G044800
MAT	S-adenosylmethionine synthetase	Potri.006G123200
MCM	s. (b)	Potri.001G070500
MIOX	myo-inositol oxygenase	Potri.018G069700
MMP	matrix metalloproteinase / interstitial collagenase	Potri.013G033200
MYB	MYB transcription factor	Potri.010G128900
NUDT	nudix hydrolase	Potri.008G134000
PAP	s. (a)	Potri.001G023400 Potri.003G030700 Potri.005G233400 Potri.010G158200 Potri.015G031400 Potri.012G042200
PK	s. (a)	Potri.001G014700 Potri.016G123300
PL	phospholipase	Potri.013G012300 Potri.001G250500
PNL	pectin lyase-like	Potri.010G042100
PP	protein phosphatase 2C	Potri.001G381000
PPase	s. (a)	Potri.008G196800
PQR	PQ-loop repeat protein	Potri.007G031800
PR	pathogenesis related protein	Potri.009G083300
PSBR	photosystem II 10 kDa polypeptide	Potri.011G142300
PSD	phosphatidylserine decarboxylase	Potri.003G061700
PUB	s. (a)	Potri.017G135000 Potri.006G202600 Potri.008G137700
rp	s. (a)	Potri.006G192900
RPA	replication protein	Potri.006G275700
SPS	sucrose phosphate synthase	Potri.013G095500
SPX	s. (a)	Potri.006G069500
SQD	s. (a)	Potri.006G228000
SULTR	sulfate transporter	Potri.005G169300
TIFY	TIFY domain protein	Potri.003G165000
TRI	tropinone reductase	Potri.005G039300
WAK	s. (a)	Potri.005G021300
WRKY		Potri.003G138600
ZAT	zinc finger protein	Potri.001G235800 Potri.014G017300 Potri.002G119300

## **2.7 Declaration**

The following data shown in this chapter have been provided:

- ICP-OES and calculations were conducted by members of the Department of Plant Ecology and Ecosystems Research (Albrecht-von-Haller-Institute for Plant Sciences, Georg-August University Göttingen).
- All laboratory steps for microarray analyses (from RNA quality determinations to raw data) were provided by the Microarray Facility (MFT Services, Tübingen, Germany).

## Chapter 3

# Phosphate uptake kinetics and tissue-specific transporter expression profiles in poplar (*Populus × canescens*) at different phosphorus availabilities

Published in similar form as open access article distributed under the terms of the Creative Commons Attribution 4.0 International License (<http://creativecommons.org/licenses/by/4.0/>). © The Author(s). 2016.

Mareike Kavka and Andrea Polle  
BMC Plant Biology (2016) 16:206  
DOI 10.1186/s12870-016-0892-3

### 3.1 Introduction

Phosphorus (P) is a major nutrient, required for growth and metabolism, but often is the least plant-available compound in soil (Holford, 1997). Plants take up phosphorus in the form of inorganic phosphate (Pi), whose concentration is usually low (< 10 µM) in soil solutions (Bieleski, 1973). P uptake and translocation is achieved by a diverse group of phosphate transporters (PHTs), which cluster in four families (Guo *et al.*, 2008; Rausch and Bucher, 2002). Most members of family 1 (PHT1) are localized in the plasma membrane (Nussaume *et al.*, 2011), of PHT2 in chloroplasts (Versaw and Harrison, 2002), of PHT3 in the mitochondria (Rausch and Bucher, 2002) and of PHT4 in various subcellular compartments, including heterotrophic plastids and the Golgi apparatus (Guo *et al.*, 2008). In *Arabidopsis*, members of the PHT1 family exhibit strong expression in roots, are responsible for P uptake from soil and for the distribution and remobilization within the plant (Baker *et al.*, 2015; Nussaume *et al.*, 2011), whereas the members of the other PHT families are required for intracellular P distribution (Guo *et al.*, 2008; Takabatake *et al.*, 1999; Versaw and Harrison, 2002).

Kinetic measurements showed that plants possess two different P uptake systems: high affinity systems that respond to the P status of the plant, and low affinity systems that



are expressed constitutively (*Schachtman et al.*, 1998). Low affinity P uptake systems are operational under high P availabilities and exhibit  $K_m$  values of 50 to several hundred  $\mu\text{M}$  (*Schachtman et al.*, 1998). In *Arabidopsis*, PHT2;1 (*Daram et al.*, 1999; *Versaw and Harrison*, 2002) and all transporters of family 4 (*Guo et al.*, 2008) were shown to be low affinity transporters. But also family 1 may contain low affinity transporters (rice: OsPHT1;2 (*Ai et al.*, 2009), barley: HvPHT1;6 (*Rae et al.*, 2003)). The expression of high affinity transporters is induced when P availability is low (*Zhang et al.*, 2014). Their  $K_m$  values are in the lower micro-molar range (*López-Arredondo et al.*, 2014). For example, *Arabidopsis* AtPHT1;1 exhibited a  $K_m$  of 3  $\mu\text{M}$  (*Mitsukawa et al.*, 1997) and transported together with AtPHT1;4 the highest proportion of phosphate into the roots under low P conditions (*Shin et al.*, 2004).

At the whole-plant level, P uptake is driven by the interplay of multiple P transporters and internal resource allocation. Whole-plant P uptake has mainly been determined for agricultural crops such as barley, maize, potato and soybean, and was about 1.8 to 5.2 times higher in P starved than in P sufficient plants (*Bhadoria et al.*, 2004; *Cogliatti and Clarkson*, 1983; *Jungk et al.*, 1990; *Lee*, 1982), but information on the involved transport systems is lacking.

*Populus* species are important woody crops (*Polle et al.*, 2013; *Polle and Chen*, 2015). With an increasing demand for woody biomass, an extension of poplar plantations is expected, especially on marginal soils where nutrients are often limited (*Polle et al.*, 2013; *Polle and Chen*, 2015). Previous studies on selected members of the PHT1 family in poplar demonstrated up-regulation when the trees were exposed to low or no P in the growth medium (*Gan et al.*, 2016; *Loth-Pereda et al.*, 2011). It was further shown that the  $K_m$  for P accumulation in roots of P starved poplars (*P. tremuloides*) was 32  $\mu\text{M}$  (*Desai et al.*, 2014). P uptake kinetics that link changes in P uptake with changes in the expression profiles in different PHT families, are still missing. Furthermore, it is not known whether modulation in P availability affects P acquisition, internal allocation and P use efficiency in poplar.

The goal of the present study was to characterize whole-plant P uptake kinetics and expression profiles of the PHT transporter families 1, 2, 3, and 4 in roots and leaves under high, intermediate and low P availability in poplar (*P. × canescens*). As pre-requisite for these studies we annotated the poplar PHT families 2, 3, and 4 in addition to the known PHT1 family (*Loth-Pereda et al.*, 2011). We further determined P

acquisition and allocation in response to different P availabilities. Our results show that intermediate P concentrations of about 6  $\mu\text{M}$ , which are often present in environments, led to a tissue-specific regulation of PHTs, a relative increase in P uptake with low  $K_m$  and high  $v_{\text{max}}$ , increased P use efficiency, but strong growth reduction.

## 3.2 Methods

### 3.2.1 Plant material and growth conditions

In vitro micropropagated (*Leple et al.*, 1992) *Populus × canescens* (INRA717 1-B4) plantlets were grown on half-strength Murashige and Skoog medium for three weeks to develop roots. Afterwards, they were planted singly into PVC tubes (5 cm diameter; 40 cm length) with one drain (*Jentschke et al.*, 1999; *Müller et al.*, 2013) filled with autoclaved sand ( $\text{\O}$  0.4-3.15 mm particle size, Melo, Göttingen, Germany) and grown in a greenhouse at an air humidity of about 65%. The plants were supplemented with additional light (EYE Clean Ace MT400DL/BH, EYE Lighting Europe, Uxbridge, UK; 50-100  $\mu\text{mol quanta m}^{-2} \text{s}^{-1}$  of photosynthetically active radiation, depending on poplar height and natural light condition) for 14 h a day from 7 am to 9 pm. The plants were automatically irrigated as described by Müller et al. (2013) every 4 hours (ca. 6.5 mL, after 45 days ca. 9 mL) with Long Ashton nutrient solution (*Hewitt and Smith*, 1974) containing either high phosphate (HP) supply (200  $\mu\text{M KNO}_3$ , 900  $\mu\text{M Ca(NO}_3)_2$ , 300.2  $\mu\text{M MgSO}_4$ , 599.9  $\mu\text{M KH}_2\text{PO}_4$ , 41.3  $\mu\text{M K}_2\text{HPO}_4$ , 10  $\mu\text{M H}_3\text{BO}_3$ , 2  $\mu\text{M MnSO}_4$ , 7  $\mu\text{M Na}_2\text{MoO}_4$ , 40 nM  $\text{CoSO}_4$ , 200 nM  $\text{ZnSO}_4$ , 128 nM  $\text{CuSO}_4$ , 10  $\mu\text{M EDTA-Fe}$ , in total: 641  $\mu\text{M P}_i$ ) or reduced  $\text{P}_i$  concentrations. Mildly  $\text{P}_i$  starved (medium phosphate, MP) poplars received long Ashton solution with 5.999  $\mu\text{M KH}_2\text{PO}_4$  and 0.413  $\mu\text{M K}_2\text{HPO}_4$  and additionally 675.8  $\mu\text{M KCl}$  and  $\text{P}_i$  starved (low phosphate, LP) plants 0.060  $\mu\text{M KH}_2\text{PO}_4$  and 0.004  $\mu\text{M K}_2\text{HPO}_4$  and additionally 682.5  $\mu\text{M KCl}$ . Plant height was measured weekly from the stem base to the apex. This experiment was repeated four times for different measurements with twelve biological replicates each time.

### 3.2.2 Labeling of the poplars with $^{33}\text{P}$ and harvest

Sixty-day-old HP, MP and LP poplars ( $n=5$  per treatment, experiment 2) were watered by hand at 7 am and 10 am with the respective nutrient solution (16 and 14 mL for HP, 4 mL for MP and 2 mL for LP) and labeled with  $\text{H}_3^{33}\text{PO}_4$  (Hartmann Analytic, Braunschweig, Germany) at 11 am: 20.25  $\mu\text{L}$  of the  $\text{H}_3^{33}\text{PO}_4$  stock solution were mixed with 5.5 mL of each of the respective nutrient solutions and 1 mL of each labeling solution was applied once to the poplars. This treatment resulted in 1.2 ( $\pm 0.013$  resp. 0.002) MBq for the HP and MP plants and 1.12 ( $\pm 0.034$ ) MBq for the LP plants (mean  $\pm$  SE,  $n=3$ ). The specific radioactivity was  $1.88 \times 10^3$  Bq  $\text{nmol}^{-1}$  P for HP,  $1.87 \times 10^5$  Bq  $\text{nmol}^{-1}$  P for MP and  $1.46 \times 10^7$  Bq  $\text{nmol}^{-1}$  P for LP poplars.

The automatic irrigation was stopped during the chase period of two days. During this time the poplars were irrigated by hand with unlabeled nutrient solution avoiding through-flow. Two days after label application, the plants were harvested. The roots were briefly washed with tap water. Each plant was divided into fine roots, coarse roots, stem and leaves. The biomass of the tissues was determined immediately after harvest and after drying at 60°C for 7 days.

### 3.2.3 Phosphorus distribution at the whole-plant level

To visualize the distribution of radioactivity, the poplars were dried at 60°C for one day pressed between paper and two glass plates. Autoradiographs were taken with a Phosphorimager (FLA 5100, Fuji, Japan) after exposure for 30 min on imaging plates (Imaging Plate BAS-MS 2040, 20  $\times$  40 cm, Fuji, Japan). The image was taken with the program Image Reader FLA-5000 (version 3.0, Fuji Film, Japan) with 100  $\mu\text{m}$  resolution and analyzed with AIDA Image Analyzer (version 4.27, raytest Isotopenmeßgeräte, Straubenhardt, Germany).

### 3.2.4 Determination of net $^{33}\text{P}$ and total P uptake

Dried plant tissues were milled (Retsch, type MM2, Haan, Germany) to a fine powder. About 25 mg of leaf or stem powder and 10 mg of fine or coarse root powder were

weighed into glass vials (20 mL, PerkinElmer Life and Analytical Sciences, Rodgau, Germany) and incinerated for 4 h at 500°C (M104, Heraeus Holding, Hanau, Germany). The residual material was mixed with 10 mL of scintillation liquid (Rotiszint® eco plus [Carl Roth, Karlsruhe, Germany]) and the radioactivity was measured by liquid-scintillation technique (Tri-Carb® 2800TR [PerkinElmer Life and Analytical Sciences, Rodgau, Germany]). The maximum count time was 10 min in normal count mode calculated against a quench set of  $^{33}\text{P}$ . All values were corrected for the half-life of  $^{33}\text{P}$ .  $^{33}\text{P}$ -activity in plants and proportion of  $^{33}\text{P}$ -uptake was calculated using following equations:

Radioactivity in plant tissue [Bq]=

$$(\text{activity in vial [Bq]} - \text{background [Bq]}) \times 0.5^{\frac{\text{date of harvest} - \text{date of measurement}}{25.3}} \times \frac{\text{dry mass tissue [g]}}{\text{sample in vial [g]}}$$

$$^{33}\text{P-recovery [\%]} = \frac{\text{radioactivity in plant [Bq]}}{\text{given radioactivity [Bq]}} \times 100$$

To determine total P uptake the specific radioactivity of the nutrient solution was used:

$$\text{P uptake [nmol]} = \frac{\text{measured radioactivity in plant [Bq]}}{\text{specific radioactivity [Bq nmol}^{-1}\text{ P]}}$$

### 3.2.5 Determination of total P contents

Dry fine root, coarse root, leaf and stem of 63-day-old HP, MP and LP poplars ( $n=4$  per treatment, experiment 1) were powdered and pressure-extracted in  $\text{HNO}_3$  (Heinrichs *et al.*, 1986). Total phosphorus concentration was measured using an inductively coupled plasma optical emission spectrometer (ICP-OES; Optima 5300 DV, PerkinElmer Life and Analytical Sciences, Rodgau, Germany). P use efficiency (PUE) was calculated as dry mass per total P content. The equation for the whole plant PUE was

$$\text{PUE [g mg}^{-1}\text{]} = \frac{\text{DM}_{\text{total}}}{\text{P conc}_L \times \text{DM}_L + \text{P conc}_S \times \text{DM}_S + \text{P conc}_{\text{FR}} \times \text{DM}_{\text{FR}} + \text{P conc}_{\text{CR}} \times \text{DM}_{\text{CR}}}$$

with DM: dry mass [g], P conc: total P concentration in fraction [ $\text{mg g}^{-1}$ ], L: leaves, S: stem, FR: fine roots, CR: coarse roots.

### 3.2.6 Phosphate uptake after glucose supply and determination of carbohydrates

Seventy-seven-day-old HP, MP and LP poplars ( $n=5$  per treatment, experiment 3) were irrigated with 80 mL HP, MP or LP Long Ashton medium with or without 400 mM glucose at 5 am. Along with turning on the additional light at 7 am, they were labeled with  $H_3^{33}PO_4$  (Hartmann Analytic, Braunschweig, Germany) in 1 mL of HP, MP or LP Long Ashton medium to yielding 1.08 ( $\pm 0.006$ ) MBq in the growth medium of HP poplars and 1.09 MBq ( $\pm 0.0008$  resp. 0.003) in the growth medium of MP and LP poplars (mean  $\pm$  SE,  $n=2$ ). At the end of the light period (9 pm), the poplars were harvested to determine biomass,  $^{33}P$  activity (as above), and the carbohydrate concentrations. Leaves (half of each leaf) and fine roots for carbohydrate determination were immediately shock frozen in liquid nitrogen and stored at  $-80^\circ C$ . The tissues were freeze-dried at  $-80^\circ C$  for three days (BETA1, Martin Christ Gefriertrocknungsanlagen, Osterode am Harz, Germany) and milled (as above). About 25 mg tissue powder was extracted in 1.5 ml dimethyl sulfoxide / hydrochloric acid (80:20 (v:v)) at  $60^\circ C$  for 30 min. After centrifugation, 200  $\mu L$  of the supernatant were mixed with 1250  $\mu L$  0.2 M citrate buffer (pH 10.6). After an additional centrifugation, 400  $\mu L$  of the supernatant were mixed with 400  $\mu L$  citrate buffer (50  $\mu M$ , pH 4.6). Two hundred  $\mu L$  were mixed with 250  $\mu L$  reaction solution (4 mM NADP, 10 mM ATP, 9 mM  $MgSO_4$ , 0.75 M triethanolamine, pH 7.6) and 300  $\mu L$   $H_2O$ . The reaction was started by subsequent addition of enzymes and the production of NADPH was determined photometrically at a wavelength of 340 nm and  $25^\circ C$  until no further increase was observed. For glucose determination 10  $\mu L$  (ca. 3.4 U; 1.7 U) of hexokinase; glucose-6-phosphate-dehydrogenase (Roche Diagnostics Deutschland, Mannheim, Germany), and subsequently for fructose 5  $\mu L$  (ca. 17.5 U) of phosphoglucose-isomerase (Roche Diagnostics, Deutschland, Mannheim, Germany) were added. To determine the amount of sucrose 400  $\mu L$  (ca. 12 U) invertase (Sigma-Aldrich Chemie, Steinheim, Germany) solution (0.1 mg invertase in 1 mL 0.32 M citrate buffer, pH 4.6) were mixed with 400  $\mu L$  of supernatant and then glucose was determined as above. Free glucose was subtracted. The concentration of glucose (fructose) was calculated for  $\Delta E = E1 - E0$  with E1 and E0 being the extinction of assay after and before addition of glucose-6-phosphate-dehydrogenase (after and before addition of phosphoglucose-isomerase) and

the extinction coefficient  $\varepsilon = 6.3 \text{ L} \times \text{mmol}^{-1} \text{ cm}^{-1}$  for NADPH. Sucrose concentration was below the detection limit in most of the samples. Each sample was measured in triplicate.

### **3.2.7 Kinetic measurements**

Roots of nine-week-old HP, MP and LP poplars (experiment 4) were washed carefully with tap water to remove the sand. The plants were transferred to aerated nutrient solution with HP, MP and LP Long Ashton nutrient solution and acclimated to this and lab conditions under continuous light (about  $10 \mu\text{mol quanta m}^{-2} \text{ s}^{-1}$  of photosynthetically active radiation, TLD18W/840, Philips Lighting, Hamburg, Germany) for 1 day. Phosphate uptake was determined with the method of Claassen and Barber (1974). The plants were removed from the nutrient solutions, the roots were cautiously surface-dried between tissue papers, washed with the experimental solution (see below), surface-dried again and placed in plastic beakers. An appropriate volume (5 to 45 ml) of Long Ashton nutrient solution which contained  $213.7 \mu\text{M Pi}$  for all plants and  $^{33}\text{P}$ -phosphoric acid (Hartmann Analytic, Braunschweig, Germany) (to about  $5375 \text{ Bq mL}^{-1}$  of experimental solution) was added. During the time course of the experiment of up to 14 h, the nutrient solution was stirred and aerated with compressed air and water loss by plant transpiration was replaced by adding deionized water up to the marked original level. Uptake of P was calculated by the decrease in  $^{33}\text{P}$  in the experimental solution. For this purpose,  $40 \mu\text{L}$  of experimental nutrient solution was removed at distinct time intervals and mixed with  $0.5 \text{ mL}$  inactive nutrient solution and  $4 \text{ mL}$  of Rotiszint® eco plus scintillation liquid (Carl Roth, Karlsruhe, Germany). Radioactivity was measured by liquid scintillation counting (Tri-Carb® 2800TR, PerkinElmer Life and Analytical Sciences, Rodgau, Germany). Samples were taken at min 0 (immediately after addition to the plants), 2.5, 5, 7.5, 10, 15, 20, 30, 45, 60 and 75 after addition to the plants, then every 30 min until 5 hours, thereafter every hour and after 8 hours every 2 hours, if needed. The experiment lasted until the LP plants showed no further uptake, but at least 7 hours. The experiment was conducted with 6 plants per P nutrient level. The plants were harvested at the end of the experiment and the biomass of the root system was measured.

The uptake rate ( $I_{k,k+1}$ ) was calculated between two time points (k and k+1) with the following equations. Because the measured radioactivity fluctuated strongly in samples of the first minutes of the experiment, only the values after stabilization were used for calculations and models.

$$C_k = C_0 \times \frac{A_k}{A_0}$$

$C_k$ : P concentration in the nutrient solution at time point k [ $\mu\text{M}$ ]

$A_k$ : activity in nutrient solution at time point k [ $\text{Bq } \mu\text{L}^{-1}$ ]

$C_0$ : P concentration at time point 0 (start of experiment) [ $\mu\text{M}$ ]

$A_0$ : activity in nutrient solution at time point 0 (start of experiment) [ $\text{Bq } \mu\text{L}^{-1}$ ]

$$I_{k,k+1} = \frac{C_{k+1} \times V - C_k \times V}{\frac{t_{k+1} - t_k}{\text{FM}}}$$

$I_{k,k+1}$ : P uptake rate between time point k and k+1 [ $\mu\text{mol min}^{-1} \text{g}^{-1}$ ]

V: volume of experimental solution [L]

$t_k, t_{k+1}$ : time point k and k+1 [min]

FM: fresh mass of fine roots [g].

Due to plant uptake, the P concentration in the nutrient solution declined during the experiment. Therefore, the P concentration ( $C_{k,k+1}$ ) at each uptake rate ( $I_{k,k+1}$ ) was calculated as:

$$C_{k,k+1} = \frac{C_k + C_{k+1}}{2}$$

To model the change in uptake rate in relation to the concentration in the nutrient solution,  $I_{k,k+1}$  and the corresponding  $C_{k,k+1}$  were plotted and a curve was fitted to determine  $v_{\text{max}}$  (the maximum uptake rate),  $C_{\text{min}}$  (the minimum concentration at which the plants can take up phosphate) and  $K_m$  (the Michaelis-Menten constant) using the following equation in a non-linear model (R-package “nlme”, *Pinheiro et al.*, 2012):

$$I_{k,k+1} = \frac{v_{\text{max}} \times (C_{k,k+1} - C_{\text{min}})}{K_m + C_{k,k+1} - C_{\text{min}}}$$

The fitted curve for these parameters was drawn; the standard errors of the predictions were used for calculation of the 95%-prediction interval (R-package “emdbook”, *Bolker*, 2013). Because the uptake rate of the control plants (HP) was slow, a linear fit without slope was defined as  $v_{\text{max}}$ . Outliers ( $>1.5$  interquartile ranges below first and above third quartile) were excluded from the linear fit.

### 3.2.8 RNA extraction and microarray analysis

The first three fully expanded leaves from the top and fine roots (< 2mm diameter) of 59-day-old HP, MP and LP poplars (experiment 2) were harvested and immediately shock frozen in liquid nitrogen. Six plants per treatment (i.e. 18 plants in total) were used and the leaves respective roots of two individual poplars were pooled yielding three biological replicates per treatment. Frozen tissue was milled in liquid nitrogen and RNA was extracted from about 1 g of plant powder according to Chang et al. (1993) with modifications: no spermidine was used, 2%  $\beta$ -mercaptoethanol was added separately from the extraction buffer and phenol:chloroform:isoamyl alcohol (Roti®-Aqua PCI, 25:24:1, Roth, Karlsruhe, Germany) was used instead of chloroform:isoamyl alcohol. RNA concentrations and purity were determined spectrophotometrically via the absorptions at 260 and 280 nm (BioPhotometer, Eppendorf, Hamburg, Germany). RNA integrity was determined with Agilent BioAnalyzer 2100 capillary electrophoresis at the Microarray Facility (MFT Services, Tübingen, Germany). Hybridization on the GeneChip® Poplar Genome Array (Affymetrix, Santa Clara, CA), washing, staining and scanning were conducted at the Microarray Facility (MFT Services, Tübingen, Germany). Raw and normalized data were uploaded into the EMBL-EBI ArrayExpress database (Kolesnikov et al., 2015) under E-MTAB-3934.

Statistical analyses of the raw data were performed as described in Janz et al. (2010) using the free statistic software R (version 2.14.2; *R Development Core Team*, 2012). Only transcripts that had a detection call of “present” (“mas5calls” function with default settings for tau (0.015), alpha1 (0.04) and alpha2 (0.06)) on all replicate chips of at least one condition were used. For annotation of the microarray probe-set, the best gene model from the annotation file of the Aspen Data Base (Tsai et al., 2011) was used. When several probe sets represented one gene, the mean value of the  $\log_2$ -expression data was used for further analysis. The  $\log_2$ -expression values  $x_i$  for each gene  $i$  of interest were normalized using z-transformation resulting in  $x_i'$ :

$$x_i' = \frac{x_i - \bar{x}}{s} \text{ with}$$

$\bar{x}$ : arithmetic mean value of all  $\log_2$ -expression data for one gene,

$s$ : standard deviation of all  $\log_2$ -expression data for one gene.

A heatmap of normalized expression values (“heatmap.2” function) was created using the R package “gplots” (Warnes, 2012).



Here, the members of the putative PHT families 1, 2, 3, and 4 (according to *Guo et al.*, 2008; *Rausch and Bucher*, 2002) were retrieved as genes of interest. To obtain the gene IDs and protein sequences for all putative poplar PHT genes, BlastP searches in the database Phytozome v9.1 (*Goodstein et al.*, 2012) were conducted. The genome of *Arabidopsis thaliana* (*Lamesch et al.*, 2012, [https://phytozome.jgi.doe.gov/pz/portal.html#!info?alias=Org\\_Athaliana](https://phytozome.jgi.doe.gov/pz/portal.html#!info?alias=Org_Athaliana)) was searched with the keyword “pht” extracting the amino acid sequences of eighteen annotated PHT genes. These sequences were used for a BlastP search (e-value cutoff at e-20) against the *Arabidopsis* genome. The Pfam database was used to identify proteins with functional domains (*Finn et al.*, 2014). Additional genes found by the BlastP search with the same domains (Mito\_carr, MFS\_1, Sugar\_tr, Pfam-B\_703, PHO4) that are present in the annotated proteins were added to the gene list. These protein sequences were used for BlastP searches against the *Populus trichocarpa* (*Tuskan et al.*, 2006), the *Oryza sativa* (*Ouyang et al.*, 2007, [https://phytozome.jgi.doe.gov/pz/portal.html#!info?alias=Org\\_Osativa](https://phytozome.jgi.doe.gov/pz/portal.html#!info?alias=Org_Osativa)) and the *Zea mays* genomes (*Schnable et al.*, 2009, [https://phytozome.jgi.doe.gov/pz/portal.html#!info?alias=Org\\_Zmays](https://phytozome.jgi.doe.gov/pz/portal.html#!info?alias=Org_Zmays)). When the resulting proteins had similar domains as *Arabidopsis* PHTs, they were used for a second BlastP against the respective genome. The resulting sequences were added to the list when the protein domains were similar to the PHT Pfam domains or when the best BlastP hit against the *Arabidopsis* genome was a PHT.

The alignment was created with ClustalW2 on the EMBL-EBI webpages (*Larkin et al.*, 2007, <http://www.ebi.ac.uk/Tools/msa/clustalw2/>) with default settings and the PHYLIP package (*Felsenstein*, 1993) was used to calculate a consensus (extended majority rule) neighbor joining phylogenetic tree using 500 replicates for bootstrapping and Jones-Taylor-Thornton model for computing distance matrices. The phylogenetic tree was displayed with MEGA6 (*Tamura et al.*, 2013, <http://www.megasoftware.net>). Based on the phylogeny, the poplar PHT2 to PHT4 genes were named. Gene IDs of the members of all putative PHTs were compiled in additional Table S3.1. The 1 kb upstream region of each poplar gene coding for a putative phosphate transporter was obtained from Phytozome using the BioMart tool on the Phytozome webpage (<https://phytozome.jgi.doe.gov/biomart/martview>) and used for a motif search with PLACE (*Higo et al.*, 1999).

### 3.2.9 Quantitative Real Time PCR of P transporter genes

RNA samples from the same samples that had been used for microarray analyses (200 ng  $\mu\text{L}^{-1}$  in 25  $\mu\text{L}$ ) were treated with Ambion® Turbo DNA-free™ kit (Life Technologies, Carlsbad, CA, USA) two times according to the manual instructions and transcribed to cDNA (0.5  $\mu\text{g}$ ) with the RevertAid First Strand cDNA Synthesis Kit and First Strand cDNA Synthesis Kit (Thermo Fisher Scientific, Braunschweig, Germany) using oligo(dT)-primers. For each gene, at least two technical replicates and three biological replicates were analyzed by quantitative Real Time PCR (qRT PCR) with a LightCycler 480® (Roche Diagnostics, Mannheim, Germany). The reaction volume (20  $\mu\text{L}$ ) consisted of 10  $\mu\text{L}$  SYBR Green I Master kit (Roche Diagnostics, Mannheim, Germany), 2  $\mu\text{L}$  of the forward and reverse primers (10  $\mu\text{M}$ , additional Table S3.2 for detailed information), 1  $\mu\text{L}$  nucleic free water and 5  $\mu\text{L}$  cDNA-solution (1:10 dilution). After pre-incubation (95°C, 5 min), 45 or 55 cycles of amplification followed: 95°C for 10 s, 57°C (55°C for *PtPHT1*;2) for 10 s and 72°C for 20 s. Melting curve (95°C for 5 s, 65°C for 1 min, then to 97°C at a rate of 0.11°C s<sup>-1</sup>) analyses implemented in the LightCycler 480® software were used to assess primer specificity.

To calculate primer efficiency, raw data were converted using LC480 conversion (version 2014.1; [www.hartfaalcentrum.nl/index.php?main=files&sub=LC480Conversion](http://www.hartfaalcentrum.nl/index.php?main=files&sub=LC480Conversion)) and loaded into LinRegPCR (version 2016.0; *Ruijter et al.*, 2009). The mean efficiency for each primer pair was calculated over all samples per gene after baseline subtraction. Cq-values were calculated using the fluorescence threshold of 3.597. Relative expression values for each sample were calculated against two reference genes (Potri.001G309500 [Actin], Potri.001G047200 [PPR-repeat gene]):

$$\text{Relative Expression} = \frac{\sqrt{E_{(\text{Ref}_1)}^{\text{Cq}} \times E_{(\text{Ref}_2)}^{\text{Cq}}}}{E_{(\text{GOI})}^{\text{Cq}}}$$

E: efficiency of primer for gene

Cq: quantification cycle value of sample for gene

(GOI): gene of interest

(Ref<sub>i</sub>): reference gene i (*Hellemans et al.*, 2007).

### 3.2.10 Statistical analyses

R (versions 2.14.2 and 3.0.2; *R Development Core Team*, 2012) was used for all statistical analyses. Mean value  $\pm$  standard error were calculated. One- or Two-Way-ANOVA and Tukey's HSD were performed on original or transformed data. Residuals were tested visually for normal distribution and homogeneity of variance. Data were transformed logarithmically ( $\log_2$ ) or by square root, if needed. For statistical comparisons of single kinetic parameters, Welsh's *t*-test was performed using the output data of the models. For percentage data on  $^{33}\text{P}$  recovery and P allocation, a general linear model with binomial distribution was fitted on underlying count data, and an analysis of deviance was used to calculate significant factor and interaction effects. A subsequent Tukey test was performed to determine the homogenous subsets. Means were considered to differ significantly between treatments, if  $p \leq 0.05$ . Differences between treatments are shown in the figures with different letters. The *p*-values calculated for gene expression data and  $v_{\max}$  for kinetic data were adjusted by Bonferroni correction. Two-Way-Repeated measurement-ANOVA with Tukey's HSD was performed for plant growth over time.

## 3.3 Results

### 3.3.1 Plant performance, P uptake and allocation in response to P deficiency

Pre-tests with five concentrations from 0.064 to 641  $\mu\text{M PO}_4^{3-}$  (further on called P) in the nutrient solution revealed a growth gradient for poplars with a strong decline in plant height and biomass between P concentration of 64 and 6.4  $\mu\text{M P}$  (additional Figure S3.1). We selected 641 (HP), 6.4 (MP) and 0.064 (LP)  $\mu\text{M P}$  in the nutrient solution for further studies because these concentrations resulted in high, intermediate and almost no growth during long-term cultivation (Figure 3.1a) and because the highest P concentration is the typical P supply in nutrient solution (*Müller et al.*, 2013), intermediate P is in the same range typically present in soil solutions and the lowest P concentration abolished growth entirely (Figure 3.1a). In comparison with HP plants,

biomass production of MP and LP poplars was significantly inhibited (Figure 3.1b, additional Figure S3.1).

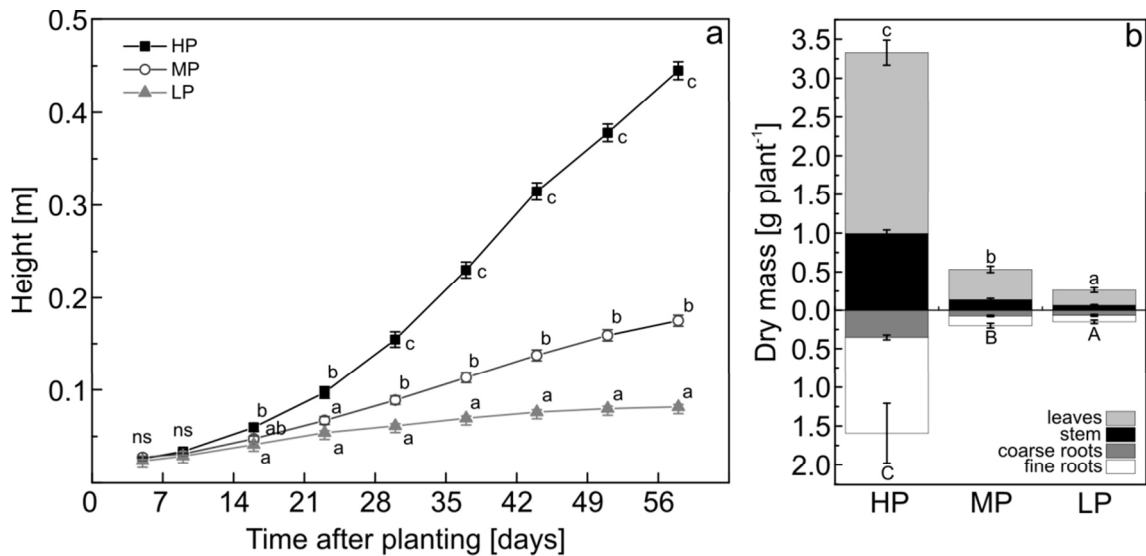


**Figure 3.1. Growth characteristics of P deficient poplar.** a) Height of poplar plants grown with high (HP: 641  $\mu\text{M}$ ), medium (MP: 6.4  $\mu\text{M}$ ) or low (LP: 0.064  $\mu\text{M}$ ) phosphate concentrations in the nutrient solution. Different letters indicate significant differences between treatments at each measuring day ( $p \leq 0.05$ , 2-Way-repeated measurement-ANOVA and Tukey's honest significance test,  $n=11-12$ , mean $\pm$ SE, ns: not significant). b) Dry mass of poplar tissues after 60 days of growth with HP, MP or LP phosphate in the nutrient solution. Different letters indicate significant differences between treatments in above- and belowground tissues ( $p \leq 0.05$ , ANOVA and Tukey's honest significance test,  $n=5$ , mean $\pm$ SE).

HP plants exhibited the highest P concentrations, MP plants intermediate and LP plants the lowest P concentrations in all tissues (Table 3.1). Because our nutrient regime also resulted in growth decline, the whole-plant P content was about 30 times higher in HP plants than in MP and 50 times higher in HP compared with LP plants (Table 3.1). The relative allocation of P in above- to belowground material was significantly affected by P starvation with a higher fraction of P belowground after MP (about 50 %) and LP (43 %) than after HP treatments (37 %,  $p \leq 0.05$ ). Exposure of HP, MP, and LP plants to  $^{33}\text{P}$  in the nutrient solution showed the highest relative uptake for the MP plants. Within two days, they acquired 25 % of the P in the labeling solution, while HP plants took up about 15 % and LP only 2.5 % of the new P (Table 3.1). It was notable that highest P

recovery of MP and LP plants was found in roots, whereas that of HP plants was more evenly distributed between roots and leaves (Table 3.1).

The differences in distribution of the newly taken up  $^{33}\text{P}$  were also qualitatively confirmed by whole plant imaging (Figure 3.2). While HP plants showed an almost even distribution across all tissues, MP plants showed a very high  $^{33}\text{P}$  concentration in the uppermost leaf and nearly no newly taken up P in the oldest leaves (Figure 3.2). LP showed very little to no  $^{33}\text{P}$  uptake in older leaves and the main aboveground allocation to the youngest leaf, while root uptake was high. All plants showed strong accumulation of  $^{33}\text{P}$  in the roots, especially in parts adjacent to the root-stem junction (Figure 3.2). Because of the different P concentrations in the nutrient solutions the calculated total P uptake (taking into account different dilution factors for  $^{33}\text{P}$  as detailed under materials and methods) corresponded to 95.7 nmol in HP plants, 1.63 in MP and  $1.94 \times 10^{-3}$  nmol in LP plants (Table 3.1). The P use efficiency was highest in LP plants ( $1.8 \pm 0.14$  g dry mass  $\text{mg}^{-1}$  P), intermediate in MP plants ( $1.0 \pm 0.10$  g dry mass  $\text{mg}^{-1}$  P) and least in HP plants ( $0.14 \pm 0.01$  g dry mass  $\text{mg}^{-1}$  P with  $p_{(\text{treatment})} \leq 0.05$ ).

**Table 3.1: In planta P and P uptake characteristics of P deficient poplar.**

		total P concentration [mg g <sup>-1</sup> ]	total P content [mg fraction <sup>-1</sup> ]	<sup>33</sup> P recovery [% fraction <sup>-1</sup> ]	P uptake [nmol fraction <sup>-1</sup> ]
HP	Leaf	6.80 ± 0.51 <sup>de</sup>	8.55 ± 0.33 <sup>e</sup>	6.79 ± 0.29 <sup>j</sup>	43.4 ± 1.82 <sup>g</sup>
	Stem	4.92 ± 0.55 <sup>d</sup>	2.56 ± 0.20 <sup>d</sup>	1.35 ± 0.15 <sup>e</sup>	8.64 ± 0.96 <sup>f</sup>
	Fine Root	11.27 ± 1.40 <sup>e</sup>	4.79 ± 1.49 <sup>de</sup>	5.79 ± 0.97 <sup>i</sup>	37.01 ± 6.20 <sup>g</sup>
	Coarse Root	6.98 ± 1.41 <sup>de</sup>	1.92 ± 0.32 <sup>d</sup>	1.04 ± 0.10 <sup>d</sup>	6.65 ± 0.65 <sup>f</sup>
MP	Leaf	1.25 ± 0.10 <sup>c</sup>	0.19 ± 0.03 <sup>bc</sup>	4.51 ± 0.38 <sup>h</sup>	0.29 ± 0.02 <sup>d</sup>
	Stem	1.11 ± 0.11 <sup>bc</sup>	0.11 ± 0.02 <sup>abc</sup>	7.22 ± 0.79 <sup>k</sup>	0.46 ± 0.05 <sup>de</sup>
	Fine Root	0.67 ± 0.12 <sup>abc</sup>	0.08 ± 0.02 <sup>ab</sup>	10.07 ± 0.69 <sup>l</sup>	0.64 ± 0.04 <sup>e</sup>
	Coarse Root	1.03 ± 0.15 <sup>bc</sup>	0.23 ± 0.03 <sup>c</sup>	3.73 ± 0.79 <sup>g</sup>	0.24 ± 0.05 <sup>d</sup>
LP	Leaf	0.69 ± 0.03 <sup>abc</sup>	0.15 ± 0.03 <sup>bc</sup>	0.08 ± 0.02 <sup>a</sup>	0.059 × 10 <sup>-3</sup> ± 0.001 × 10 <sup>-3 a</sup>
	Stem	0.62 ± 0.17 <sup>ab</sup>	0.05 ± 0.02 <sup>a</sup>	0.12 ± 0.03 <sup>b</sup>	0.088 × 10 <sup>-3</sup> ± 0.003 × 10 <sup>-3 a</sup>
	Fine Root	0.41 ± 0.10 <sup>a</sup>	0.05 ± 0.01 <sup>a</sup>	1.94 ± 0.47 <sup>f</sup>	1.48 × 10 <sup>-3</sup> ± 0.35 × 10 <sup>-3 c</sup>
	Coarse Root	0.49 ± 0.03 <sup>ab</sup>	0.10 ± 0.01 <sup>abc</sup>	0.41 ± 0.19 <sup>c</sup>	0.32 × 10 <sup>-3</sup> ± 0.15 × 10 <sup>-3 b</sup>
<i>p</i> -value	<i>p</i> <sub>(treatment)</sub>	< 0.001	< 0.001	< 0.001	< 0.001
<i>p</i> -value	<i>p</i> <sub>(fraction)</sub>	0.225	< 0.001	< 0.001	< 0.001
<i>p</i> -value	<i>p</i> <sub>(treatment×fraction)</sub>	< 0.01	< 0.001	< 0.001	< 0.001
HP	whole plant	7.10 ± 0.58 <sup>C</sup>	17.82 ± 1.38 <sup>C</sup>	14.98 ± 1.36 <sup>B</sup>	95.69 ± 8.71 <sup>C</sup>
MP	whole plant	1.03 ± 0.11 <sup>B</sup>	0.61 ± 0.05 <sup>B</sup>	25.52 ± 1.84 <sup>C</sup>	1.63 ± 0.12 <sup>B</sup>
LP	whole plant	0.56 ± 0.04 <sup>A</sup>	0.34 ± 0.06 <sup>A</sup>	2.55 ± 0.64 <sup>A</sup>	1.94 × 10 <sup>-3</sup> ± 0.49 × 10 <sup>-3 A</sup>
<i>p</i> -value		< 0.001	< 0.001	< 0.001	< 0.001

Total P concentration and total P content per dry mass, <sup>33</sup>P recovery and calculated uptake of P after 2 days in tissues of and whole poplar plants grown with one of three different P concentrations in the nutrient solution in sand (HP: 641 μM, MP: 6.4 μM, LP: 0.064 μM). Different letters indicate significant differences ( $p \leq 0.05$ , Two-Way-ANOVA and Tukey's honest significance test, mean ± SE,  $n=4-5$ ).

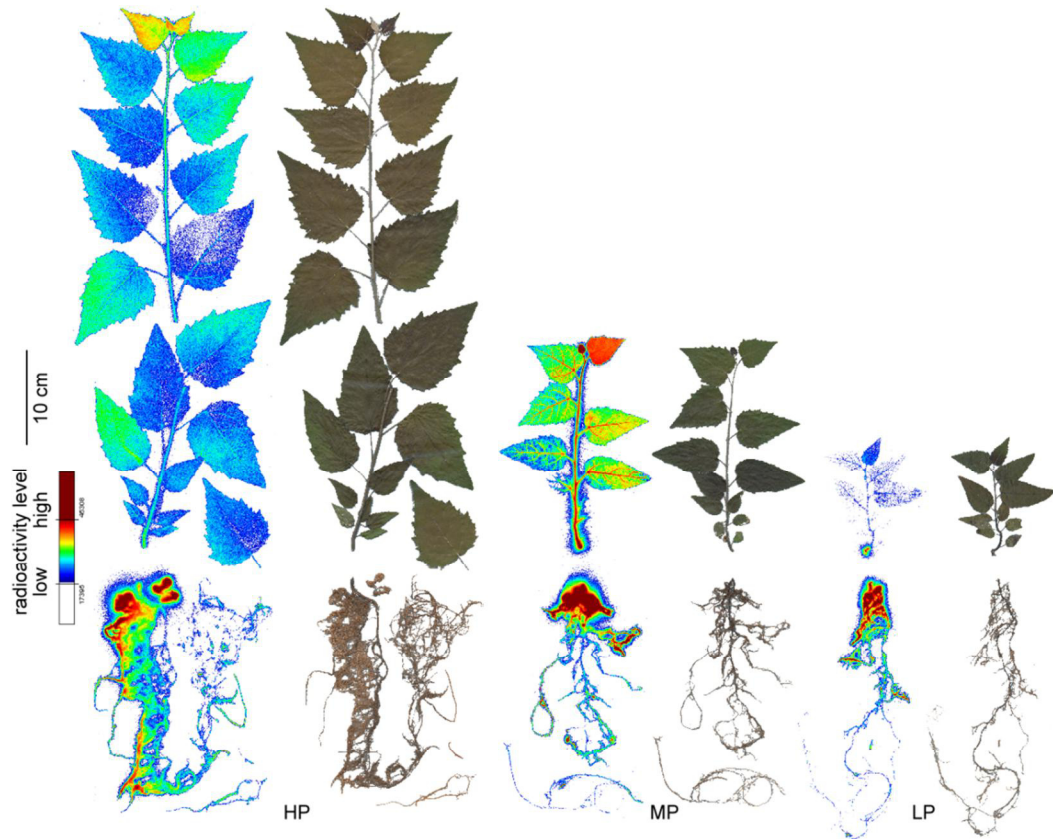


**Figure 3.2.**  $^{33}\text{P}$  allocation in P deficient poplar. Autoradiographs of the  $^{33}\text{P}$  distribution in poplars grown with different P concentrations in the nutrient solution (HP: 641  $\mu\text{M}$ , MP: 6.4  $\mu\text{M}$ , LP: 0.064  $\mu\text{M}$ ) and scans of the corresponding plants. Autoradiographs were taken of whole plants 2 days after exposure to  $^{33}\text{P}$  as described under materials and methods. Uptake intensity is indicated by false color images with red indicating high and blue low radioactivity.

### 3.3.2 P uptake is not energy limited

Because LP plants showed lower relative P uptake than MP or HP plants, we tested whether P uptake was inhibited by energy depletion. For this purpose, the growth medium was supplemented with glucose before adding the  $^{33}\text{P}$ -labeled nutrient solution. There was no difference in P uptake between the glucose-fed and the non-fed control plants. As before, MP plants showed the highest, HP intermediate and LP plants the lowest P recovery (Figure 3.3a), but the overall levels were lower because we used only 14 h exposure time instead of 48 h to avoid confounding effects of microbial growth. The soluble carbohydrate concentrations in fine roots were unaffected by glucose treatment (Figure 3.3b). The concentration of soluble carbohydrates was about 4-fold higher in the fine roots of P-depleted poplars (MP, LP) than in HP plants (Figure 3.3b).

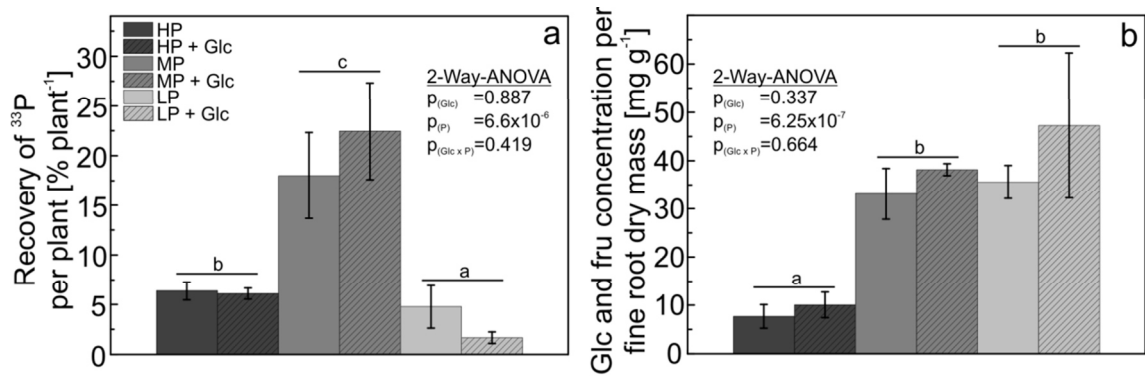


**Figure 3.3.  $^{33}\text{P}$  uptake and carbohydrate concentrations in P deficient poplar supplied with glucose in the nutrient solution.** a) The recovery of  $^{33}\text{P}$  in whole plants relative to the total amount of  $^{33}\text{P}$  added to the nutrient solution. b) Soluble carbohydrate concentrations as the sum of fructose and glucose in roots of poplars. The plants were grown with three different phosphate concentrations in the nutrient solutions (HP: 641  $\mu\text{M}$ , MP: 6.4  $\mu\text{M}$ , LP: 0.064  $\mu\text{M}$ ) that were supplemented with 400 mM glucose for 2 h before adding 1 mL  $^{33}\text{P}$  labeled nutrient solution. Controls received no glucose. Different letters indicate significant differences between treatments ( $p \leq 0.05$ , Two-Way-ANOVA and Tukey's honest significance test,  $n=5$ , mean  $\pm$  SE).

### 3.3.3 Low P concentrations in the nutrient solution limit P uptake

To investigate plant acclimation to decreasing P availabilities in the nutrient solution, P uptake kinetics of HP, MP, and LP plants were determined. The modeled Michaelis-Menten-curves for the P uptake of LP and MP plants showed a steep increase of the P uptake rate at low P concentrations in the nutrient solution and leveled off to different maximum uptake rates (Figure 3.4, Table 3.2). The highest P uptake rate was found in MP plants and was similar to that of the LP plants (Table 3.2). The maximum P uptake rate was more than 13 times higher in LP plants than in the HP plants (Table 3.2, Figure 3.4). The  $K_m$  was 25.9 ( $\pm 9.9$ )  $\mu\text{M}$  in the MP and 19.9 ( $\pm 8.1$ )  $\mu\text{M}$  in the LP plants. The minimum concentration  $C_{\min}$ , at which net uptake took place, was reached at 1.1  $\mu\text{M}$  (Figure 3.4, insert) and was similar for LP and MP poplars. HP plants exhibited very slow P uptake kinetics and therefore determination of  $K_m$  and  $C_{\min}$  was not possible under our experimental conditions, where the maximum P concentration tested was 200  $\mu\text{M}$ .



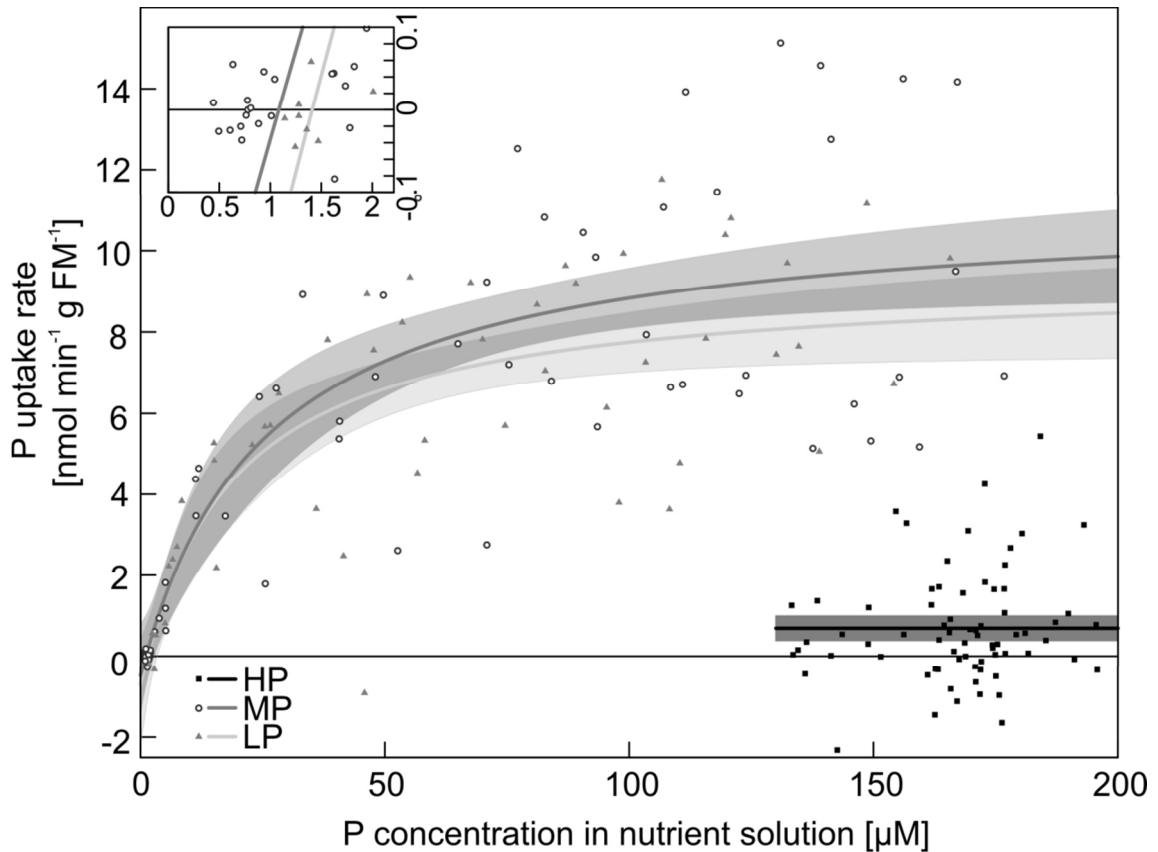


**Figure 3.4. Model of kinetic parameters for P uptake of P deficient poplars at different P concentrations.** P uptake rate per gram of fine root mass of plants grown with different P concentrations in the nutrient solution (black squares: HP, 641  $\mu\text{M}$ ; open circles: MP, 6.4  $\mu\text{M}$ ; grey triangles: LP, 0.064  $\mu\text{M}$ ) during exposure to different P concentrations. Data points from six different plants per treatment. Modeled curves (HP: black, MP: dark grey, LP: light grey) with parameters from Table 3.2 and 95%-prediction interval in grey. The insert shows an enlargement of the curves at intermediate and low P concentrations around the concentration of  $C_{\min}$ .

**Table 3.2: Kinetic parameters for P uptake of P deficient poplar.**

	HP	MP	LP
$v_{\max}$ [ $\text{nmol min}^{-1} \text{g}^{-1}$ ]	0.689 ( $\pm 0.164$ ) <sup>a</sup>	11.140 ( $\pm 1.065$ ) <sup>b</sup>	9.311 ( $\pm 0.908$ ) <sup>b</sup>
$K_m$ [ $\mu\text{M}$ ]	n.d.	25.87 ( $\pm 9.87$ ) <sup>ns</sup>	19.85 ( $\pm 8.11$ ) <sup>ns</sup>
$C_{\min}$ [ $\mu\text{M}$ ]	n.d.	1.08 ( $\pm 0.91$ ) <sup>ns</sup>	1.41 ( $\pm 1.19$ ) <sup>ns</sup>

Kinetic parameters (estimate  $\pm$  standard error) for the uptake of P in plants grown with one of three different P concentrations in the nutrient solution in sand (HP: 641  $\mu\text{M}$ , MP: 6.4  $\mu\text{M}$ , LP: 0.064  $\mu\text{M}$ ). Model calculated with data from 6 different plants per treatment. Different letters in rows indicate significant differences at  $p \leq 0.05$ .  $v_{\max}$ : maximum uptake rate,  $K_m$ : Michaelis-Menten constant,  $C_{\min}$ : minimal concentration needed for uptake, n.d.: not determined

### 3.3.4 Low P availabilities lead to differential regulation of P transporters

As the pre-requisite to analyze the response of poplar P transporters from different families, we annotated all putative PHTs in the poplar genome based on homology searches using *Arabidopsis*, rice and maize (additional Figure S3.2, Table S3.1). We found a total of 36 genes in poplar belonging to 4 different clades, of which 31 had probe sets on Affymetrix microarrays. Among those genes, 21 were expressed in roots and leaves (Figure 3.5a, additional Table S3.1, Table S3.3). We selected four genes for validation of their expression in different tissues and in response to different P supply (Figure 3.5b) and found a strong correlation between qRT PCR and microarray data (additional Figure S3.3).

The expression pattern of the 21 PHT genes clearly distinguished roots and leaves (Figure 3.5a). *PtPHT1;1*, *PtPHT1;2*, *PtPHT1;4*, *PtPHT1;7*, *PtPHT1;9*, *PtPHT1;12*, *PtPHT3;1*, *PtPHT3;2*, *PtPHT3;6*, *PtPHT4;6*, *PtPHT4;7* and *PtPHT4;8* exhibited generally higher transcript levels in roots than in leaves (Figure 3.5a). In leaves, the transcript abundances of *PtPHT1;3*, *PtPHT2;1*, *PtPHT2;2*, *PtPHT3;5*, *PtPHT4;1*, *PtPHT4;2*, *PtPHT4;3*, *PtPHT4;4* and *PtPHT4;5* were generally higher than in roots (Figure 3.5a). It was notable that among the putative plasma membrane P transporters only *PtPHT1;3* was higher expressed in leaves than in roots and with almost 10-fold higher transcript abundance than in roots (Figure 3.5b). The expression of *PtPHT1;1* and *PtPHT1;2* was root-specific because we could not detect any signal in leaves with specific primers in the qRT PCR analysis (Figure 3.5b) and on microarrays the measured transcript abundance of these genes in leaves were classified with the expression probability “absent (for the definition, see materials and methods). The putative chloroplastic P transporters (*PtPHT2;1*, *PtPHT2;2*) showed higher expression levels in leaves than in roots.

The transcript levels of most PHTs, which had been classified into the “root” group showed strong responsiveness to P starvation in both tissues, roots and leaves, whereas the PHT members classified into the “leaf” group did not respond to variation in P supply, with few exceptions (*PtPHT1;3*, *PtPHT4;2*, *PtPHT4;5*) (Figure 3.5a). It is also important to note that the PHT members *PtPHT1;4*, *PtPHT1;7*, *PtPHT1;9*, and

*PtPHT3;6* showed the highest transcript abundances in roots under MP and in leaves under LP conditions (Figure 3.5a).

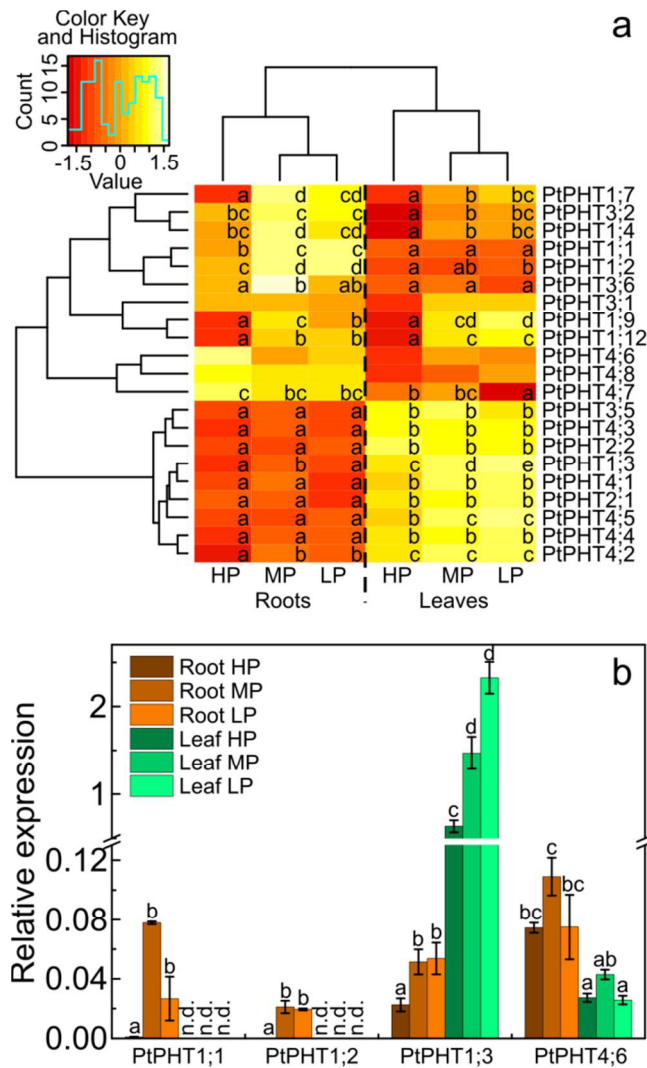


**Figure 3.5. Expression of phosphate transporters in P deficient poplars.** a) Heatmap of the relative expression of putative phosphate transporters in the three uppermost leaves and fine roots of poplar plants grown with different P concentrations in the nutrient solution (HP: 641 μM, MP: 6.4 μM, LP: 0.064 μM). Red colors indicate lower and yellow to white color higher values after z-transformation of the transcript abundances of each gene across all analyzed tissues and P conditions. b) Relative expression of selected *PtPHTs* measured by qRT PCR (mean ± SE). Values were normalized to the expression of two reference genes (Actin, PPR-repeat) in the samples. Different letters indicate significant differences in expression of each gene (adj.  $p \leq 0.05$ , ANOVA and Tukey's honest significance test,  $n=3$ ).

Our annotation of the PHT family members also uncovered P1BS (PHR1 binding sequence) elements, known to be involved in the P response (*Bustos et al.*, 2010) in the upstream regions of the genes (additional Table S3.1). P1BS elements were mainly present in PHT1 promoters (additional Table S3.1). Among the P starvation responsive genes in family 1 *PtPHT1;1*, *PtPHT1;4*, *PtPHT1;7* and *PtPHT1;9* had a P1BS element in the 1 kb promoter region and in family PHT4 it was present in the promoter region of *PtPHT4;5*. However, the P1BS element was not found in the 1 kb upstream region of other P starvation responsive genes of the PHT1, 3 and 4 families: *PtPHT1;2*, *PtPHT1;3*, *PtPHT1;12*, *PtPHT3;2*, *PtPHT3;6* and *PtPHT4;2*, while it was present in *PtPHT3;1*, a gene, which showed no P starvation response under our experimental conditions.

## 3.4 Discussion

### 3.4.1 P uptake and allocation

Here, we characterized the uptake, allocation and PHT expression levels of *Populus × canescens* grown under different P availabilities. Similar as in *P. tremuloides* (*Desai et al.*, 2014), we found that P availabilities below 60  $\mu\text{M}$  resulted in strong reduction in height growth and biomass. These reductions were accompanied by a strong decline in tissue phosphorus concentrations, with the strongest decline in fine roots. The phosphorus concentrations found in leaves and fine roots of MP poplars in our study were similar to those found in conventional poplar plantations, as reported for example by Ge et al. (2015). Poplar plantations are often established on marginal sites and therefore information on the uptake characteristics and allocation in the trees is an essential pre-requisite for sustainable management (*Ge et al.*, 2015). Values indicating sufficient P supply of young *Populus × canescens* leaves range from 1.7 to 2.7  $\text{mg g}^{-1}$  dry mass (*Burg*, 1985). According to these values, the MP and LP poplars in our study suffered from strong and very strong deficiency, whereas the P concentrations in the HP poplars indicate luxurious P supply. Luxurious P concentrations cannot be used for growth and consequently, PUE of *P. × canescens* increased when the P availability declined as was also shown for other poplar species and crops (*Akhtar et al.*, 2007; *Gan et al.*, 2016; *Huang et al.*, 2011). It is further notable that the allocation pattern of newly

taken up P was shifted towards leaves in the MP compared with LP or HP poplars. While usually the young leaves were the predominant aboveground sink, our imaging analyses showed that in MP plants also older leaves exhibited significant uptake of newly acquired P, resulting in an allocation shift. Nevertheless, no measurable newly acquired P was allocated to the oldest leaves. Belowground, the new P was mainly concentrated in those parts of root system that were close to the root-shoot junction, regardless of the P supply. This finding was surprising because under severe P limitation one may have expected preferential allocation of P to growing tissues such as the fine root tips and the shoot apex. The observed P accumulation suggests that the root-shoot junction constitutes an obstacle to P below-aboveground translocation. Studies on heavy metal transport (cadmium, zinc) suggested that the root-shoot junction serves as a control barrier for translocation of those elements into the shoot probably due to changes in the anatomical structure of the xylem at transition from root to shoot xylem (Martinka *et al.*, 2014). The molecular and cellular basis for the supposed control function is unknown and must be addressed in future research. Our data suggest that an improved allocation from roots to the shoot could perhaps contribute to enhance PUE. This suggestion is currently speculative, but worthwhile to be addressed in future studies.

Under P starvation, the poplars showed not only differences in allocation and an increased P use but also higher uptake efficiency than the well-supplied trees, as indicated by the increased recovery of  $^{33}\text{P}$  from the nutrient solution in MP compared with HP plants. While this finding is in agreement with crops and *Arabidopsis* (Bhadoria *et al.*, 2004; Cogliatti and Clarkson, 1983; Dong *et al.*, 1999; Jungk *et al.*, 1990; Lee, 1982), severely P-starved poplars were not able to increase the relative P uptake compared with that of HP plants and even exhibited a significant decline in uptake efficiency. We considered whether energy limitation might have resulted in the reduction of P uptake efficiency. Because phosphorus occurs in the environment often in bound forms, P-starved poplars enhance the production and exudation of organic acids to increase the mobilization of external P (Desai *et al.*, 2014). Consequently, large amounts of photo-assimilates are lost when the plants attempt to counteract P deficiency. Furthermore, P-starved plants accumulate carbohydrates in chloroplasts because the export of the carbon skeletons into the cytosol is inhibited (Hammond and White, 2008). Nevertheless, for some plants an increased carbohydrate translocation to

the roots and even an accumulation in roots was shown under P deprivation (*Hammond and White, 2008*). Also here, an accumulation of carbohydrates in roots of both MP and LP compared with HP plants was found and exposure to additional glucose could not stimulate P uptake under any of the tested P concentrations in the growth medium. It is known that glucose is taken up by plants from the medium via monosaccharide transporters (*Yamada et al., 2011*) into the cytoplasm of root cells, i.e., the same compartment into which sugars from source tissues are unloaded (*Lemoine et al., 2013*). Therefore, the availability of sugar taken up from the medium does not differ from plant-derived sugar and thus, we could exclude energy limitation as the reason for the decrease in  $^{33}\text{P}$ -recovery of severely P-stressed poplars.

P uptake is further governed by the kinetic properties of the uptake systems. We found a threshold concentration of 1  $\mu\text{M}$  in the medium required for net P uptake. One reason for such a threshold could be the efflux of newly acquired  $^{33}\text{P}$  from the roots back into the medium at very low external P concentrations because of the steep concentration gradient. Another reason could be that the ratio of the monovalent form of P ( $\text{H}_2\text{PO}_4^-$ ), which is taken up by plants (*Schachtman et al., 1998*), was shifted to the acid form at the membrane due to an excess of protons under very low external P concentrations (*Poirier and Bucher, 2002*) and then was not available for plant uptake.

Here, we showed that the  $K_m$  for P uptake of the root system of MP poplars did not decrease significantly when the phosphate concentration in the nutrient solution was further decreased.. This finding suggests that the uptake systems operate at their limits under these conditions. *Desai et al. (2014)* found a similar  $K_m$  value of about 30  $\mu\text{M}$  for P accumulation in *P. tremuloides* across a range of low P concentrations. The apparent  $K_m$  values for P uptake of P-starved poplars are, however, higher than phosphate concentrations in soil solutions in many non-fertilized ecosystems, for instance 5  $\mu\text{M}$  in forests beneath the organic layer (*Asano et al., 2006; Fitzhugh et al., 2001; Ranger et al., 2001; van Hees et al., 2003*). These soil concentrations are too low for sufficient P nutrition and the up-regulation of uptake systems would only ensure net uptake that occurred above the threshold concentration of 1  $\mu\text{M}$  P. Thus, neither decreases in  $K_m$  values nor increases in  $v_{\text{max}}$  by up-regulation of phosphate transporters would be sufficient to combat P deficiency in natural environments (*Lambers et al., 2006*). Under field conditions poplar roots are colonized by mycorrhizal fungi with different abilities for P acquisition (*Baum and Makeschin, 2000; Danielsen et al., 2013, 2012; Gehring et*

*al.*, 2006; *Seven and Polle*, 2014). Mycorrhizal roots usually show lower  $K_m$  values for P uptake (*Cress et al.*, 1979; *Van Tichelen and Colpaert*, 2000) and higher tissue P concentrations than non-mycorrhizal roots (*Danielsen and Polle*, 2014). In poplar the reduction in  $K_m$  of P accumulation after colonization with the mycorrhizal fungus *Laccaria bicolor* was moderate (about 6  $\mu\text{M}$  instead of 30  $\mu\text{M}$  (*Desai et al.*, 2014)). In *Pinus sylvestris*, mycorrhizal colonization decreased not only the  $K_m$  from 12.1  $\mu\text{M}$  to 3.5  $\mu\text{M}$ , but also the minimum threshold concentration for net P uptake of 2  $\mu\text{M}$  to 0.2  $\mu\text{M}$  (*Van Tichelen and Colpaert*, 2000). Altogether, these findings underpin that without the help of microbes, P nutrition of poplars is critical in nature and may often fall below the threshold for net uptake.

### **3.4.2 Regulation of the poplar PHT families in response to P starvation**

P uptake and intracellular distribution is achieved by four P transporter families, with different number of genes in different plant species. Our *in silico* annotation of the PHTs of poplars showed that the PHT1 family was the largest with 12 members, followed by PHT4 with 9 members, while PHT3 and PHT2 contained 6 and 2 members respectively. These findings demonstrate that not only poplar PHT1 (*Loth-Pereda et al.*, 2011), but also the other families exhibit an expansion compared to *Arabidopsis* (*Guo et al.*, 2008; *Poirier and Bucher*, 2002). The PHT2, PHT3 and PHT4 families contain organelle membrane located transporters, which assure together photosynthetic and respiration processes (*López-Arredondo et al.*, 2014). The presence of the putative P responsive element P1BS in the 1 kb upstream region was confirmed for PHT1 family members and was further demonstrated for some members of the PHT3 and PHT4 families, but was unrelated to P starvation responsiveness as reports previously for the poplar PHT1 (*Loth-Pereda et al.*, 2011).

Here, the putative chloroplastic P transporters *PtPHT2;1* and *PtPHT2;2* exhibited low transcript abundance in roots and high in leaves, but were not responsive to P starvation. Similar results have been reported for the only member *AtPHT2;1* in *Arabidopsis* (*Versaw and Harrison*, 2002) suggesting that the functional properties have been maintained. The results for the mitochondrial PHTs are more divergent because *AtPHT3;1* was unresponsive to P starvation, whereas its homologs in poplar (*PtPHT3;1* and *PtPHT3;2*) showed increased transcript levels (this study; *Morcuende et al.*, 2007).

Poplar *PtPHT3;5*, an ortholog to the mitochondrial *Arabidopsis AtPHT3;3* was unresponsive to P deprivation in both plant species (this study; *Morcuende et al.*, 2007). The PHT4 family showed an interesting clustering with *PtPHT4;6*, *PtPHT4;7* and *PtPHT4;8*, the orthologs of *AtPHT4;6*, *AtPHT4;2* and *AtPHT4;3*, respectively, exhibiting higher transcript levels in roots than in leaves, and higher transcript abundances in leaves than in roots for *PtPHT4;1*, *PtPHT4;2*, *PtPHT4;3*, *PtPHT4;4* and *PtPHT4;5*, which are the orthologs to *AtPHT4;1*, *AtPHT4;4* and *AtPHT4;5*. An expression pattern similar to that in poplar was reported for *Arabidopsis* with higher transcript levels in roots for *AtPHT4;6*, and *AtPHT4;2* and higher levels in leaves for *AtPHT4;1*, *AtPHT4;4* and *AtPHT4;5* (*Guo et al.*, 2008). The latter transporters were localized to chloroplasts, while *AtPHT4;6* was localized in the Golgi membrane (*Guo et al.*, 2008). In poplar, the members of PHT4 were not or only little regulated by P starvation. Still, they have important function for intracellular trafficking of P. For example, deletion of the Golgi-membrane localized *AtPHT4;6* leads to severe growth impairment and symptoms of P starvation, despite normal tissue P concentrations (*Hassler et al.*, 2012). Altogether, similar tissue-specific expression pattern and P responsiveness of many organelle-related P transporters suggest that their functions are conserved in *Arabidopsis* and poplar.

The members of PHT1 family are localized to the plasma membrane and catalyze P uptake from the soil and long distance transport in plants (*Nussaume et al.*, 2011; *Poirier and Bucher*, 2002; *Poirier and Jung*, 2015). Each of the nine *Arabidopsis* and all analyzed poplar PHT1 members show increased transcript abundance after exposure to low P supply (this study; *Loth-Pereda et al.*, 2011; *Morcuende et al.*, 2007), although some genotype-related exception were found (*Loth-Pereda et al.*, 2011). While three of the nine *Arabidopsis* PHT1 genes (*AtPHT1;3*, *AtPHT1;5*, *AtPHT1;6*) exhibited higher expression in leaves than in roots (*Morcuende et al.*, 2007), in poplar, only *PtPHT1;3* showed this pattern. *PtPHT1;3* was phylogenetically related to *AtPHT1;4* and *AtPHT1;7*, but showed a higher distance to these *Arabidopsis* genes than the poplar genes *PtPHT1;4*, *PtPHT1;5* and *PtPHT1;7*. This observation suggests that *PtPHT1;3* may have evolved more rapidly and already acquired additional functions compared to the *Arabidopsis* genes.

The expression patterns of poplar *PtPHT1;9* and *PtPHT1;12* were similar in roots and in leaves with activation in response to P deficiency. Their orthologs in *Arabidopsis*



(*AtPHT1;9* and *AtPHT1;8* for *PtPHT1;9*) mediated high-affinity P uptake in roots (Remy *et al.*, 2012) and *AtPHT1;5* (for *PtPHT1;12*) was located in the vascular system (Mudge *et al.*, 2002) suggesting important roles for uptake and long-distance transport under P starvation. The expression of these transporters was most strongly stimulated by P deficiency in *P. trichocarpa* (Loth-Pereda *et al.*, 2011). In contrast to those results, we found the strongest responsiveness to P starvation for *PtPHT1;1*, *PtPHT1;2*, *PtPHT1;12* and *PtPHT1;7*, which underline genotype-related differences in the expression patterns. In *Arabidopsis*, *AtPHT1;1* and *AtPHT1;4*, orthologs to those poplar genes, are expressed in the epidermal layer of roots and mediate high-affinity root uptake (Misson *et al.*, 2004; Mudge *et al.*, 2002; Shin *et al.*, 2004). The pre-dominant expression of those poplar transporters in roots and their strong root-specific up-regulation upon P limitation, suggests that these functions are conserved in *P. × canescens* and *Arabidopsis thaliana*.

### 3.4.3 Conclusions

Here, we annotated the four PHT families in poplar and demonstrated tissue-specific expression patterns in response to P starvation. P transporters that were higher expressed in young leaves than in fine roots belonged to the organelle-related families and showed no response to P starvation, with the exception of *PtPHT1;3*. The transcript abundance of the latter transporter in leaves was high under high P supply, but further increased massively under P starvation suggesting an important role of this gene for foliar P supply in accordance with highest allocations to the youngest leaves. Other members of the PHT1 family also showed strong up-regulation in response to P starvation, but were generally higher expressed in roots than in leaves underpinning their role in P uptake from the environment. The root-specific increment in *PtPHT1;1* and *PtPHT1;2* expression suggests a major role for these transporters in combating P deficiency in poplar. In accordance with the enhanced expression of PHT members in roots, P uptake efficiency was enhanced at the intermediate P level which represents a concentration that can occur in soil solution. Furthermore, P starved poplars showed the highest allocation of newly acquired P to fine roots, suggesting that these organs were preferentially supplied with P to maintain their physiological activities.

We found that the threshold for net P uptake was about 1  $\mu\text{M}$  and the apparent  $K_m$  for the whole-root system about 26  $\mu\text{M}$ . These findings indicate that under low P availabilities, which occur often in soil solutions, bare-rooted poplars are prone to suffer from P limitations. Mycorrhizal colonization of the roots can increase net P uptake (Casieri *et al.*, 2013), but which fungal species are the most useful to combat P deficiency is an open question, which needs to be addressed for sustainable poplar plantation management.

### **3.5 Acknowledgements**

We are grateful to Gabriele Lehmann, Bernd Kopka, Thomas Klein (Labor für Radioisotope, LARI, Georg-August Universität Göttingen), and Christine Kettner for expert technical assistance. We thank Dennis Janz for introducing statistical and microarray analyses in R to MK.

The Georg-August University of Göttingen funded the PhD position of MK. The Deutsche Forschungsgemeinschaft (DFG), Priority Program SPP 1685 “Ecosystem Nutrition” provided financial support for this research project under grant number Po362/22-2. The publication fund of the University of Göttingen and the Deutsche Forschungsgemeinschaft supported open access publication of this article. The funders had no role in the design of the study, the collection, analysis, and interpretation of data and in writing the manuscript.

### 3.6 References

- Ai, P., Sun, S., Zhao, J., Fan, X., Xin, W., Guo, Q., Yu, L., Shen, Q., Wu, P., Miller, A.J., Xu, G.* (2009): Two rice phosphate transporters, OsPht1;2 and OsPht1;6, have different functions and kinetic properties in uptake and translocation. *Plant J.* 57, 798–809.
- Akhtar, M.S., Oki, Y., Adachi, T., Murata, Y., Khan, M.H.R.* (2007): Relative phosphorus utilization efficiency, growth response, and phosphorus uptake kinetics of *Brassica* cultivars under a phosphorus stress environment. *Commun. Soil Sci. Plant Anal.* 38, 1061–1085.
- Asano, Y., Compton, J.E., Church, M.R.* (2006): Hydrologic flowpaths influence inorganic and organic nutrient leaching in a forest soil. *Biogeochemistry* 81, 191–204.
- Baker, A., Ceasar, S.A., Palmer, A.J., Paterson, J.B., Qi, W., Muench, S.P., Baldwin, S.A.* (2015): Replace, reuse, recycle: improving the sustainable use of phosphorus by plants. *J. Exp. Bot.* 66, 3523–3540.
- Baum, C., Makeschin, F.* (2000): Effects of nitrogen and phosphorus fertilization on mycorrhizal formation of two poplar clones (*Populus trichocarpa* and *P. tremula* x *tremuloides*). *J. Plant Nutr. Soil Sci.* 163, 491–497.
- Bhadoria, P.S., Dessougi, H.E., Liebersbach, H., Claassen, N.* (2004): Phosphorus uptake kinetics, size of root system and growth of maize and groundnut in solution culture. *Plant Soil* 262, 327–336.
- Bielecki, R.L.* (1973): Phosphate pools, phosphate transport, and phosphate availability. *Annu. Rev. Plant Physiol.* 24, 225–252.
- Bolker, B.* (2013): emdbook: Ecological Models and Data in R. R package version 1.3.4.
- Burg, J. van den* (1985): Foliar analysis for determination of tree nutrient status- a compilation of literature data. *Rapp. Rijksinst. Voor Onderz. Bos- En Landschapsbouw Dorschkamp Neth.*
- Bustos, R., Castrillo, G., Linhares, F., Puga, M.I., Rubio, V., Pérez-Pérez, J., Solano, R., Leyva, A., Paz-Ares, J.* (2010): A central regulatory system largely controls transcriptional activation and repression responses to phosphate starvation in *Arabidopsis*. *PLoS Genet* 6, e1001102.
- Casieri, L., Lahmidi, N.A., Doidy, J., Veneault-Fourrey, C., Migeon, A., Bonneau, L., Courty, P.-E., Garcia, K., Charbonnier, M., Delteil, A., Brun, A., Zimmermann, S., Plassard, C., Wipf, D.* (2013): Biotrophic transportome in mutualistic plant–fungal interactions. *Mycorrhiza* 23, 597–625.

- Chang, S., Puryear, J., Cairney, J. (1993): A simple and efficient method for isolating RNA from pine trees. *Plant Mol. Biol. Report.* 11, 113–116.
- Claassen, N., Barber, S.A. (1974): A method for characterizing the relation between nutrient concentration and flux into roots of intact plants. *Plant Physiol.* 54, 564–568.
- Cogliatti, D.H., Clarkson, D.T. (1983): Physiological changes in, and phosphate uptake by potato plants during development of, and recovery from phosphate deficiency. *Physiol. Plant.* 58, 287–294.
- Cress, W.A., Throneberry, G.O., Lindsey, D.L. (1979): Kinetics of phosphorus absorption by mycorrhizal and nonmycorrhizal tomato roots. *Plant Physiol.* 64, 484–487.
- Danielsen, L., Lohaus, G., Sirrenberg, A., Karlovsky, P., Bastien, C., Pilate, G., Polle, A. (2013): Ectomycorrhizal colonization and diversity in relation to tree biomass and nutrition in a plantation of transgenic poplars with modified lignin biosynthesis. *PLOS ONE* 8, e59207.
- Danielsen, L., Polle, A. (2014): Poplar nutrition under drought as affected by ectomycorrhizal colonization. *Environ. Exp. Bot.* 108, 89–98.
- Danielsen, L., Thürmer, A., Meinicke, P., Buée, M., Morin, E., Martin, F., Pilate, G., Daniel, R., Polle, A., Reich, M. (2012): Fungal soil communities in a young transgenic poplar plantation form a rich reservoir for fungal root communities. *Ecol. Evol.* 2, 1935–1948.
- Daram, P., Brunner, S., Rausch, C., Steiner, C., Amrhein, N., Bucher, M. (1999): *Pht2;1* encodes a low-affinity phosphate transporter from *Arabidopsis*. *Plant Cell Online* 11, 2153–2166.
- Desai, S., Naik, D., Cumming, J.R. (2014): The influence of phosphorus availability and *Laccaria bicolor* symbiosis on phosphate acquisition, antioxidant enzyme activity, and rhizospheric carbon flux in *Populus tremuloides*. *Mycorrhiza* 24, 369–382.
- Dong, B., Ryan, P.R., Rengel, Z., Delhaize, E. (1999): Phosphate uptake in *Arabidopsis thaliana*: dependence of uptake on the expression of transporter genes and internal phosphate concentrations. *Plant Cell Environ.* 22, 1455–1461.
- Felsenstein, J. (1993): PHYLIP (Phylogeny Inference Package) version 3.5c. Distributed by the author. Department of Genetics, University of Washington, Seattle.
- Finn, R.D., Bateman, A., Clements, J., Coghill, P., Eberhardt, R.Y., Eddy, S.R., Heger, A., Hetherington, K., Holm, L., Mistry, J., Sonnhammer, E.L.L., Tate, J., Punta, M. (2014): Pfam: the protein families database. *Nucleic Acids Res.* 42, D222–D230.

- Fitzhugh, R.D., Driscoll, C.T., Groffman, P.M., Tierney, G.L., Fahey, T.J., Hardy, J.P.* (2001): Effects of soil freezing disturbance on soil solution nitrogen, phosphorus, and carbon chemistry in a northern hardwood ecosystem. *Biogeochemistry* 56, 215–238.
- Gan, H., Jiao, Y., Jia, J., Wang, X., Li, H., Shi, W., Peng, C., Polle, A., Luo, Z.-B.* (2016): Phosphorus and nitrogen physiology of two contrasting poplar genotypes when exposed to phosphorus and/or nitrogen starvation. *Tree Physiol.* 36, 22–38.
- Ge, X., Tian, Y., Tang, L.* (2015): Nutrient distribution indicated whole-tree harvesting as a possible factor restricting the sustainable productivity of a poplar plantation system in China. *PLOS ONE* 10, e0125303.
- Gehring, C.A., Mueller, R.C., Whitham, T.G.* (2006): Environmental and genetic effects on the formation of ectomycorrhizal and arbuscular mycorrhizal associations in cottonwoods. *Oecologia* 149, 158–164.
- Goodstein, D.M., Shu, S., Howson, R., Neupane, R., Hayes, R.D., Fazo, J., Mitros, T., Dirks, W., Hellsten, U., Putnam, N., Rokhsar, D.S.* (2012): Phytozome: a comparative platform for green plant genomics. *Nucleic Acids Res.* 40, D1178–D1186.
- Guo, B., Jin, Y., Wussler, C., Blancaflor, E.B., Motes, C.M., Versaw, W.K.* (2008): Functional analysis of the *Arabidopsis* PHT4 family of intracellular phosphate transporters. *New Phytol.* 177, 889–898.
- Hammond, J.P., White, P.J.* (2008): Sucrose transport in the phloem: integrating root responses to phosphorus starvation. *J. Exp. Bot.* 59, 93–109.
- Hassler, S., Lemke, L., Jung, B., Möhlmann, T., Krüger, F., Schumacher, K., Espen, L., Martinoia, E., Neuhaus, H.E.* (2012): Lack of the Golgi phosphate transporter PHT4;6 causes strong developmental defects, constitutively activated disease resistance mechanisms and altered intracellular phosphate compartmentation in *Arabidopsis*. *Plant J.* 72, 732–744.
- Heinrichs, H., Brumsack, H.-J., Löffel, N., König, N.* (1986): Verbessertes Druckaufschlußsystem für biologische und anorganische Materialien. *Z. Für Pflanzenernähr. Bodenkd.* 149, 350–353.
- Hellemans, J., Mortier, G., De Paepe, A., Speleman, F., Vandesompele, J.* (2007): qBase relative quantification framework and software for management and automated analysis of real-time quantitative PCR data. *Genome Biol.* 8, R19.
- Hewitt, E.J., Smith, T.A.* (1974): Plant Mineral Nutrition. English University Press, London, p. 298 pp.
- Higo, K., Ugawa, Y., Iwamoto, M., Korenaga, T.* (1999): Plant cis-acting regulatory DNA elements (PLACE) database: 1999. *Nucleic Acids Res.* 27, 297–300.

- Holford, I.C.R. (1997): Soil phosphorus: its measurement, and its uptake by plants. *Soil Res.* 35, 227–240.
- Huang, C.Y., Shirley, N., Genc, Y., Shi, B., Langridge, P. (2011): Phosphate utilization efficiency correlates with expression of low-affinity phosphate transporters and noncoding RNA, IPS1, in barley. *Plant Physiol.* 156, 1217–1229.
- Janz, D., Behnke, K., Schnitzler, J.-P., Kanawati, B., Schmitt-Kopplin, P., Polle, A. (2010): Pathway analysis of the transcriptome and metabolome of salt sensitive and tolerant poplar species reveals evolutionary adaptation of stress tolerance mechanisms. *BMC Plant Biol.* 10, 150.
- Jentschke, G., Brandes, B., Heinzemann, J., Marschner, P., Godbold, D.L. (1999): Sand culture of mycorrhizal plants. *J. Plant Nutr. Soil Sci.* 162, 107–112.
- Jungk, A., Asher, C.J., Edwards, D.G., Meyer, D. (1990): Influence of phosphate status on phosphate uptake kinetics of maize (*Zea mays*) and soybean (*Glycine max*). *Plant Soil* 124, 175–182.
- Kolesnikov, N., Hastings, E., Keays, M., Melnichuk, O., Tang, Y.A., Williams, E., Dylag, M., Kurbatova, N., Brandizi, M., Burdett, T., Megy, K., Pilicheva, E., Rustici, G., Tikhonov, A., Parkinson, H., Petryszak, R., Sarkans, U., Brazma, A. (2015): ArrayExpress update--simplifying data submissions. *Nucleic Acids Res.* 43, D1113–D1116.
- Lambers, H., Shane, M.W., Cramer, M.D., Pearse, S.J., Veneklaas, E.J. (2006): Root structure and functioning for efficient acquisition of phosphorus: Matching morphological and physiological traits. *Ann. Bot.* 98, 693–713.
- Lamesch, P., Berardini, T.Z., Li, D., Swarbreck, D., Wilks, C., Sasidharan, R., Muller, R., Dreher, K., Alexander, D.L., Garcia-Hernandez, M., Karthikeyan, A.S., Lee, C.H., Nelson, W.D., Ploetz, L., Singh, S., Wensel, A., Huala, E. (2012): The *Arabidopsis* Information Resource (TAIR): improved gene annotation and new tools. *Nucleic Acids Res.* 40, D1202–D1210.
- Larkin, M.A., Blackshields, G., Brown, N.P., Chenna, R., McGettigan, P.A., McWilliam, H., Valentin, F., Wallace, I.M., Wilm, A., Lopez, R., Thompson, J.D., Gibson, T.J., Higgins, D.G. (2007): Clustal W and Clustal X version 2.0. *Bioinformatics* 23, 2947–2948.
- Lee, R.B. (1982): Selectivity and kinetics of ion uptake by barley plants following nutrient deficiency. *Ann. Bot.* 50, 429–449.
- Lemoine, R., Camera, S.L., Atanassova, R., Dédaldéchamp, F., Allario, T., Pourtau, N., Bonnemain, J.-L., Laloi, M., Coutos-Thévenot, P., Maurousset, L., Faucher, M., Girousse, C., Lemonnier, P., Parrilla, J., Durand, M. (2013): Source-to-sink transport of sugar and regulation by environmental factors. *Front. Plant Sci.* 4, 272.

- Leple, J.C., Brasileiro, A.C.M., Michel, M.F., Delmotte, F., Jouanin, L. (1992): Transgenic poplars: expression of chimeric genes using four different constructs. *Plant Cell Rep.* 11, 137–141.
- López-Arredondo, D.L., Leyva-González, M.A., González-Morales, S.I., López-Bucio, J., Herrera-Estrella, L. (2014): Phosphate nutrition: Improving low-phosphate tolerance in crops. *Annu. Rev. Plant Biol.* 65, 95–123.
- Loth-Pereda, V., Orsini, E., Courty, P.-E., Lota, F., Kohler, A., Diss, L., Blaudez, D., Chalot, M., Nehls, U., Bucher, M., Martin, F. (2011): Structure and expression profile of the phosphate Pht1 transporter gene family in mycorrhizal *Populus trichocarpa*. *Plant Physiol.* 156, 2141–2154.
- Martinka, M., Vaculík, M., Lux, A. (2014): Plant cell responses to cadmium and zinc, in: Nick, P., Opatrný, Z. (eds.): Applied plant cell biology. Springer Berlin Heidelberg, Berlin, Heidelberg, pp. 209–246.
- Misson, J., Thibaud, M.-C., Bechtold, N., Raghothama, K., Nussaume, L. (2004): Transcriptional regulation and functional properties of *Arabidopsis* Pht1;4, a high affinity transporter contributing greatly to phosphate uptake in phosphate deprived plants. *Plant Mol. Biol.* 55, 727–741.
- Mitsukawa, N., Okumura, S., Shirano, Y., Sato, S., Kato, T., Harashima, S., Shibata, D. (1997): Overexpression of an *Arabidopsis thaliana* high-affinity phosphate transporter gene in tobacco cultured cells enhances cell growth under phosphate-limited conditions. *Proc. Natl. Acad. Sci. U. S. A.* 94, 7098–7102.
- Morcuende, R., Bari, R., Gibon, Y., Zheng, W., Pant, B.D., Bläsing, O., Usadel, B., Czechowski, T., Udvardi, M.K., Stitt, M., Scheible, W.-R. (2007): Genome-wide reprogramming of metabolism and regulatory networks of *Arabidopsis* in response to phosphorus. *Plant Cell Environ.* 30, 85–112.
- Mudge, S.R., Rae, A.L., Diatloff, E., Smith, F.W. (2002): Expression analysis suggests novel roles for members of the Pht1 family of phosphate transporters in *Arabidopsis*. *Plant J.* 31, 341–353.
- Müller, A., Volmer, K., Mishra-Knyrim, M., Polle, A. (2013): Growing poplars for research with and without mycorrhizas. *Front. Plant Sci.* 4, 332.
- Nussaume, L., Kanno, S., Javot, H., Marin, E., Pochon, N., Ayadi, A., Nakanishi, T.M., Thibaud, M.-C. (2011): Phosphate import in plants: Focus on the PHT1 transporters. *Front. Plant Sci.* 2, 83.
- Ouyang, S., Zhu, W., Hamilton, J., Lin, H., Campbell, M., Childs, K., Thibaud-Nissen, F., Malek, R.L., Lee, Y., Zheng, L., Orvis, J., Haas, B., Wortman, J., Buell, C.R. (2007): The TIGR rice genome annotation resource: improvements and new features. *Nucleic Acids Res.* 35, D883–D887.

Pinheiro, J.C., Bates, D.M., DebRoy, S., the R Development Core Team (2012): The R Core Team nlme: Linear and Nonlinear Mixed Effects Models. R package version 3.1-103.

Poirier, Y., Bucher, M. (2002): Phosphate transport and homeostasis in *Arabidopsis*. *Arab. Book* e0024.

Poirier, Y., Jung, J.-Y. (2015): Phosphate transporters, in: Plaxton, W.C., Lambers, H. (eds.): Annual Plant Reviews Volume 48. John Wiley & Sons, Inc., Hoboken, NJ, USA, pp. 125–158.

Polle, A., Chen, S. (2015): On the salty side of life: molecular, physiological and anatomical adaptation and acclimation of trees to extreme habitats. *Plant Cell Environ.* 38, 1794–1816.

Polle, A., Janz, D., Teichmann, T., Lipka, V. (2013): Poplar genetic engineering: promoting desirable wood characteristics and pest resistance. *Appl. Microbiol. Biotechnol.* 97, 5669–5679.

R Development Core Team (2012): R: a language and environment for statistical computing. R Foundation for Statistical Computing, Vienna, Austria.

Rae, A.L., Cybinski, D.H., Jarmey, J.M., Smith, F.W. (2003): Characterization of two phosphate transporters from barley; evidence for diverse function and kinetic properties among members of the Pht1 family. *Plant Mol. Biol.* 53, 27–36.

Ranger, J., Marques, R., Jussy, J.-H. (2001): Forest soil dynamics during stand development assessed by lysimeter and centrifuge solutions. *For. Ecol. Manag.* 144, 129–145.

Rausch, C., Bucher, M. (2002): Molecular mechanisms of phosphate transport in plants. *Planta* 216, 23–37.

Remy, E., Cabrito, T.R., Batista, R.A., Teixeira, M.C., Sá-Correia, I., Duque, P. (2012): The Pht1;9 and Pht1;8 transporters mediate inorganic phosphate acquisition by the *Arabidopsis thaliana* root during phosphorus starvation. *New Phytol.* 195, 356–371.

Ruijter, J.M., Ramakers, C., Hoogaars, W.M.H., Karlen, Y., Bakker, O., Hoff, M.J.B. van den, Moorman, A.F.M. (2009): Amplification efficiency: linking baseline and bias in the analysis of quantitative PCR data. *Nucleic Acids Res.* 37, e45–e45.

Schachtman, D.P., Reid, R.J., Ayling, S.M. (1998): Phosphorus uptake by plants: from soil to cell. *Plant Physiol.* 116, 447–453.

Schnable, P.S., Ware, D., Fulton, R.S., Stein, J.C., Wei, F., Pasternak, S., Liang, C., Zhang, J., Fulton, L., Graves, T.A., Minx, P., Reily, A.D., Courtney, L., Kruchowski, S.S., Tomlinson, C., Strong, C., Delehaunty, K., Fronick, C., Courtney, B., Rock, S.M.,



Belter, E., Du, F., Kim, K., Abbott, R.M., Cotton, M., Levy, A., Marchetto, P., Ochoa, K., Jackson, S.M., Gillam, B., Chen, W., Yan, L., Higginbotham, J., Cardenas, M., Waligorski, J., Applebaum, E., Phelps, L., Falcone, J., Kanchi, K., Thane, T., Scimone, A., Thane, N., Henke, J., Wang, T., Ruppert, J., Shah, N., Rotter, K., Hodges, J., Ingenthron, E., Cordes, M., Kohlberg, S., Sgro, J., Delgado, B., Mead, K., Chinwalla, A., Leonard, S., Crouse, K., Collura, K., Kudrna, D., Currie, J., He, R., Angelova, A., Rajasekar, S., Mueller, T., Lomeli, R., Scarra, G., Ko, A., Delaney, K., Wissotski, M., Lopez, G., Campos, D., Braidotti, M., Ashley, E., Golser, W., Kim, H., Lee, S., Lin, J., Dujmic, Z., Kim, W., Talag, J., Zuccolo, A., Fan, C., Sebastian, A., Kramer, M., Spiegel, L., Nascimento, L., Zutavern, T., Miller, B., Ambroise, C., Muller, S., Spooner, W., Narechania, A., Ren, L., Wei, S., Kumari, S., Faga, B., Levy, M.J., McMahan, L., Buren, P.V., Vaughn, M.W., Ying, K., Yeh, C.-T., Emrich, S.J., Jia, Y., Kalyanaraman, A., Hsia, A.-P., Barbazuk, W.B., Baucom, R.S., Brutnell, T.P., Carpita, N.C., Chaparro, C., Chia, J.-M., Deragon, J.-M., Estill, J.C., Fu, Y., Jeddeloh, J.A., Han, Y., Lee, H., Li, P., Lisch, D.R., Liu, S., Liu, Z., Nagel, D.H., McCann, M.C., SanMiguel, P., Myers, A.M., Nettleton, D., Nguyen, J., Penning, B.W., Ponnala, L., Schneider, K.L., Schwartz, D.C., Sharma, A., Soderlund, C., Springer, N.M., Sun, Q., Wang, H., Waterman, M., Westerman, R., Wolfgruber, T.K., Yang, L., Yu, Y., Zhang, L., Zhou, S., Zhu, Q., Bennetzen, J.L., Dawe, R.K., Jiang, J., Jiang, N., Presting, G.G., Wessler, S.R., Aluru, S., Martienssen, R.A., Clifton, S.W., McCombie, W.R., Wing, R.A., Wilson, R.K. (2009): The B73 maize genome: Complexity, diversity, and dynamics. *Science* 326, 1112–1115.

Seven, J., Polle, A. (2014): Subcellular nutrient element localization and enrichment in ecto- and arbuscular mycorrhizas of field-grown beech and ash trees indicate functional differences. *PLOS ONE* 9, e114672.

Shin, H., Shin, H.-S., Dewbre, G.R., Harrison, M.J. (2004): Phosphate transport in *Arabidopsis*: Pht1;1 and Pht1;4 play a major role in phosphate acquisition from both low- and high-phosphate environments. *Plant J.* 39, 629–642.

Takabatake, R., Hata, S., Taniguchi, M., Kouchi, H., Sugiyama, T., Izui, K. (1999): Isolation and characterization of cDNAs encoding mitochondrial phosphate transporters in soybean, maize, rice, and *Arabidopsis*. *Plant Mol. Biol.* 40, 479–486.

Tamura, K., Stecher, G., Peterson, D., Filipowski, A., Kumar, S. (2013): MEGA6: Molecular Evolutionary Genetics Analysis Version 6.0. *Mol. Biol. Evol.* 30, 2725–2729.

Tsai, C.-J., Ranjan, P., DiFazio, S., Tuskan, G., Johnson, V. (2011): Poplar genome microarrays, in: Joshi, C., DiFazio, S., Kole, C. (eds.): Genetics, genomics and breeding of poplars. Science Publishers, Enfield, NH, pp. 112–127.

Tuskan, G.A., DiFazio, S., Jansson, S., Bohlmann, J., Grigoriev, I., Hellsten, U., Putnam, N., Ralph, S., Rombauts, S., Salamov, A., Schein, J., Sterck, L., Aerts, A., Bhalerao, R.R., Bhalerao, R.P., Blaudez, D., Boerjan, W., Brun, A., Brunner, A., Busov, V., Campbell, M., Carlson, J., Chalot, M., Chapman, J., Chen, G.-L., Cooper, D.,

Coutinho, P.M., Couturier, J., Covert, S., Cronk, Q., Cunningham, R., Davis, J., Degroeve, S., Déjardin, A., dePamphilis, C., Detter, J., Dirks, B., Dubchak, I., Duplessis, S., Ehling, J., Ellis, B., Gendler, K., Goodstein, D., Gribskov, M., Grimwood, J., Groover, A., Gunter, L., Hamberger, B., Heinze, B., Helariutta, Y., Henrissat, B., Holligan, D., Holt, R., Huang, W., Islam-Faridi, N., Jones, S., Jones-Rhoades, M., Jorgensen, R., Joshi, C., Kangasjärvi, J., Karlsson, J., Kelleher, C., Kirkpatrick, R., Kirst, M., Kohler, A., Kalluri, U., Larimer, F., Leebens-Mack, J., Leplé, J.-C., Locascio, P., Lou, Y., Lucas, S., Martin, F., Montanini, B., Napoli, C., Nelson, D.R., Nelson, C., Nieminen, K., Nilsson, O., Pereda, V., Peter, G., Philippe, R., Pilate, G., Poliakov, A., Razumovskaya, J., Richardson, P., Rinaldi, C., Ritland, K., Rouzé, P., Ryaboy, D., Schmutz, J., Schrader, J., Segerman, B., Shin, H., Siddiqui, A., Sterky, F., Terry, A., Tsai, C.-J., Uberbacher, E., Unneberg, P., Vahala, J., Wall, K., Wessler, S., Yang, G., Yin, T., Douglas, C., Marra, M., Sandberg, G., Peer, Y.V. de, Rokhsar, D. (2006): The genome of black cottonwood, *Populus trichocarpa* (Torr. & Gray). *Science* 313, 1596–1604.

van Hees, P.A.W., Vinogradoff, S.I., Edwards, A.C., Godbold, D.L., Jones, D.L. (2003): Low molecular weight organic acid adsorption in forest soils: effects on soil solution concentrations and biodegradation rates. *Soil Biol. Biochem.* 35, 1015–1026.

Van Tichelen, K.K., Colpaert, J.V. (2000): Kinetics of phosphate absorption by mycorrhizal and non-mycorrhizal Scots pine seedlings. *Physiol. Plant.* 110, 96–103.

Versaw, W.K., Harrison, M.J. (2002): A chloroplast phosphate transporter, PHT2;1, influences allocation of phosphate within the plant and phosphate-starvation responses. *Plant Cell Online* 14, 1751–1766.

Warnes, G.R. (2012): gplots: Various R programming tools for plotting data. R package version 2.11.0.

Yamada, K., Kanai, M., Osakabe, Y., Ohiraki, H., Shinozaki, K., Yamaguchi-Shinozaki, K. (2011): Monosaccharide absorption activity of *Arabidopsis* roots depends on expression profiles of transporter genes under high salinity conditions. *J. Biol. Chem.* 286, 43577–43586.

Zhang, Z., Liao, H., Lucas, W.J. (2014): Molecular mechanisms underlying phosphate sensing, signaling, and adaptation in plants: Phosphate sensing and signaling in plants. *J. Integr. Plant Biol.* 56, 192–220.

### 3.7 Supporting information

**Table S3.1:** In silico analyses of putative poplar phosphate transporters.

**Table S3.2:** Primers used for qRT PCR of putative P transporter genes.

**Table S3.3:** Transcript abundances of phosphate transporter genes

**Figure S3.1.** Biomass and performance of poplar grown with five different P concentrations.

**Figure S3.2.** Neighbor-Joining tree (Jones-Taylor-Thornton model, 500 bootstraps) of the amino acid sequences for inorganic phosphate transporters in poplar.

**Figure S3.3.** Correlations of absolute microarray expression data ( $\log_2$ -value) and qRT PCR relative expression values ( $\log_2$ ) for PtPHTs.

**Table S3.1: In silico analyses of putative poplar phosphate transporters.**

GeneID	Gene name or Family	PLACE	Affy IDs	Comments	Ath protein homolog (% identity)
		P1BS-Localization			
Potri.010G072000	<i>PtPHT1;1</i>	54	PtpAffx.215047.1.S1_s_at PtpAffx.208712.1.S1_at PtpAffx.219484.1.S1_s_at		AtPHT1;5 (77.5)
Potri.010G071700	<i>PtPHT1;2</i>		PtpAffx.219485.1.S1_s_at		AtPHT1;5 (78.7)
Potri.010G071500	<i>PtPHT1;3</i>		PtpAffx.54440.1.A1_at		AtPHT1;4 (82.5), AtPHT1;7 (82.0)
Potri.005G223500	<i>PtPHT1;4</i>	404	PtpAffx.141538.1.S1_s_at Ptp.5181.2.S1_at PtpAffx.69535.1.A1_s_at		AtPHT1;4 (83.0), AtPHT1;7 (84.7)
Potri.002G038900	<i>PtPHT1;5</i>	169		NA	AtPHT1;4 (84.5), AtPHT1;7 (83.6)
Potri.005G175500	<i>PtPHT1;6</i>		PtpAffx.223352.1.S1_s_at	n.d.	AtPHT1;6 (64.5), At4G08895 (53.3)
Potri.005G223600	<i>PtPHT1;7</i>	911	PtpAffx.205756.1.S1_x_at PtpAffx.205756.1.S1_at PtpAffx.69535.2.A1_s_at	n.d.	AtPHT1;4 (85.9), AtPHT1;7 (86.9)
Potri.019G061900	<i>PtPHT1;8</i>		PtpAffx.215592.1.S1_at PtpAffx.223434.1.S1_at PtpAffx.223434.1.S1_s_at	n.d. n.d. n.d.	-
Potri.002G005500	<i>PtPHT1;9</i>	334	PtpAffx.62481.1.A1_s_at		AtPHT1;8 (60.4),
Potri.015G022800	<i>PtPHT1;10</i>	489, 581, 826	PtpAffx.201523.1.S1_at PtpAffx.218285.1.S1_at	n.d. n.d.	AtPHT1;9 (62.9) -
Potri.005G256100	<i>PtPHT1;11</i>	514		NA	AtPHT1;8 (61.0), AtPHT1;9 (64.2)
Potri.001G318500	<i>PtPHT1;12</i>		PtpAffx.201089.1.S1_at		AtPHT1;5 (78.9)
Potri.005G175700	Fam. 1		PtpAffx.205527.1.S1_at	n.d.	AtPHT1;6 (66.5), At4G08895 (53.3)
Potri.005G223700	Fam. 1		PtpAffx.205757.1.S1_at	n.d., tr.	-
Potri.006G109800	Fam. 4	434	PtpAffx.206360.1.S1_at	n.d., tr.	-
Potri.010G071600	Fam. 1			NA	AtPHT1;5 (78.9)
Potri.013G089800	Fam. 1	449, 472		NA, tr.	-
Potri.008G186600	PtPHT2;1		PtpAffx.208289.1.S1_at		AtPHT2;1 (81.7)
Potri.010G046300	PtPHT2;2		PtpAffx.208671.1.S1_at		AtPHT2;1 (73.3)

**Table S3.1 (continued)**

GeneID	Gene name or Family	PLACE P1BS-Localization	Affy IDs	Comments	Ath protein homolog (% identity)
Potri.017G060800	<i>PtPHT3;1</i>	305	PtpAffx.223426.1.S1_at	n.d.	AtPHT3;1 (88.3)
Potri.001G322300	<i>PtPHT3;2</i>		PtpAffx.51641.2.S1_at PtpAffx.7845.1.A1_s_at Ptp.2106.1.A1_s_at PtpAffx.51641.1.S1_s_at PtpAffx.201077.1.S1_at		AtPHT3;1 (88.8)
Potri.012G105100	<i>PtPHT3;3</i>			NA	-
Potri.015G104400	<i>PtPHT3;4</i>	277	Ptp.6141.1.S1_at	n.d.	-
Potri.004G207200	<i>PtPHT3;5</i>		PtpAffx.172.1.S1_at		AtPHT3;3 (75.2)
Potri.005G098800	<i>PtPHT3;6</i>		PtpAffx.222497.1.S1_s_at PtpAffx.205286.1.S1_at PtpAffx.13003.1.S1_at		AtPHT3;3 (72.7)
Potri.006G062300	<i>PtPHT4;1</i>		PtpAffx.216795.1.S1_at	n.d.	AtPHT4;5 (71.7)
Potri.018G121600	<i>PtPHT4;2</i>		Ptp.850.1.S1_at PtpAffx.214529.1.S1_at PtpAffx.214529.1.S1_x_at PtpAffx.157223.1.S1_at Ptp.6820.1.S1_at		AtPHT4;5 (67.0)
Potri.001G249800	<i>PtPHT4;3</i>		Ptp.7586.1.S1_at		AtPHT4;1 (75.6)
Potri.009G043800	<i>PtPHT4;4</i>		PtpAffx.95515.1.S1_at		AtPHT4;1 (75.4)
Potri.014G085700	<i>PtPHT4;5</i>	958	PtpAffx.59699.2.A1_a_at		AtPHT4;4 (73.8)
Potri.009G168200	<i>PtPHT4;6</i>		PtpAffx.147587.1.A1_at PtpAffx.204370.1.S1_at	n.d.	AtPHT4;6 (78.7)
Potri.016G111000	<i>PtPHT4;7</i>		Ptp.5773.1.S1_at		AtPHT4;2 (73.8)
Potri.001G248200	<i>PtPHT4;8</i>		PtpAffx.107855.1.A1_a_at PtpAffx.112006.1.S1_s_at PtpAffx.107855.1.A1_at PtpAffx.200753.1.S1_at PtpAffx.112006.1.S1_at	n.d.	AtPHT4;3 (77.0)
Potri.009G042000	<i>PtPHT4;9</i>		PtpAffx.204925.1.S1_at	n.d.	AtPHT4;3 (64.3)
Potri.004G061400	uncl.		PtpAffx.203816.1.S1_at	n.d.	-
Potri.013G095600	uncl.		PtpAffx.211244.1.S1_at	n.d., tr.	-

GeneID: Poplar gene IDs in genome annotation version v3, PLACE P1BS-Localization: location of P1BS-motif(s) in 1 kb upstream region of the gene, Affy IDs: probe names on annotated for the gene by Tsai et al. (2011), Ath protein homolog: closest *Arabidopsis* protein homolog after Figure S1 and its identity (%) with the poplar protein, n.d.: expression not detected on microarray, NA: gene is not on array, tr.: truncated; uncl: unclustered.

**Table S3.2: Primers used for qRT PCR of putative P transporter genes.**

Potri.ID	Affy IDs	Primer name	Primer sequence (5'-3')	Design	Reference
Potri.010G072000 (PtPHT1;1)	PtpAffx.215047.1.S1_s_at PtpAffx.208712.1.S1_at PtpAffx.219484.1.S1_s_at	PtPH1f PtPH1r	GCGATTCACGAGGTTTTTCA GGCGAAGAAAAAGGTCAACG		Loth-Pereda et al. (2011)
Potri.010G071700 (PtPHT1;2)	PtpAffx.219485.1.S1_s_at	PcPHT1;2_fw PcPHT1;2_rev2	CACAGACCGAACGAAGACTG ATCACACTGAAGCCATCCTAGG		(after) Loth-Pereda et al. (2011)
Potri.010G071500 (PtPHT1;3)	PtpAffx.54440.1.A1_at	PcPHT1;3_fw PcPHT1;3_rev	CGACAACCGAATTGGCTTCG CAAGTGGACCTCAGTCTCG	intron spanning	after Loth-Pereda et al. (2011)
Potri.009G168200 (PtPHT4;6)	PtpAffx.147587.1.A1_at PtpAffx.204370.1.S1_at	PcPHT4;6_fw PcPHT4;6_rev	CGCTCGCTGCCAATCTTAC GTCTAGGGATGTTCCACCC	intron spanning	
Potri.001G047200 (PPR-repeat as reference gene)	PtpAffx.200189.1.S1_at	Pc001G047200_fw Pc001G047200_rev	GGCTGAGGAATGTCGAATGG AGAACGCAACATCATGGAAACC	Exon- Exon junction	
Potri.001G309500 (Actin as reference gene)	Ptp.6486.1.S1_s_at PtpAffx.1258.1.S1_s_at PtpAffx.1258.4.S1_s_at	Aktin9_fw Aktin9_rev	TGGTGGTTCCACTATGTTCC TGGAATCCACATCTGCTGG	Exon- Exon junction	Janz et al. (2012)

Genes are indicated by their Potri.IDs, Affy IDs for probe sets on microarray, indication of special design, and reference. When published primers were not available, they were designed with OligoExplorer 1.5 and checked with OligoAnalyzer 1.5 (both Gene Link, Hawthorne, NY, USA). Primers were adapted to *P. × canescens* (sequences from AspenDB) when the nucleotide sequence differed from *P. trichocarpa*.

**Table S3.3: Transcript abundances of phosphate transporter genes.**

Raw expression values for the PHT genes on microarrays (means of  $n = 3$ ) used for z-normalization to construct the heatmap shown in Figure 5a. Poplar plants were grown with nutrient solutions differing in phosphate concentration (641  $\mu\text{M}$  P (HP), 6.4  $\mu\text{M}$  P (MP), 0.064  $\mu\text{M}$  P (LP)).

	Fine Roots			Uppermost Leaves		
	HP	MP	LP	HP	MP	LP
PtPHT1;1	44.6	3699.2	2721.1	6.2	6.7	7.2
PtPHT1;2	250.2	6658.6	6268.9	4.7	7.3	9.6
PtPHT1;3	18.0	35.5	22.5	386.1	818.6	1251.1
PtPHT1;4	196.7	423.4	287.6	70.7	179.9	199.1
PtPHT1;7	14.3	195.4	129.4	11.6	43.7	79.1
PtPHT1;9	20.6	169.2	84.2	14.1	195.4	304.6
PtPHT1;12	6.8	205.5	211.4	5.7	323.1	451.6
PtPHT2;1	7.3	7.0	5.8	15.5	18.0	19.0
PtPHT2;2	6.3	5.3	7.3	162.9	103.2	96.7
PtPHT3;1	101.2	99.8	98.3	78.8	106.2	103.3
PtPHT3;2	348.7	457.0	445.7	207.4	308.5	327.6
PtPHT3;5	6.7	7.7	6.4	18.4	21.6	16.6
PtPHT3;6	22.5	32.7	23.3	18.6	19.3	17.5
PtPHT4;1	54.4	63.6	48.7	112.1	146.1	156.3
PtPHT4;2	15.7	22.2	20.1	39.0	47.6	46.1
PtPHT4;3	4.5	7.1	5.4	33.1	34.0	34.1
PtPHT4;4	15.7	30.0	33.5	156.0	230.2	268.2
PtPHT4;5	21.6	18.5	25.1	215.4	616.5	728.6
PtPHT4;6	57.0	41.2	46.1	31.8	42.5	38.6
PtPHT4;7	134.4	118.8	119.2	90.3	101.8	63.5
PtPHT4;8	35.7	34.5	34.0	26.2	27.5	30.4

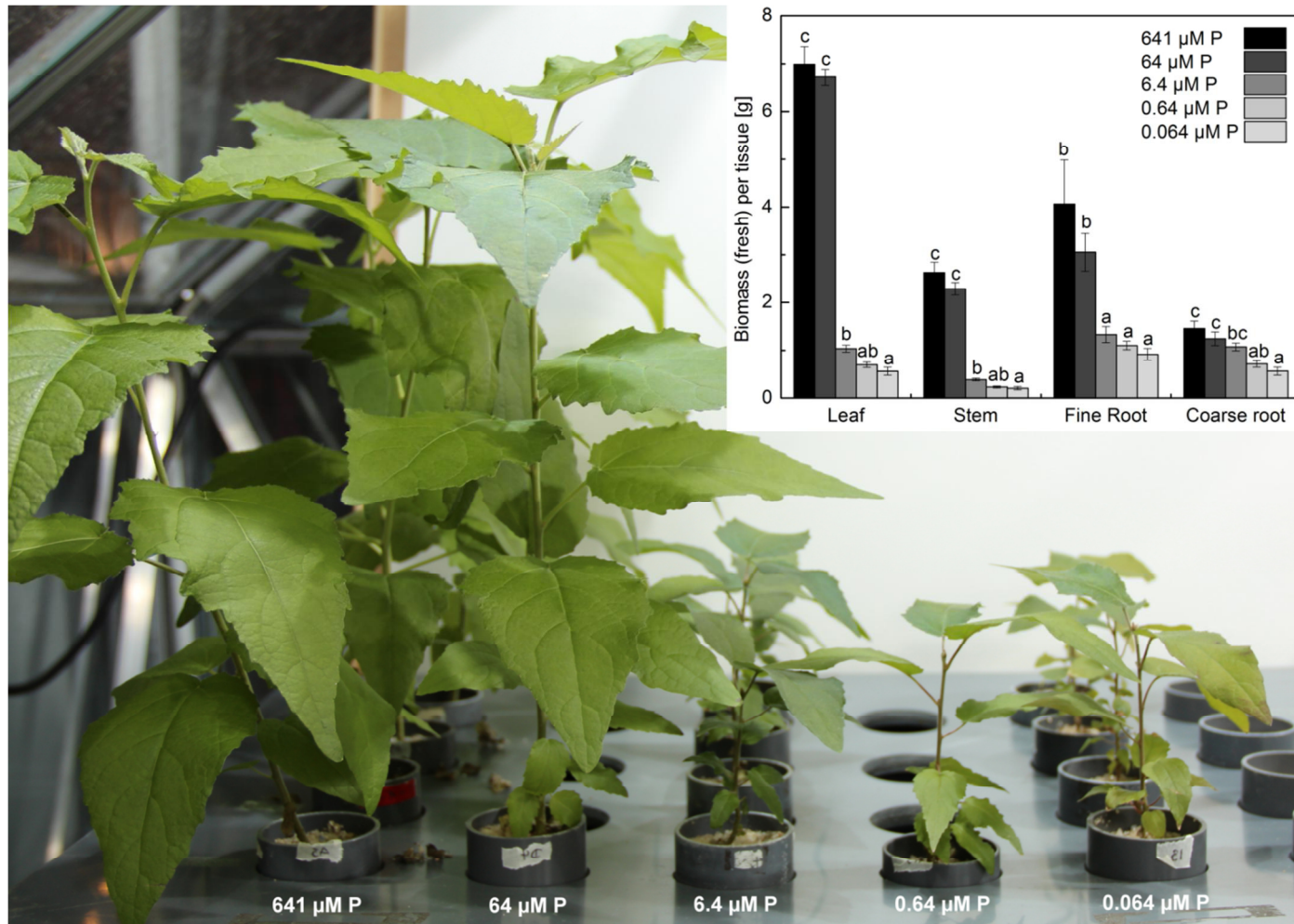


**Figure S3.1. Biomass and performance of poplar grown with five different P concentrations.** *Populus × canescens* plants were grown for about 2 months in nutrient solutions differing in phosphate concentrations (641 μM P (HP), 64 μM P, 6.4 μM P (MP), 0.64 μM P, 0.064 μM P (LP)). Biomass data are means for n=11-12 (±SE).



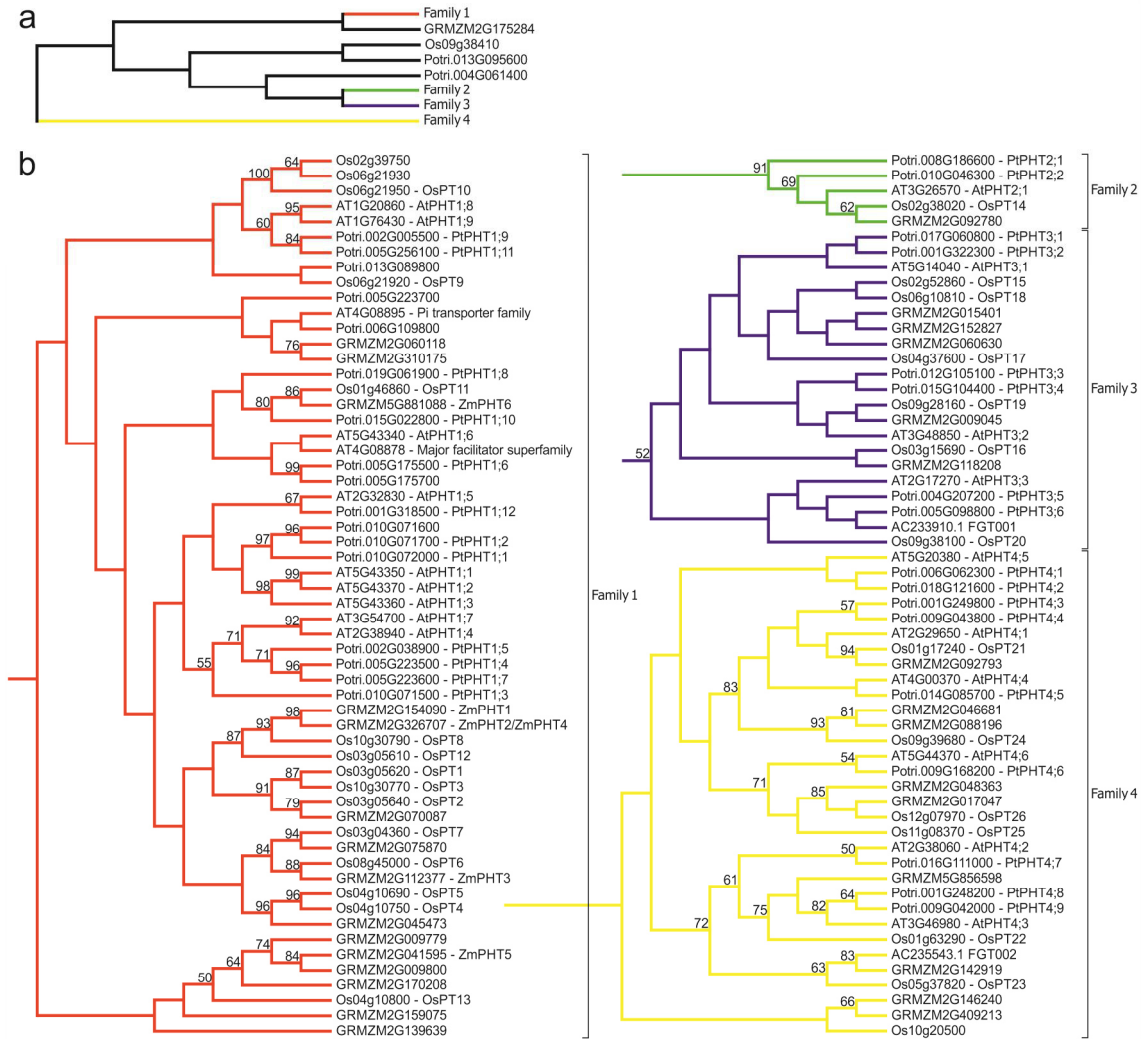


**Figure S3.2. Neighbor-Joining tree (Jones-Taylor-Thornton model, 500 bootstraps) of the amino acid sequences for inorganic phosphate transporters in poplar.** Poplar (Potri), *Arabidopsis* (AT), rice (Os) and maize (GRMZM and AC) sequences were used; A: unrooted compressed phylogenetic tree; B: expanded view of the four families, names according to Fan et al. (2013), Liu et al. (2011) and Phytozome, names for newly annotated poplar genes according to tree structure. Only bootstrap values  $\geq 50$  are displayed.

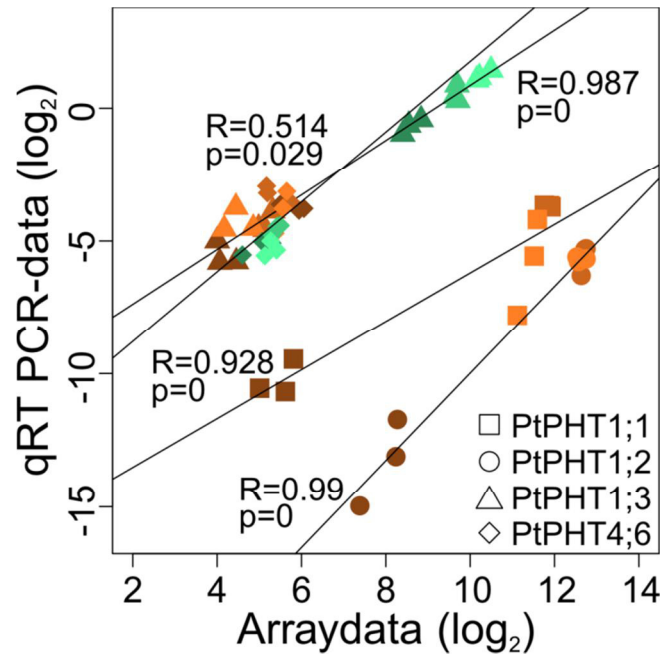


**Figure S3.3. Correlations of absolute microarray expression data ( $\log_2$ -value) and qRT PCR relative expression values ( $\log_2$ ) for PtPHTs.** P-value and R-value of correlation (R function cor.test) are given, red: root samples, green: leaf samples, dark: HP, middle: MP, light: LP; expression of *PtPHT1;1* and *PtPHT1;2* could not be detected by qRT PCR in leaves. Absolute expression values are given for the microarray data and relative expression values to two reference genes (Actin, PPR-repeat) for qRT PCR data.

**References for supplements Chapter 3**

Fan, C., Wang, X., Hu, R., Wang, Y., Xiao, C., Jiang, Y., Zhang, X., Zheng, C., Fu, Y.-F. (2013): The pattern of Phosphate transporter 1 genes evolutionary divergence in *Glycine max* L. *BMC Plant Biol.* 13, 48.

Janz, D., Lautner, S., Wildhagen, H., Behnke, K., Schnitzler, J.-P., Rennenberg, H., Fromm, J., Polle, A. (2012): Salt stress induces the formation of a novel type of “pressure wood” in two *Populus* species. *New Phytol.* 194, 129–141.

Liu, F., Chang, X.-J., Ye, Y., Xie, W.-B., Wu, P., Lian, X.-M. (2011): Comprehensive sequence and whole-life-cycle expression profile analysis of the phosphate transporter gene family in rice. *Mol. Plant* 4, 1105–1122.

Loth-Pereda, V., Orsini, E., Courty, P.-E., Lota, F., Kohler, A., Diss, L., Blaudez, D., Chalot, M., Nehls, U., Bucher, M., Martin, F. (2011): Structure and expression profile of the phosphate Pht1 transporter gene family in mycorrhizal *Populus trichocarpa*. *Plant Physiol.* 156, 2141–2154.

Tsai, C.-J., Ranjan, P., DiFazio, S., Tuskan, G., Johnson, V. (2011): Poplar genome microarrays, in: Joshi, C., DiFazio, S., Kole, C. (eds.): Genetics, genomics and breeding of poplars. Science Publishers, Enfield, NH, pp. 112–127.

### **3.8 Authors' contributions**

MK conducted experiments, analyzed data and wrote the manuscript. AP designed the experiments, analyzed data and wrote the manuscript. Both authors read and approved the final manuscript.

### **3.9 Declaration**

The following data shown in this chapter have been provided:

- ICP-OES and calculations were conducted by members of the Department of Plant Ecology and Ecosystems Research (Albrecht-von-Haller-Institute for Plant Sciences, Georg-August University Göttingen).
- All laboratory steps for microarray analyses (from RNA quality determinations to raw data) were provided by the Microarray Facility (MFT Services, Tübingen, Germany).

## Chapter 4

# Phosphate acquisition by poplar: Phylogeny, tissue-specific expression, and activity of root secreted purple acid phosphatases

### 4.1 Introduction

Plants take up phosphorus (P) only in the inorganic form, phosphate (*Schachtman et al.*, 1998). But phosphate is present in soil solutions in only low concentrations of below 10  $\mu\text{M}$  (*Bielecki*, 1973). Therefore, the inorganic phosphate pool has to be replenished constantly from other phosphorus pools. Up to 80 % of the total soil P sources is bound in organic P compounds (*Schachtman et al.*, 1998). Enzymes that cleave inorganic phosphate from organic P are phosphatases. The largest group of phosphatases, the purple acid phosphatases (PAPs) (*Olczak et al.*, 2003) have a pH optimum in acidic conditions present in most soils. PAPs have a purple color in concentrated solutions due to a ferric ligand in the active center of the enzyme (*Vincent and Averill*, 1990).

Most PAPs have a broad substrate spectrum (*Olczak et al.*, 2003). They acquire phosphate from organic P in the soil but also from internal P sources (*Duff et al.*, 1994). *Zhu et al.* (2005) found that 16 of 29 *Arabidopsis* PAPs were expressed in roots, seven AtPAPs were solely expressed in flowers, highlighting the role of PAPs for other functions than phosphate acquisition from soil.

The acid phosphatase activities in the whole plant are enhanced under P deprivation as was shown for *Arabidopsis* (*Del Pozo et al.*, 1999; *Wang et al.*, 2014), poplar (*Gan et al.*, 2016), and *Carpinus pubescens* and *Eurycorymbus cavaleriei* (*Zhang et al.*, 2015). AtPAP17 is one of the acid phosphatases with highest activity increment under low P (*Del Pozo et al.*, 1999). It was shown that the expression of *AtPAP17* is induced not only by P starvation but also by senescence, salt stress, abscisic acid and hydrogen peroxide suggesting a role in P mobilization in response to those stresses (*Del Pozo et al.*, 1999). An enhanced acid phosphatase activity on roots under P limited conditions was shown for *Arabidopsis* (*Wang et al.*, 2014) and tomato (*Bozzo et al.*, 2006). Experiments with *Arabidopsis* mutants have shown that AtPAP12 and AtPAP26 are the

main secreted phosphatases and responsible for most of the phosphatase activity in the medium under low P conditions, whereas AtPAP10 is the main root-associated phosphatase under low P conditions (Wang *et al.*, 2014).

The transcript levels of most, but not all PAPs are induced by P starvation (e.g. in soybean (Li *et al.*, 2012), maize (González-Muñoz *et al.*, 2015), rice (Zhang *et al.*, 2011) and *Arabidopsis* (Li *et al.*, 2002; Lohrasebi *et al.*, 2007)). In poplar (*Populus. simonii* and *P. × euramericana*), the expression of one PAP (Potri.010G158400) was studied and found to be increased upon P starvation in roots and leaves in congruence with enhanced acid phosphatase activity in these tissues (Gan *et al.*, 2016). But it is not known, which phosphatases contribute to root derived soil phosphatase activity in low P conditions of poplar.

The main goals of this study were to investigate acid phosphatase activities of poplar (*Populus × canescens*) roots under low P conditions and to reveal which phosphatases, that might acquire P from organic P sources, are released into the growth medium under control and low P conditions. To achieve this, transcriptome and proteome analyses were combined with phosphatase activity assays. Additionally, changes in root morphology in response to low P availabilities as method for increased root surface and therefore PAP secretion area were assessed.

## 4.2 Materials and Methods

### 4.2.1 Measurement of root-associated acid phosphatase activity *in vivo*

*Populus × canescens* (INRA717 1-B4) was micropropagated and rooted on MS-medium as described in Müller *et al.* (2013). For –P plants, potassium dihydrogenphosphate was substituted by equimolar concentration of potassium chloride in the MS-medium. Phosphatase activities on the roots were measured by two methods essentially after Wang *et al.* (2011) with modifications: For measurements with 4-nitrophenyl phosphate disodium salt (pNPP; Sigma-Aldrich Chemie, Munich, Germany), the plants (height about 5 cm) were transferred after three weeks to 1.5 mL Long Ashton nutrient solution with or without P<sub>i</sub> in an 2 mL tube and adapted to laboratory conditions under slight mixing (130 rpm, GFL 3018, Gesellschaft für Labortechnik, Burgwedel, Germany).

Nutrient solution was refilled to 1.5 mL regularly. Air humidity was maintained by covering each plant with a 50 mL tube (Figure 4.1).

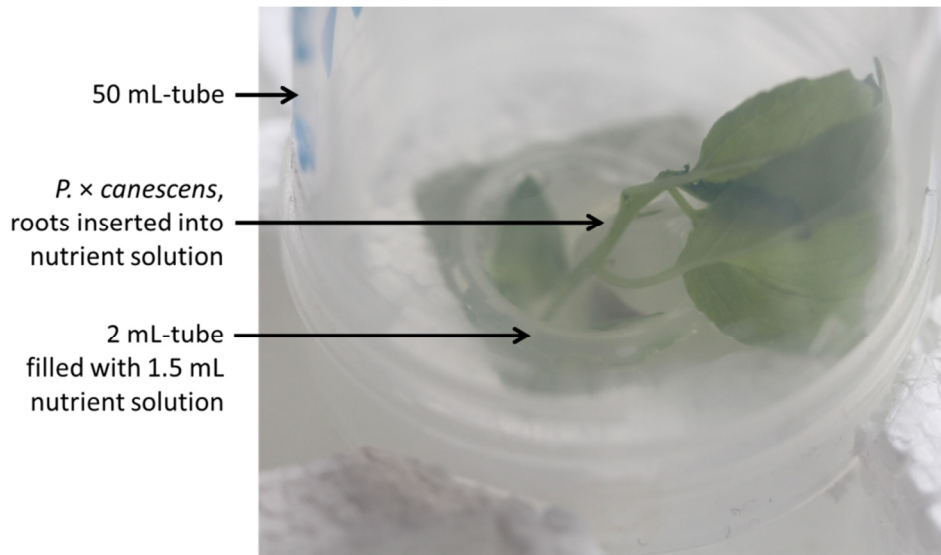


**Figure 4.1. Experimental setup for measurement of root-associated acid phosphatase activity *in vivo***

After two days, the plants were transferred to fresh Long Ashton solution (1.5 mL, without  $P_i$  for -P plants and with or without  $P_i$  for +P plants to distinguish between activity capacity and possible inhibition by P) and 200  $\mu\text{L}$  pNPP ( $1\text{mg mL}^{-1}$ ). After 1 h with slight shaking the plants were removed and 300  $\mu\text{L}$  0.4 M NaOH were added to the solution. This solution (500  $\mu\text{L}$ ) was measured in three technical replicates photometrically at 410 nm. A calibration curve with 4-nitrophenol (FLUKA, Sigma-Aldrich Chemie, Munich, Germany) was prepared for calculation of phosphatase activity. 4-nitrophenol was diluted to different amounts (0, 0.00575, 0.0115, 0.023, 0.046, 0.092, 0.184 nmol) per 1.7 mL sample with +P or -P nutrient solution (as for the plant roots) and treated in the same way. Calibration curves did not differ between +P and -P solution.

For measurement of acid phosphatase activity with 5-bromo-4-chloro-3-indolyl phosphate disodium salt (BCIP; Carl Roth, Karlsruhe, Germany), the micropropagated and to laboratory conditions adapted plants in nutrient solution were transferred to fresh Long Ashton solution (1.5 mL) containing 4 mM BCIP. After 1 h with slight shaking the plants were removed. From the solution, 0.6 mL were taken and 1 mL HCl (1 M) was added (two technical replicates per sample). The samples were mixed, incubation

for 25 min at room temperature and centrifuged for 5 min at 10000 g. The supernatant was discarded. The pellet was diluted in 1 mL dimethyl sulfoxide. Two technical replicates of this solution (500  $\mu$ L) were measured photometrically at 635 nm. Acid phosphatase activity was recorded in 4-nitrophenol produced [nmol] per hour per gram fresh mass of root or per  $\text{cm}^2$  of root surface (for measurement with pNPP) or as absorption at 635 nm ( $A_{635}$ , for measurement with BCIP) per hour per gram fresh mass of root or per  $\text{cm}^2$  of root surface, measured as described below.

For staining of phosphatase activity on the roots, micropropagated and rooted -P and +P poplars were planted into MS-medium without phosphate by placing the roots into warm but still liquid medium (about 50°C), containing 0.01 % BCIP and 0.5 % agar (Micro-Agar, Duchefa Biochemie, Haarlem, The Netherlands) in Petri dishes (12 cm x 12 cm; Greiner Bio-One, Frickenhausen, Germany) and scanned after 4 h (HP Scanjet G4050, Hewlett-Packard, Böblingen, Germany).

#### **4.2.2 Purple acid phosphatases in apoplastic washing fluid (AWF)**

Poplar plants (micropropagated and grown for three weeks on MS-medium, n=8) were cultivated in Long Ashton nutrient solution with 641  $\mu$ M or with 0.064  $\mu$ M P (missing K added as KCl) for 3 months (for medium see *Kavka and Polle, 2016*). AWF was collected after Floerl et al. (2008) with modifications: Roots were washed with tap water and infiltrated with cold 100 mM KCl (20 kPa for 15 min). Roots were patted dry, rolled into plastic foil and placed vertically into centrifuge tubes (4°C, 950 g, 8 min). AWF was collected and stored at -80°C until further analyzes. Four biological samples were pooled to result in two biological replicates per treatment. Per replicate, two samples of up to 1 mL were lyophilized at -80°C. One of these samples was used for a proteomic approach and one for protein gel electrophoresis.

For the gel electrophoresis, the lyophilized sample was dissolved in 20  $\mu$ L solution containing 50 mM sodium acetate (pH 4.9) and 10 mM  $\text{MgCl}_2$ . Two  $\mu$ L were used for measuring the protein concentration in a micro Bradford assay (Coomassie plus reagent, Thermo Scientific, Waltham, MA, USA) following the instructions manual. The protein concentration was calculated against a bovine serum albumin standard curve (12.5, 25, 50, 100 and 200  $\mu\text{g mL}^{-1}$ ). For the in-gel assay of acid phosphatase activity, the method of Wang et al. (2011) was used with modifications: The same amount of protein



(0.3 µg) for each sample was diluted in 13 µl solution as above, mixed with 13 µl sample buffer without SDS (0.06 M Tris-(hydroxymethyl)-aminomethanhydrochlorid HCl, 10 % glycerol, 0.025 % bromphenol blue (w:v)) and loaded on a Amersham ECL<sup>TM</sup> Gel 12 % (GE Healthcare Life Sciences, Freiburg, Germany). The gel was run as indicated in the manual instructions for 1.25 h, cooled on ice. The gel was washed in cold distilled water (6 times 10 min at about 50 rpm) and then in 50 mM sodium acetate (pH 4.9), 10 mM MgCl<sub>2</sub> (2 times 15 min at about 50 rpm). The gel was stained with 100 mL 50 mM sodium acetate (pH 4.9), 10 mM MgCl<sub>2</sub> solution containing 15 mg 2-naphthyl phosphate sodium salt (Sigma-Aldrich Chemie, Munich, Germany) and 75 mg Fast Black K salt (Serva, Heidelberg, Germany) at 37°C overnight with slight shaking (about 50 rpm) and scanned.

For the proteomic approach with Liquid-Chromatography Electrospray-Ionization Mass Spectrometer (LC-ESI-MS), the second aliquot of the lyophilized samples was dissolved in 80 µl 20 mM ammonium bicarbonate, 80 mM D-1,4-dithiothreitol and centrifuged at 2000 rpm for 3 min. 75 µl of 2,2,2-trifluoroethanol was added to 75 µl sample, shaken for 15 min by using a Vortex mixer, sonicated for 5 min (RK 100 H, Bandelin electronic, Berlin, Germany), shaken again for 15 min and incubated for 30 min at 60°C. After centrifugation (10 min, 16000g), 100 µl supernatant was collected into a 1.5 ml LoBind tube (Eppendorf, Hamburg, Germany). Proteins were alkylated by adding 5 µl 500 mM iodoacetamide and incubated for 30 min in dark and thereafter diluted with 50 µl water.

Proteins were purified according to Wessel and Flügge (1984) using chloroform/methanol precipitation. In short, methanol was added to the protein sample, mixed and centrifuged, and then chloroform was added, the sample mixed and centrifuged. Proteins precipitate in the interphase. The upper phase with methanol was removed and the sample again washed with methanol and centrifuged. The supernatant was removed and the protein pellet dried. Precipitates were suspended in 50 µl Tris-(hydroxymethyl)-aminomethanhydrochlorid (100 mM, pH 8.0) by sonication (RK 100 H, Bandelin electronic, Berlin, Germany) for about 3 min. Proteins in the samples were digested overnight at 37°C in a water bath after adding 5 µl trypsin solution (100 ng/µl in 10mM HCl (MS grade, Promega)). The digestion was stopped by adding 20 µl ammonium formate (20 mM, pH 10). Samples were mixed and centrifuged (20 min, 16000 g). 60 µl of sample were immediately purified by using StageTips (Stop-and-go-

extraction tips) (*Rappsilber et al.*, 2007) prepared from three layers of Empore 3M-C18 filter (3M, USA) and conditioned with ammonium formate (20 mM, pH 10). The peptides were eluted from the tips with 60 % acetonitrile (Ultima LC-MS grade, Fisher Scientific) in ammonium formate (20 mM). After drying for 10 min in a vacuum concentrator (Concentrator 5301, Eppendorf, Hamburg, Germany) peptides were stored at -20°C. Peptides were dissolved in 5 µl 2 % acetonitrile in water with 0.1 % formic acid (all solvents in Ultima LC-MS quality) and analyzed by “trap & elute” mode (Eksigent 420, Sciex, USA) using a 2.5 cm 100 µm id pre-column packed with 5 µm Reprosil-Pur C18-AQ (Dr. Maisch GmbH, Ammerbuch, Germany) and 30 cm 50 µm id analytical column packed with 3 µm Reprosil-Gold C18. Samples were separated in a gradient mode at 260 nL min<sup>-1</sup> solvent flow with solvent A (100 % water with 0.1 % formic acid in water (Optima Gold quality, Thermo Fisher Scientific, Braunschweig, Germany). Solvent B consisted of 0.1 % formic acid in acetonitrile (Optima Gold quality, Thermo Fisher Scientific, Braunschweig, Germany) and served as the eluent in the following gradient: initially 5 %, 100 min to 35 %, 20 min to 50 % and 2 min to 95 %. The mass spectrometry system consisted of Hybrid Quadrupole-TOF LC/MS/MS Mass Spectrometer TripleTOF 5600+ (Sciex, USA), nano-spray source Nanospray III (Sciex) and Analyst 1.7 software. MS spectra in the positive mode were detected in a range of 300 to 2000 Da and 30 most intensive ions with charge 2+ to 5+ were fragmented in the MS/MS mode. Analyses of MS spectra and protein identification were performed by ProteinPilot 5.0 (Sciex, Darmstadt, Germany). The protein identification database consisted of *Populus trichocarpa* protein sequences (JGI; *Tuskan et al.*, 2006) combined with a common contaminants dataset (Sciex, Darmstadt, Germany). Carbamidomethylation of cysteine and trypsin cleavage were set as fixed modifications. Searches were performed in “false discovery rate” mode with thorough settings including biological modifications and amino acid substitutions. Results were filtered for at least two peptides per protein and an unused score of at least four to exclude proteins from the results that were not sufficiently supported by peptide sequences.

### 4.2.3 Gene expression analysis

The microarrays with the accession number E-MTAB-3934 (*Kavka and Polle, 2016*) from the EMBL-EBI ArrayExpress database (<http://www.ebi.ac.uk/arrayexpress/>) were used: In this experiment, poplar plants were grown in sand culture irrigated with Long Ashton nutrient solution containing three different phosphate concentrations (641  $\mu\text{M}$  - HP, 6.4  $\mu\text{M}$  - MP, 0.064  $\mu\text{M}$  - LP) with three biological replicates per treatment with uppermost leaves and fine roots as samples. For annotation of the Affy probe set IDs to gene model IDs, the best hit in the annotation file of the AspenDB (*Tsai et al., 2011*) was used. For each purple acid phosphatase, the mean expression value of the three replicates was calculated. When there were more than one probe set per gene, the mean value of all probe sets were calculated. The  $\log_2$ -expression values for each gene were z-transformed across all arrays. Heatmap of normalized expression values was created using “heatmap.2” function implemented in the R (*R Development Core Team, 2012*) package “gplots” (*Warnes, 2012*).

### 4.2.4 Quantitative Real Time PCR

To remove contaminating DNA, an aliquot of the RNA samples that were also used for microarray analyses (200 ng  $\mu\text{L}^{-1}$  in 25  $\mu\text{l}$ ) were treated with Ambion® Turbo DNA-free™ kit (Life Technologies, Carlsbad, CA, USA) two times according to the manual instructions and transcribed to cDNA (0.5  $\mu\text{g}$ ) with the RevertAid First Strand cDNA Synthesis Kit and First Strand cDNA Synthesis Kit (Thermo Fisher Scientific, Braunschweig, Germany) using oligo(dT)-primers. To validate the microarray, four genes were chosen (PtPAP1 (Potri.005G233400), PtPAP30 (Potri.012G042200), Potri.013G005700, Potri.007G089000) with different expression patterns over all samples on the microarrays. Primers used for quantitative Real Time PCR (qRT PCR) were described in Janz et al. (2012; Potri.013G005700, Potri.007G089000, Potri.001G309500) or designed using OligoExplorer 1.5 and checked with OligoAnalyzer 1.5 (both Gene Link, Hawthorne, NY, USA, Table 4.1 for detailed information). At least one primer for each gene was designed to cross an exon-exon junction. For each gene and sample (three biological replicates per treatment, fine roots and leaves), at least two technical replicates were analyzed by qRT PCR with

LightCycler 480® (Roche Diagnostics, Mannheim, Germany). The reaction volume of 20 µl consisted of 10 µl SYBR Green I Master kit (Roche Diagnostics, Mannheim, Germany), 2 µl of forward and reverse primer (10 µM), 1 µl nucleic free water and 5 µl cDNA-solution (1:10 dilution). After pre-incubation (95°C, 5 min), 45 or 55 cycles of amplification followed: 95°C for 10 s, 57°C for 10 s and 72°C for 20 s. Melting curve (95°C 5 s, 65°C 1 min to 97°C with 0.11°C/s) analyses implemented in the LightCycler 480® software were used to assess primer specificity.

To calculate efficiency, raw data were converted using LC480 conversion (version 2014.1; [www.hartfaalcentrum.nl/index.php?main=files&sub=LC480Conversion](http://www.hartfaalcentrum.nl/index.php?main=files&sub=LC480Conversion)) and loaded into LinRegPCR (version 2016.0; *Ruijter et al.*, 2009). The mean efficiency for each primer pair was calculated over all samples after baseline subtraction and given in Table 1. Quantification cycle-values were calculated using the fluorescence threshold of 3.597 (lowest threshold of all genes). Relative expressions for each sample were calculated against two reference genes using the formula

$$\text{Relative Expression} = \frac{\sqrt{E_{(\text{Ref}_1)}^{Cq} \times E_{(\text{Ref}_2)}^{Cq}}}{E_{(\text{GOI})}^{Cq}}$$

E: efficiency of primer for gene

Cq: quantification cycle value

(GOI): efficiency and Cq for gene of interest

(Ref<sub>i</sub>): efficiency and Cq for reference gene *i* (*Hellemans et al.*, 2007).

**Table 4.1: Primers used for qRT PCR.**

Potri.ID	Affy IDs	Primer name	Primer sequence (5'-3')	Primer efficiency
Potri.005G233400 (PtPAP1)	PtpAffx.33535.1.A1_at	Pc005_fw	GTTGCATACAACATCGTGAACG	1.870
	PtpAffx.33535.3.S1_at	Pc005_rev	CTGTCATGCTGGTCACTAATC	
Potri.012G042200 (PtPAP30)	Ptp.6082.1.S1_at	Pc012_fw	AGCACAAGTTAAGCCTTCACC	1.924
		Pc012_rev	TTCAGCCAATTCAGCATCGAC	
Potri.013G005700 (Xyloglucan Endotransglucosylase)	Ptp.3948.1.S1_at	Pc013G005700_fw	CCACAAAGAATCATTCTCTCTG	1.836
	PtpAffx.102427.1.A1_at	Pc013G005700_rev	AAACTAGAGTAAATTCTCATTGG	
Potri.007G089000 (Myo-Inositol-1-Phosphate Synthase)	PtpAffx.102427.1.A1_s_at			1.874
	PtpAffx.249.474.S1_at	Pc007G089000_fw	CCCATGGTGAACCCAGATG	
	PtpAffx.249.570.S1_a_at	Pc007G089000_rev	TCAGGGTCGTAAATTCCAGG	
	PtpAffx.249.570.S1_at			
Potri.001G047200 (PPR-repeat as reference gene)	PtpAffx.36446.1.A1_at			1.908
	PtpAffx.200189.1.S1_at	Pc001G047200_fw	GGCTGAGGAATGTCTGAATGG	
Potri.001G309500 (Actin as reference gene)		Pc001G047200_rev	AGAACGCAACATCATGGAAACC	1.876
	Ptp.6486.1.S1_s_at	Aktin9_fw	TGGTGGTTCCACTATGTTCC	
	PtpAffx.1258.1.S1_s_at	Aktin9_rev	TGGAAATCCACATCTGCTGG	
	PtpAffx.1258.4.S1_s_at			

Corresponding Potri.IDs and Affy IDs for probe sets on microarray and primer efficiency calculated by LinRegPCR are given; primers for Potri.013G005700, Potri.007G089000 and Potri.001G309500 were obtained from Janz et al. (2012).

### 4.2.5 Assessment of root morphological parameters

For measuring the root surface and root length in different width classes, roots were scanned (HP Scanjet G4050, Hewlett-Packard, Böblingen, Germany) before drying and analyzed with WinRhizo (version 2012b, Regent Instruments Inc., Ottawa, Canada). To get optimal scans, following parameters for a transmitted-light-scan were set: scanning resolution of 300 dpi, greyscale, middle tone: -30, bright image areas: -100, shadows: -100, gamma: 1.0.

Roots from acid phosphatase activity measurements were scanned directly after the experiment.

HP, MP and LP fine roots were taken from another plant set and washed before scanning. In the case of HP roots only an aliquot was scanned.

Photos of root hairs were taken in water with a digital camera (DFC420 C, Leica Microsystems Ltd., Germany) attached to a stereomicroscope (M205 FA, Leica Microsystems Ltd., Wetzlar, Germany).

### 4.2.6 Phylogeny of PAPs in poplar compared with *Arabidopsis*, rice and maize

All protein sequences and gene IDs were obtained from Phytozome v9.1 ([www.phytozome.net](http://www.phytozome.net), Goodstein *et al.*, 2012). For domain comparisons the Pfam database ([pfam.xfam.org](http://pfam.xfam.org)) was used. All annotated (Wang *et al.*, 2014) *Arabidopsis* PAP protein sequences ([http://phytozome.jgi.doe.gov/pz/portal.html#!info?alias=Org\\_Athaliana](http://phytozome.jgi.doe.gov/pz/portal.html#!info?alias=Org_Athaliana)) were used for a BlastP search (e-value cutoff at  $e^{-20}$ ) against the *Populus trichocarpa*, *Oryza sativa* ([http://phytozome.jgi.doe.gov/pz/portal.html#!info?alias=Org\\_Osativa](http://phytozome.jgi.doe.gov/pz/portal.html#!info?alias=Org_Osativa)) and *Zea mays* proteomes ([http://phytozome.jgi.doe.gov/pz/portal.html#!info?alias=Org\\_Zmays](http://phytozome.jgi.doe.gov/pz/portal.html#!info?alias=Org_Zmays)), but only proteins with a Metallophos or Metallophos C domain were kept, as these were present in every *Arabidopsis* PAP. The alignment was performed using the online tool ClustalW2 ([www.ebi.ac.uk/Tools/msa/clustalw2/](http://www.ebi.ac.uk/Tools/msa/clustalw2/)) with default settings. The PHYLIP package (Felsenstein, 1993) was used to calculate a consensus (extended majority rule) neighbor joining phylogenetic tree using 500 replicates for bootstrapping and Jones-

Taylor-Thornton model for computing distance matrices. MEGA6 (Tamura *et al.*, 2013) was used to display and edit the phylogenetic trees. Phylogenetic subgroups were named after Li *et al.* (2002). Poplar PAPs were named according to their position in the phylogenetic tree, rice PAP names are according to Zhang *et al.* (2011), maize PAP names according to González-Muñoz *et al.* (2015) and *Arabidopsis* PAP names according to Li *et al.* (2002). The 1 kb upstream region of each poplar gene coding for a putative PAP was obtained from Phytozome using the BioMart tool (<http://phytozome.jgi.doe.gov/biomart/martview/16e565cddceb03f127d3e5b55e576a6f>) and used for a motif search with PLACE (Higo *et al.*, 1999). Protein sequences were used for prediction of the subcellular locations of the proteins with TargetP v. 1.1 (<http://www.cbs.dtu.dk/services/TargetP/>; Emanuelsson *et al.*, 2000).

#### **4.2.7 Statistical analyses**

R (versions 2.14.2 and 3.0.2, *R Development Core Team*, 2012, [www.r-project.org](http://www.r-project.org)) was used for statistical analyses. One-Way-ANOVA and Tukey's HSD were performed on original or transformed data. Residuals were checked visually for normal distribution and homogeneity of variance and transformed logarithmically ( $\log_2$ ) or by square root if needed. Means were considered to differ significantly between treatments, if  $P \leq 0.05$ . The P-value was Bonferroni adjusted for ANOVAs on gene expression data. Figures show mean value  $\pm$  standard error.

### **4.3 Results**

#### **4.3.1 Phylogeny of PAPs**

The PAPs proteins of poplar clustered into the three main clades (I, II and III) known from *Arabidopsis* (Figure 4.2A) with three subclades in cluster I (Ia with Ia-1 to Ia-3 and five unclustered maize and rice PAPs, Ib-1 and Ib-2), three subclades in cluster II (IIa to IIc) and two subclades (IIIa and IIIb) in cluster III (Figure 4.2B). We found 33 poplar PAPs, compared with the 29 PAPs known from *Arabidopsis*. Our search revealed 30 rice PAPs: the 26 PAPs found by Zhang *et al.* (2011) and four additional

ones (Figure 4.2). Of the 33 maize PAPs found by González-Muñoz et al. (2015) not all were retrieved because ZmPAP7c and ZmPAP28b were not found by our approach.

As expected, the nearest homologs of poplar PAPs were *Arabidopsis* PAPs (Figure 4.2B). In the PAP clusters Ib-1, Ib-2 and IIIa, there was a direct orthologous group of poplar and *Arabidopsis* proteins for each group of rice and maize proteins (Figure 4.2B). In all other clusters, there was mostly one branch each with monocot and dicot proteins (Figure 4.2B). Cluster Ia-1 consisted of only *Arabidopsis* proteins, in cluster IIc no *Arabidopsis* proteins but two poplar proteins were present. Four poplar proteins were orthologous to the two *Arabidopsis* proteins AtPAP10 and AtPAP12, one rice protein (OsPAP10a) and one maize protein (ZmPAP10); three poplar proteins were orthologous to AtPAP26, OsPAP26 and ZmPAP26. Additionally multiplied poplar genes were found for AtPAP1, AtPAP17, and AtPAP14 compared with *Arabidopsis*, rice and maize.

Among the 33 poplar PAPs 28 were targeted to the secretion pathway; one member of cluster Ia-2 (Potri.004G160100) to mitochondria and four had no distinct target sequence (Table 4.2).

P1BS elements, which are known to play a role in the up-regulation of gene expression in response to phosphate starvation (Bustos et al., 2010), were present in the 1 kb upstream sequence of ten poplar PAP genes from clusters I and III.



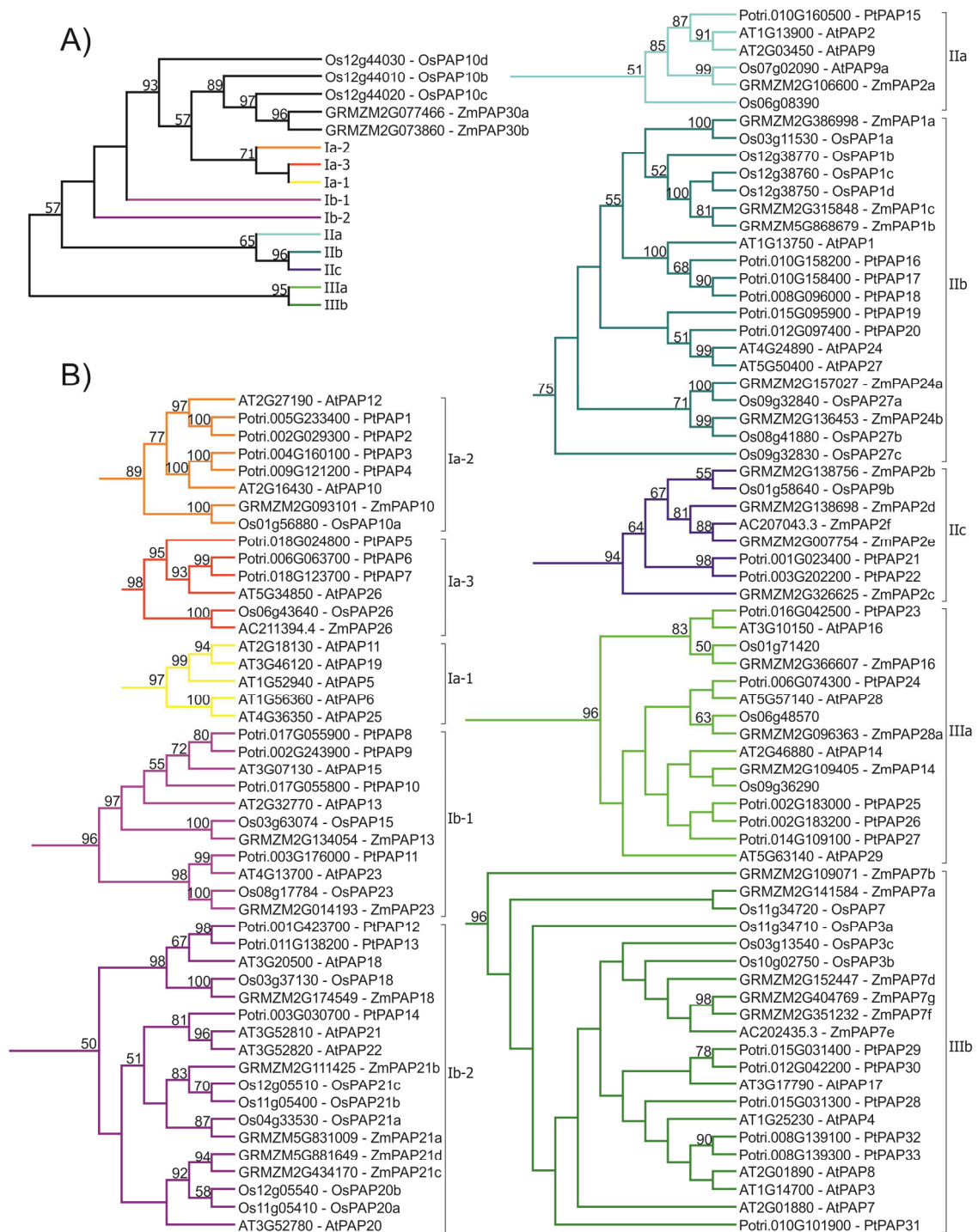


**Figure 4.2. Neighbor-Joining tree (Jones-Taylor-Thornton model, 500 bootstraps) of the amino acid sequences for purple acid phosphatases in poplar.** Poplar (Potri), *Arabidopsis* (AT), rice (Os) and maize (GRMZM and AC); A: unrooted compressed phylogenetic tree; B: expanded view of the clusters, names of clusters modified after Li et al. (2002), names for OsPAPs from Zhang et al. (2011), names for ZmPAPs from González-Muñoz et al. (2015). Only bootstrap values  $\geq 50$  are displayed.

**Table 4.2: Summary of in silico analyses for poplar purple acid phosphatases.**

Cluster	GeneID	Gene name	PLACE P1BS- Locali- zation	TargetP		Affy IDs
				Locali- zation	RC	
Ia-2	Potri.002G029300	<i>PtPAP2</i>	603	–	4	PtpAffx.33535.2.A1_at
	Potri.004G160100	<i>PtPAP3</i>		M	5	PtpAffx.662.1.A1_at
	Potri.005G233400	<i>PtPAP1</i>		S	1	PtpAffx.33535.3.S1_at PtpAffx.33535.1.A1_at
	Potri.009G121200	<i>PtPAP4</i>		–	5	PtpAffx.662.3.A1_at (n.d.)
Ia-3	Potri.006G063700	<i>PtPAP6</i>	927	S	1	PtpAffx.38937.2.A1_at (n.d.) PtpAffx.45845.1.S1_at
	Potri.018G024800	<i>PtPAP5</i>	635	S	2	PtpAffx.125017.1.S1_at (n.d.) PtpAffx.125017.1.S1_s_at (n.d.) Ptp.1772.1.A1_at PtpAffx.214211.1.S1_at
	Potri.018G123700	<i>PtPAP7</i>	298	S	1	NA
Ib-1	Potri.002G243900	<i>PtPAP9</i>	449	S	1	Ptp.5137.1.S1_at PtpAffx.66415.1.A1_s_at PtpAffx.203446.1.S1_at
	Potri.003G176000	<i>PtPAP11</i>		–	3	PtpAffx.94885.1.S1_s_at (n.d.) PtpAffx.213843.1.S1_at (n.d.)
	Potri.017G055800	<i>PtPAP10</i>		S	1	PtpAffx.121479.1.A1_at PtpAffx.213844.1.S1_at (n.d.)
	Potri.017G055900	<i>PtPAP8</i>		S	1	
Ib-2	Potri.001G423700	<i>PtPAP12</i>	544	S	1	PtpAffx.145701.1.S1_s_at PtpAffx.211221.1.S1_at PtpAffx.160811.1.S1_s_at
	Potri.003G030700	<i>PtPAP14</i>	925	S	2	PtpAffx.221489.1.S1_at PtpAffx.221491.1.S1_at
	Potri.011G138200	<i>PtPAP13</i>		S	1	PtpAffx.160811.2.S1_at PtpAffx.145392.1.A1_at
IIa	Potri.010G160500	<i>PtPAP15</i>		S	1	PtpAffx.77953.1.S1_at
IIb	Potri.008G096000	<i>PtPAP18</i>		S	1	PtpAffx.124035.1.S1_s_at PtpAffx.207897.1.S1_at (n.d.) PtpAffx.101405.1.A1_at (n.d.)
	Potri.010G158200	<i>PtPAP16</i>		–	2	PtpAffx.35988.1.A1_at PtpAffx.35988.4.A1_a_at
	Potri.010G158400	<i>PtPAP17</i>		S	1	PtpAffx.140167.1.A1_at
	Potri.012G097400	<i>PtPAP20</i>		S	2	PtpAffx.143041.1.S1_s_at PtpAffx.138433.1.S1_s_at (n.d.) Ptp.2985.1.S1_at PtpAffx.210647.1.S1_s_at
	Potri.015G095900	<i>PtPAP19</i>		S	2	PtpAffx.212872.1.S1_s_at

**Table 4.2 (continued)**

Cluster	GeneID	Gene name	PLACE P1BS- Locali- zation	TargetP		Affy IDs
				Locali- zation	RC	
IIc	Potri.001G023400	<i>PtPAP21</i>		S	2	PtpAffx.200148.1.S1_at (n.d.) PtpAffx.34917.2.S1_a_at PtpAffx.34917.1.S1_at
	Potri.003G202200	<i>PtPAP22</i>		S	1	PtpAffx.203537.1.S1_at (n.d.)
IIIa	Potri.002G183000	<i>PtPAP25</i>		S	3	PtpAffx.3736.1.S1_at
	Potri.002G183200	<i>PtPAP26</i>	892	S	3	NA
	Potri.006G074300	<i>PtPAP24</i>		S	1	NA
	Potri.014G109100	<i>PtPAP27</i>		S	2	NA
	Potri.016G042500	<i>PtPAP23</i>	676	S	1	PtpAffx.213280.1.S1_at
IIIb	Potri.008G139100	<i>PtPAP32</i>		S	1	PtpAffx.95224.1.A1_at
	Potri.008G139300	<i>PtPAP33</i>		S	1	NA
	Potri.010G101900	<i>PtPAP31</i>		S	5	PtpAffx.208843.1.S1_at (n.d.)
	Potri.012G042200	<i>PtPAP30</i>	477, 523, 531	S	2	Ptp.6082.1.S1_at
	Potri.015G031300	<i>PtPAP28</i>		S	1	NA
	Potri.015G031400	<i>PtPAP29</i>		S	1	PtpAffx.7937.1.A1_at

GeneID: Poplar gene IDs in genome v3; PLACE P1BS-Localization: location of P1BS-motif(s) in 1 kb upstream region of the gene; TargetP Localization: predicted localization of protein (M: mitochondria, S: secreted, \_: none of above and not chloroplast and cytoplasm, RC: Reliability Class (best 1 to 5); Affy IDs: probe names on annotated for the gene by Tsai et al. (2011), n.d.: expression not detected, NA: gene is not on array

### 4.3.2 Expression of poplar PAPs is enhanced under phosphate deprivation in roots and leaves

Six of the poplar PAPs present in the phylogenetic tree were not present as probe sets on the Affymetrix microarray (*PtPAP7*, *PtPAP24*, *PtPAP26-28*, *PtPAP33*). Four PAPs (*PtPAP4*, *PtPAP8*, *PtPAP22*, *PtPAP31*) could neither be detected under control conditions nor under phosphate deprivation regardless the tissue analyzed (Table 4.2). The genes had no truncated sequence compared with sequences of expressed genes. Therefore, they may be expressed in tissues or conditions not analyzed here.

The microarray data were validated by qRT PCR for two PAPs (*PtPAP1*, *PtPAP30*) with strong increase under P limitation and two genes with opposing expression patterns (Potri.013G005700 (xyloglucan endotransglucosylase), Potri.007G089000 (myo-

inositol-1-phosphate synthase)). qRT PCR and transcript abundance data of the microarray showed a strong correlation (Figure 4.3).

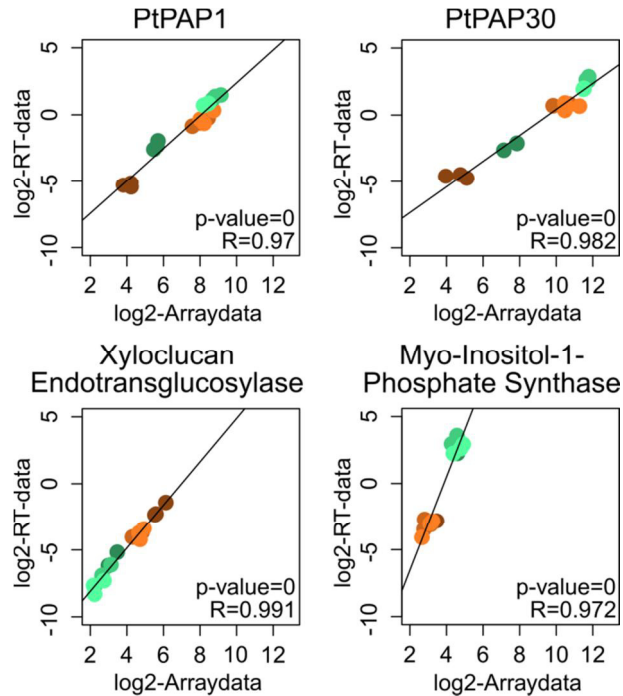


**Figure 4.3. Verification of array data by qRT PCR.** Red: root samples, green: leaf samples, dark: HP, middle: MP, light: LP; log<sub>2</sub>-value for expression with p-value and R-value of correlation (R function cor.test)

Based on their z-transformed expression values under control (HP) and low P (MP, LP) the PAPs of poplar could be divided into three groups (Figure 4.4). The first group consisted of PAPs that are upregulated under P deprivation in both roots and leaves. Among them, *PtPAP17*, *PtPAP18* and *PtPAP32* exhibited a higher expression in roots than in leaves, *PtPAP1*, *PtPAP16*, *PtPAP21*, *PtPAP29* and *PtPAP30* a higher expression in leaves than in roots, while the expression of *PtPAP9* and *PtPAP14* did not differ between roots and leaves (Figure 4.4).

The second group contained four genes with highest expression under HP conditions that were unresponsive to or showed lower transcript abundance in low P conditions (Figure 4.4). These genes were all from cluster I: *PtPAP3*, *PtPAP5*, *PtPAP6* and *PtPAP12*.

The third group was formed by genes with higher expressions in leaves than in roots only under low P conditions (*PtPAP11*, *PtPAP15* and *PtPAP23*), and genes with generally higher transcript levels in leaves (*PtPAP2*, *PtPAP19*, *PtPAP25*). *PtPAP10* had

the highest transcript level in HP leaves and *PtPAP13* and *PtPAP20* exhibited no significant differences in expression (Figure 4.4).

The presence of a P1BS-element in the 1 kb promoter sequence had no clear influence on the expression under P deprivation, because half of the eight genes containing a P1BS-element in the promoter on the array that were analyzed here did not show any up-regulation in low P<sub>i</sub> (*PtPAP2*, *PtPAP5*, *PtPAP6*, *PtPAP12*). The other four genes were upregulated in roots and leaves (*PtPAP14*, and *PtPAP30* with three P1BS elements) or only in leaves (*PtPAP11*, *PtPAP23*) under low P<sub>i</sub> availability.

Based on the expression values of the PAP family the tissues were clustered into one group with HP tissues and one group containing the clusters MP and LP roots and MP and LP leaves (Figure 4.4). Only *PtPAP5* had different expression between MP and LP with lower expression in LP leaves compared to MP and also HP leaves.

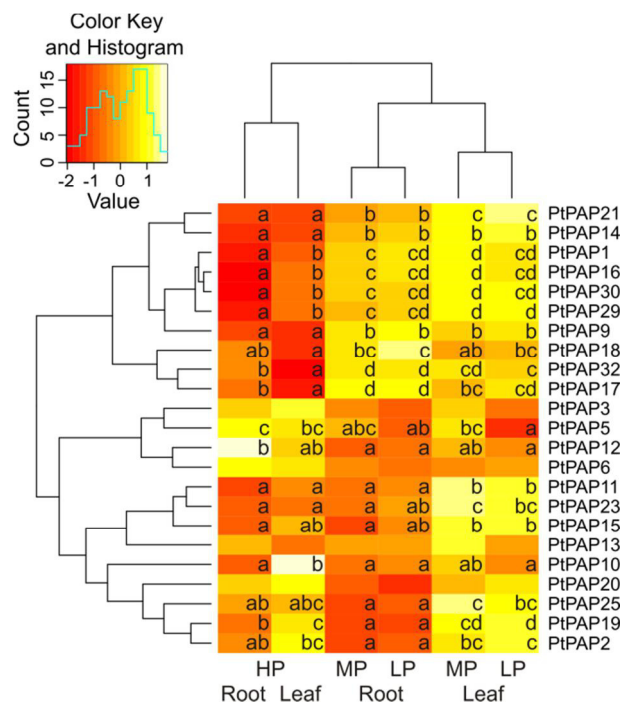


**Figure 4.4. Expression of purple acid phosphatases in P deficient poplars.** Heatmap of the relative expression of putative purple acid phosphatases in the three uppermost leaves and fine roots of poplar plants grown with different P concentrations in the nutrient solution (HP: 641  $\mu$ M, MP: 6.4  $\mu$ M, LP: 0.064  $\mu$ M). Red colors indicate lower and yellow to white color higher values after z-transformation of the transcript abundances of each gene across all analyzed tissues and P conditions. Different letters indicate significant differences in expression of each gene (adj.  $P \leq 0.05$ , ANOVA and Tukey's honest significance test,  $n=3$ , mean of normalized expression for each gene is color coded).

### 4.3.3 Roots of P deprived poplar have altered root morphology and higher acid phosphatase activity

Changes in root morphology of three-week-old micropropagated poplars *in vitro* grown in agar medium were visible upon P deprivation (Figure 4.5A). Plants grown with 625  $\mu\text{M}$  P had a rounded root tip with a distinct root cap (Figure 4.5B), whereas plants grown without P developed long peaked root tips (Figure 4.5C). Root hairs were longer and in greater number in -P plants (Figure 4.5C). Mean root diameter was higher in -P plants than in +P plants (Figure 4.6A). This change was also detected in fine root morphology after growth in sand culture. Only in HP plants very fine roots with less than 2 mm diameter were present in high numbers (Figure 4.6B). The roots of MP and LP plants had longer and more root hairs than roots of HP plants (Figure 4.7).

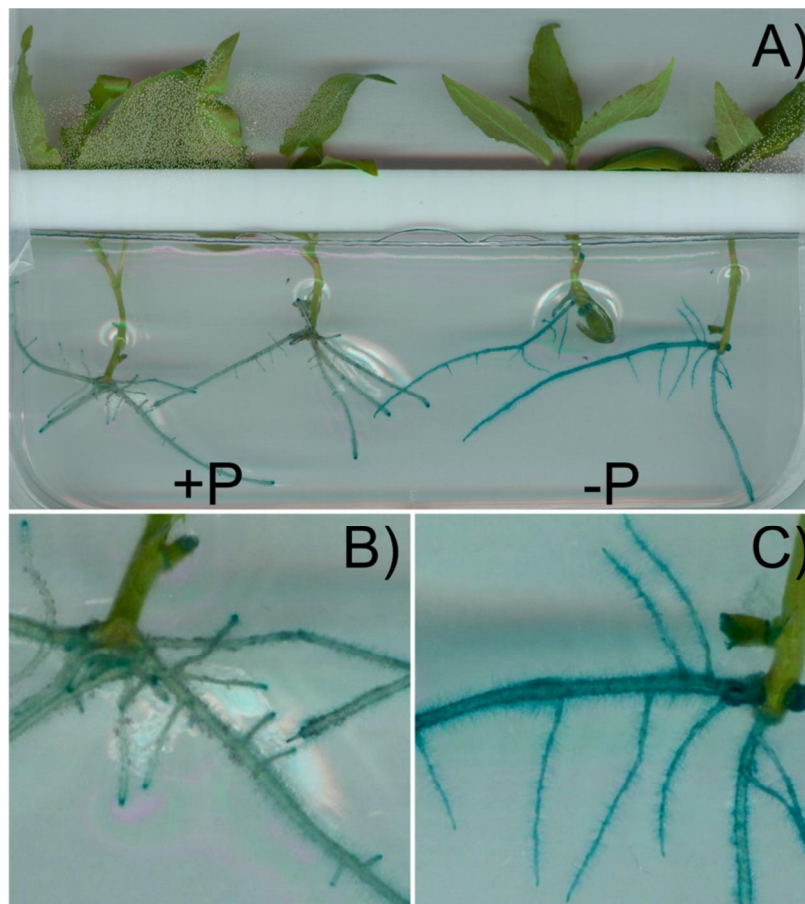


**Figure 4.5. Poplar roots grown with or without Pi stained for acid phosphatase activity.** 0.01 % BCIP in medium, staining for 4 h. Blue color indicates phosphatase activity, A) side length of picture: 12 cm, zoom on roots of +P (B), -P (C) plants, zoomed picture side length: 1.5 cm

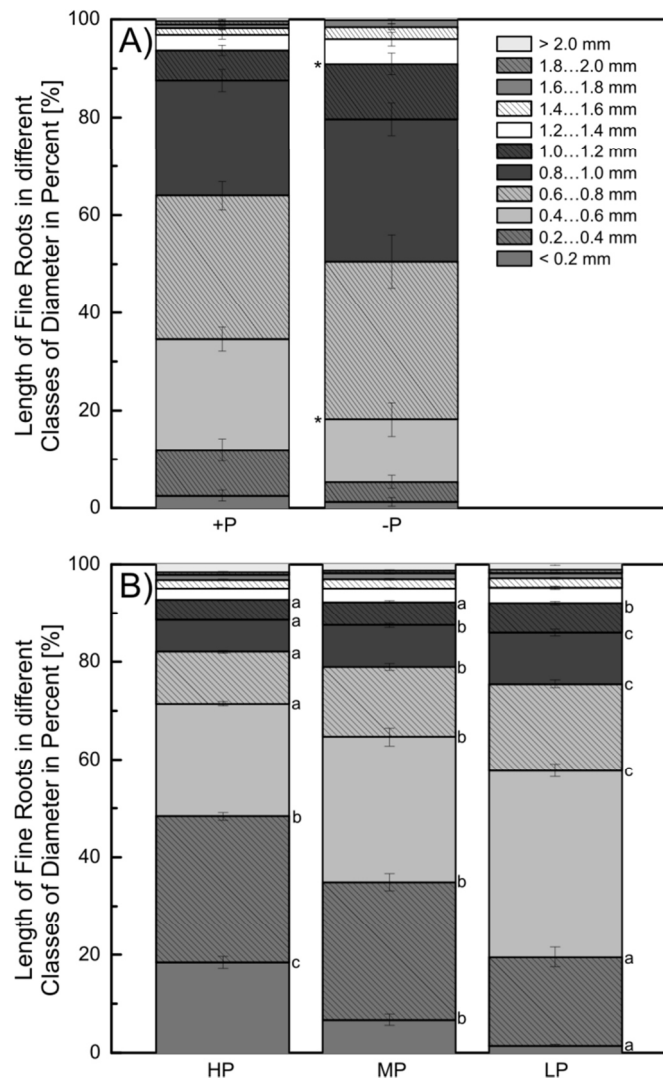


**Figure 4.6. Length of roots in different root diameter classes in percent of total root length.** A) micopropagated plants from measurement of acid phosphatase activity in vivo (n=24 for +P, n=12 for -P), and B) HP, MP and LP plants (n=8). Stars and different letters indicate significant differences at  $P \leq 0.05$ , ANOVA and Tukey's honest significance test.

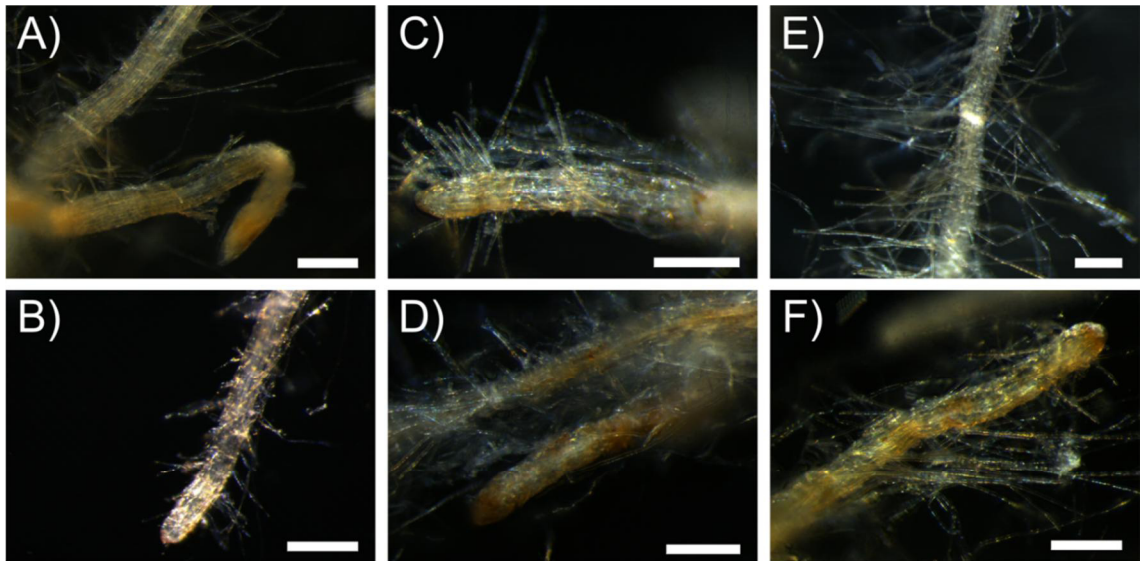


**Figure 4.7. Roots hairs of poplars grown with different P availabilities.** A,B) HP, C,D) MP, E,F) LP plants, scale bar = 200  $\mu\text{m}$ .

Roots of  $-P$  poplar showed higher root-associated PAP activity than those of  $+P$  plants grown with  $625 \mu\text{M P}$  (Figure 4.5A). In  $+P$  roots, the PAP activity was high in root caps and in small patches across the root surface, but otherwise negligible (Figure 4.5B). Strong PAP activity was distributed across root surface and root hairs of  $-P$  roots (Figure 4.5C). These results were also confirmed for *Arabidopsis* (Supplemental materials). To test which AtPAP contribute to root-associated PAP activity, roots of different *Arabidopsis* mutants were stained for PAP activity. But only in the *pap10*-mutant PAP staining was suppressed (Supplemental material).

The two tests (BCIP and pNPP) for quantification of PAP activity of poplar roots grown in agar medium showed consistently a higher PAP activity for  $-P$  roots than for  $+P$  roots (Figure 4.8). Because PAP activity was shown to be inhibited by P, the root PAP activity of  $+P$  plants was tested for two reaction media: with P (PAP activity of roots in growth medium) and without P (possible PAP activity of roots). The PAP activity was slightly but not significantly inhibited in  $P_i$  consisting medium (Figure 4.8).



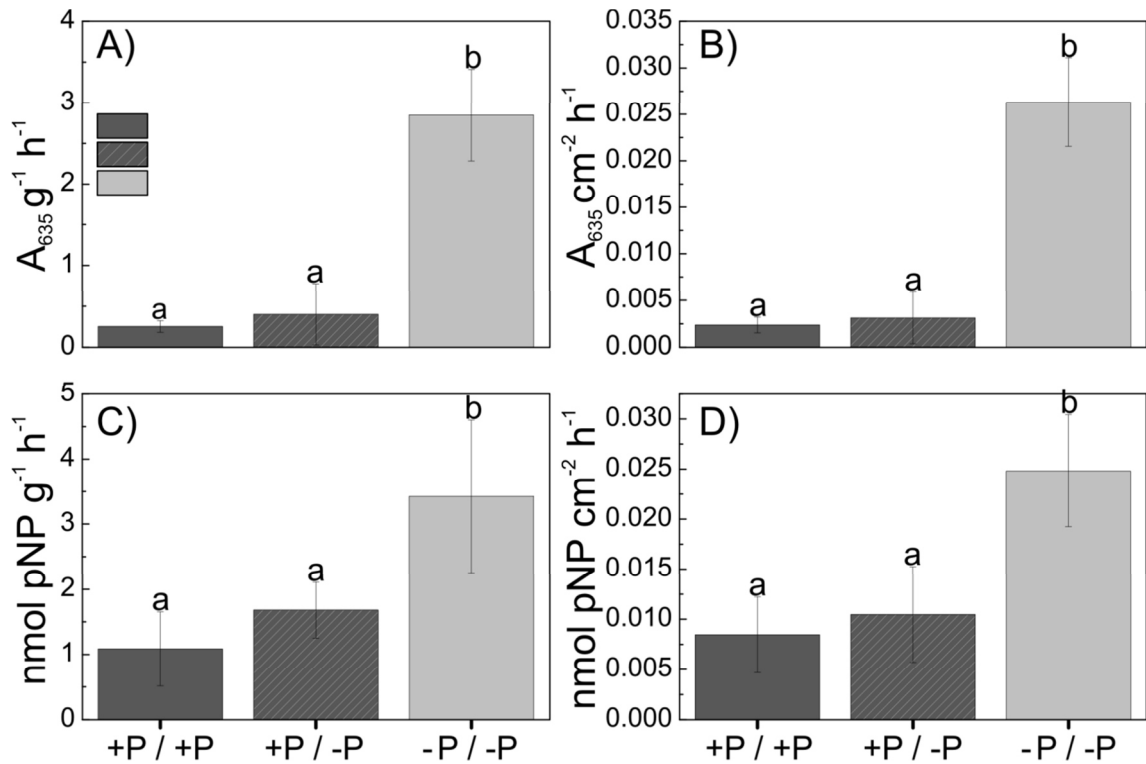


**Figure 4.8. Root associated acid phosphatase activity of poplar.** Poplar grown with phosphate and measured in solution with phosphate (+P/+P), measured in solution without phosphate (+P/-P) and grown and measured in solution without phosphate (-P/-P). A), B) measured with BCIP as substrate, C), D) measured with pNPP as substrate, activity calculated A), C) per gram root fresh mass, B), D) per cm<sup>2</sup> root surface

#### 4.3.4 Roots of P deprived poplar secrete additionally PtPAP1

PAP staining of native gels revealed one PAP band for AWFs of HP poplars and two bands for those of LP poplars (Figure 4.9). The staining showed a higher PAP activity in LP PAPs than in HP PAPs (Figure 4.9). In proteins of HP and LP AWFs was one isoform with slow running behavior (E1) that was stained only slightly. A second isoform (E2) only seen in the LP samples had a slightly faster running behavior and was stained stronger than the slower isoform.

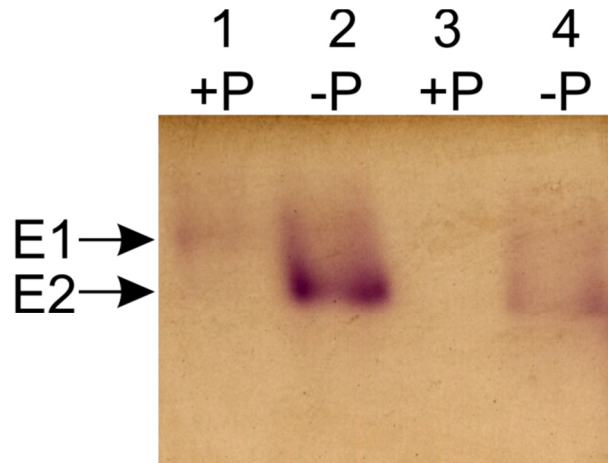


**Figure 4.9. In gel-assay of acid phosphatase activity from poplar root AWF.** Poplars were grown with (+P) or without phosphate (-P), E1 and E2: phosphatase isoforms

To identify the PAPs present in the apoplast, proteomic analyses were conducted. In general, AWFs from LP roots contained a lower number of proteins than those from HP roots (Table S4.1). In the AWF of HP plants, we detected PtPAP4 and PtPAP17 or the homologous PtPAP18 with PtPAP4 being most abundant. Of these PAPs, PtPAP4 had no secretion signal (Table 4.2). Although there were less total protein numbers present, PtPAP1 was found only in LP samples. This PAP was not present in HP AWF.

To test whether PtPAP1 could rescue PAP staining of the *atpap10*-mutant at low P conditions, the *PtPAP1* coding sequence was transformed into the *Arabidopsis pap10*-mutant (Supplemental material). Cloning and transformation of *PtPAP1* was successful, but expression in *Arabidopsis* was not yet successful (Supplemental material).

## 4.4 Discussion

Here, the complete phylogeny of the purple acid phosphatase family in poplar is presented in comparison with the model plant *Arabidopsis* and the model monocotyledonous crop plants rice and maize. Although the total numbers of sequences found for PAPs in poplar were similar to those of *Arabidopsis*, rice and maize, phylogenetic clustering suggested evolutionary differences. For example, sub-cluster Ia-1 consisted of only *Arabidopsis* PAPs implying involvement of these proteins in *Arabidopsis*. AtPAP5 of this cluster plays a role in resistance to pathogens and is

upregulated during the early stages of pathogen defense (Ravichandran *et al.*, 2013). For other *Arabidopsis* PAPs, duplicated or multiplied genes were found in poplar. Relatively fast substitutions in the *Arabidopsis* genome and genome duplication events in the evolution of poplar (Van de Peer *et al.*, 2009) led to this phylogenetic clustering. The four poplar PAPs that were not detected under our conditions at expression level in roots and leaves are duplicated genes compared to *Arabidopsis*. Therefore, these genes may have already lost their function or they may be expressed under different conditions or in different tissues than those in this study. Other poplar PAPs may have gained functional diversification during duplication. For example the closely related *PtPAP1* and *PtPAP2* have different expression patterns: *PtPAP1* was transcriptionally upregulated during P starvation in both roots and leaves whereas *PtPAP2* had the highest transcript abundances in leaves and was unresponsive to P starvation.

In this study, enhanced acid phosphatase activity of poplar roots during P starvation was shown for *P. × canescens*. This was shown before for different P deficient poplar species (*P. tremuloides*, *P. simonii*, *P. × euramericana*; Desai *et al.*, 2014; Gan *et al.*, 2016) without knowledge of the participating enzymes. In this study, two PAP isoforms were detected by in-gel PAP staining of AWF proteins. Low activity of one phosphatase isoform was detected in AFW proteins from LP and HP plants. One isoform with high activity was found only in LP samples.

The expression levels of *PtPAP17*, *PtPAP18* and *PtPAP32* were higher in roots than in leaves. Other PAPs (*PtPAP1*, *PtPAP9*, *PtPAP14*, *PtPAP16*, *PtPAP21*, *PtPAP29*, *PtPAP30*) exhibited up-regulation in roots under P deprivation. These PAPs may play a role in P acquisition from soil and the latter ones in the enhanced PAP activities on roots of P starved poplar. In *Arabidopsis*, AtPAP12 and AtPAP26 are the main secreted PAPs under low P conditions, whereas AtPAP10 is primarily associated with the root cell-walls (Wang *et al.*, 2014). AtPAP10 and AtPAP12 are homologous to PtPAP1 to PtPAP4, AtPAP26 to PtPAP5 to PtPAP7. The detection of PtPAP4 and PtPAP1 proteins in the AWF of poplar roots suggested a conserved function for these enzymes with *Arabidopsis* AtPAP12. Especially PtPAP1 may be responsible for the enhanced PAP activity of poplar roots under low P conditions as this PAP was found only in AWF of P starved poplar roots and is transcriptionally upregulated. Whether another poplar PAP is bound to root cell-walls and could therefore not be detected in the AWF, remains open. Further tests have to reveal whether PtPAP1 is a suitable candidate gene

to engineer -P tolerant poplars for natural soils with organic P sources. Firstly, it has to be tested, whether the acid phosphatase isoform with high activity in AWF of poplar roots grown under low P conditions is PtPAP1. Further, it should be tested, whether enhanced expression of PtPAP1 leads to enhanced P acquisition from organic P sources and better plant performance under low phosphate conditions. First experiments with transient expression in *Arabidopsis* have been initiated (Supplemental materials) but were not yet successful. Overexpression in poplar would be a further step.

Additionally to their function in soil P acquisition, PAPs release P from internal stores (Duff *et al.*, 1994). As newly taken up P in poplar is mainly transported to the youngest, growing leaves (Kavka and Polle, 2016), a recycling of P from storage pools in older leaves is likely, especially in P starved plants. PtPAPs highly expressed or up-regulated in leaves upon P starvation may have a role in plant internal P recycling (e.g. PtPAP2, PtPAP11, PtPAP15, PtPAP23).

Besides the enzymatic changes towards higher P acquisition and P recycling in the plant, plants also have to alter their root system and morphology to increase the access to phosphate in soil (Lambers and Plaxton, 2015). Increased root hair length and density is an early and specific response to P deprivation (Niu *et al.*, 2013) and could be seen in very young as well as in long term P stressed poplars in this study. Poplars also changed the root morphology towards longer exploring root tips as was seen in maize. Maize roots show a reduced root diameter in the apical region (Mollier and Pellerin, 1999) which was also detected in poplar. Reduced root diameter as in *Arabidopsis* Col-0 is not a universal response to reduced P availability in plants (Lambers *et al.*, 2006). In poplar, the root diameter distribution changed from thin to more thick roots under P deprivation.

In this study, it was shown that P starved *P. × canescens* roots had higher PAP activity than well P-supplied plants. PtPAP4 was secreted into the growth medium under high and low P conditions, whereas PtPAP1 was secreted into the growth medium only under low P conditions. Therefore, PtPAP1 may play a role in enhanced P acquisition of P starved poplars. Additionally, P deprived poplars increased their root surface by increasing the number and length of root hairs, which allows them to explore a greater soil volume in search for P sources.

## 4.5 References

- Bielecki, R.L. (1973): Phosphate pools, phosphate transport, and phosphate availability. *Annu. Rev. Plant Physiol.* 24, 225–252.
- Bozzo, G.G., Dunn, E.L., Plaxton, W.C. (2006): Differential synthesis of phosphate-starvation inducible purple acid phosphatase isozymes in tomato (*Lycopersicon esculentum*) suspension cells and seedlings. *Plant Cell Environ.* 29, 303–313.
- Bustos, R., Castrillo, G., Linhares, F., Puga, M.I., Rubio, V., Pérez-Pérez, J., Solano, R., Leyva, A., Paz-Ares, J. (2010): A central regulatory system largely controls transcriptional activation and repression responses to phosphate starvation in *Arabidopsis*. *PLoS Genet* 6, e1001102.
- Del Pozo, J.C., Allona, I., Rubio, V., Leyva, A., De La Peña, A., Aragoncillo, C., Paz-Ares, J. (1999): A type 5 acid phosphatase gene from *Arabidopsis thaliana* is induced by phosphate starvation and by some other types of phosphate mobilising/oxidative stress conditions. *Plant J.* 19, 579–589.
- Desai, S., Naik, D., Cumming, J.R. (2014): The influence of phosphorus availability and *Laccaria bicolor* symbiosis on phosphate acquisition, antioxidant enzyme activity, and rhizospheric carbon flux in *Populus tremuloides*. *Mycorrhiza* 24, 369–382.
- Duff, S.M., Sarath, G., Plaxton, W.C. (1994): The role of acid phosphatases in plant phosphorus metabolism. *Physiol. Plant.* 90, 791–800.
- Emanuelsson, O., Nielsen, H., Brunak, S., von Heijne, G. (2000): Predicting subcellular localization of proteins based on their N-terminal amino acid sequence. *J. Mol. Biol.* 300, 1005–1016.
- Felsenstein, J. (1993): PHYLIP (Phylogeny Inference Package) version 3.5c. Distributed by the author. Department of Genetics, University of Washington, Seattle.
- Floerl, S., Druebert, C., Majcherczyk, A., Karlovsky, P., Kües, U., Polle, A. (2008): Defence reactions in the apoplastic proteome of oilseed rape (*Brassica napus* var. *napus*) attenuate *Verticillium longisporum* growth but not disease symptoms. *BMC Plant Biol.* 8, 129.
- Gan, H., Jiao, Y., Jia, J., Wang, X., Li, H., Shi, W., Peng, C., Polle, A., Luo, Z.-B. (2016): Phosphorus and nitrogen physiology of two contrasting poplar genotypes when exposed to phosphorus and/or nitrogen starvation. *Tree Physiol.* 36, 22–38.
- González-Muñoz, E., Avendaño-Vázquez, A.-O., Montes, R.A.C., de Folter, S., Andrés-Hernández, L., Abreu-Goodger, C., Sawers, R.J.H. (2015): The maize (*Zea mays* ssp. *mays* var. B73) genome encodes 33 members of the purple acid phosphatase family. *Front. Plant Sci.* 6, 341.

- Goodstein, D.M., Shu, S., Howson, R., Neupane, R., Hayes, R.D., Fazo, J., Mitros, T., Dirks, W., Hellsten, U., Putnam, N., Rokhsar, D.S. (2012): Phytozome: a comparative platform for green plant genomics. *Nucleic Acids Res.* 40, D1178–D1186.
- Hellemans, J., Mortier, G., De Paepe, A., Speleman, F., Vandesompele, J. (2007): qBase relative quantification framework and software for management and automated analysis of real-time quantitative PCR data. *Genome Biol.* 8, R19.
- Higo, K., Ugawa, Y., Iwamoto, M., Korenaga, T. (1999): Plant cis-acting regulatory DNA elements (PLACE) database: 1999. *Nucleic Acids Res.* 27, 297–300.
- Janz, D., Lautner, S., Wildhagen, H., Behnke, K., Schnitzler, J.-P., Rennenberg, H., Fromm, J., Polle, A. (2012): Salt stress induces the formation of a novel type of “pressure wood” in two *Populus* species. *New Phytol.* 194, 129–141.
- Kavka, M., Polle, A. (2016): Phosphate uptake kinetics and tissue-specific transporter expression profiles in poplar (*Populus × canescens*) at different phosphorus availabilities. *BMC Plant Biol.* 16, 206.
- Lambers, H., Plaxton, W.C. (2015): Phosphorus: Back to the roots, in: Plaxton, W.C., Lambers, H. (eds.): Annual Plant Reviews Volume 48. John Wiley & Sons, Inc., Hoboken, NJ, USA, pp. 1–22.
- Lambers, H., Shane, M.W., Cramer, M.D., Pearse, S.J., Veneklaas, E.J. (2006): Root structure and functioning for efficient acquisition of phosphorus: Matching morphological and physiological traits. *Ann. Bot.* 98, 693–713.
- Li, C., Gui, S., Yang, T., Walk, T., Wang, X., Liao, H. (2012): Identification of soybean purple acid phosphatase genes and their expression responses to phosphorus availability and symbiosis. *Ann. Bot.* 109, 275–285.
- Li, D., Zhu, H., Liu, K., Liu, X., Leggewie, G., Udvardi, M., Wang, D. (2002): Purple acid phosphatases of *Arabidopsis thaliana*, comparative analysis and differential regulation by phosphate deprivation. *J. Biol. Chem.* 277, 27772–27781.
- Lohrasebi, T., Malboobi, M.A., Samaeian, A., Sanei, V. (2007): Differential expression of *Arabidopsis thaliana* acid phosphatases in response to abiotic stresses. *Iran. J. Biotechnol.* 5, 130–39.
- Mollier, A., Pellerin, S. (1999): Maize root system growth and development as influenced by phosphorus deficiency. *J. Exp. Bot.* 50, 487–497.
- Müller, A., Volmer, K., Mishra-Knyrim, M., Polle, A. (2013): Growing poplars for research with and without mycorrhizas. *Front. Plant Sci.* 4, 332.

Niu, Y.F., Chai, R.S., Jin, G.L., Wang, H., Tang, C.X., Zhang, Y.S. (2013): Responses of root architecture development to low phosphorus availability: a review. *Ann. Bot.* 112, 391–408.

Olczak, M., Morawiecka, B., Watorek, W. (2003): Plant purple acid phosphatases - genes, structures and biological function. *Acta Biochim. Pol.* 50, 1245–1256.

R Development Core Team (2012): R: a language and environment for statistical computing. R Foundation for Statistical Computing, Vienna, Austria.

Rappsilber, J., Mann, M., Ishihama, Y. (2007): Protocol for micro-purification, enrichment, pre-fractionation and storage of peptides for proteomics using StageTips. *Nat. Protoc.* 2, 1896–1906.

Ravichandran, S., Stone, S.L., Benkel, B., Prithiviraj, B. (2013): Purple Acid Phosphatase 5 is required for maintaining basal resistance against *Pseudomonas syringae* in *Arabidopsis*. *BMC Plant Biol.* 13, 107.

Ruijter, J.M., Ramakers, C., Hoogaars, W.M.H., Karlen, Y., Bakker, O., Hoff, M.J.B. van den, Moorman, A.F.M. (2009): Amplification efficiency: linking baseline and bias in the analysis of quantitative PCR data. *Nucleic Acids Res.* 37, e45.

Schachtman, D.P., Reid, R.J., Ayling, S.M. (1998): Phosphorus uptake by plants: from soil to cell. *Plant Physiol.* 116, 447–453.

Tamura, K., Stecher, G., Peterson, D., Filipowski, A., Kumar, S. (2013): MEGA6: Molecular Evolutionary Genetics Analysis Version 6.0. *Mol. Biol. Evol.* 30, 2725–2729.

Tsai, C.-J., Ranjan, P., DiFazio, S., Tuskan, G., Johnson, V. (2011): Poplar genome microarrays, in: Joshi, C., DiFazio, S., Kole, C. (eds.): Genetics, genomics and breeding of poplars. Science Publishers, Enfield, NH, pp. 112–127.

Tuskan, G.A., DiFazio, S., Jansson, S., Bohlmann, J., Grigoriev, I., Hellsten, U., Putnam, N., Ralph, S., Rombauts, S., Salamov, A., Schein, J., Sterck, L., Aerts, A., Bhalerao, R.R., Bhalerao, R.P., Blaudez, D., Boerjan, W., Brun, A., Brunner, A., Busov, V., Campbell, M., Carlson, J., Chalot, M., Chapman, J., Chen, G.-L., Cooper, D., Coutinho, P.M., Couturier, J., Covert, S., Cronk, Q., Cunningham, R., Davis, J., Degroove, S., Déjardin, A., dePamphilis, C., Detter, J., Dirks, B., Dubchak, I., Duplessis, S., Ehrling, J., Ellis, B., Gendler, K., Goodstein, D., Gribskov, M., Grimwood, J., Groover, A., Gunter, L., Hamberger, B., Heinze, B., Helariutta, Y., Henrissat, B., Holligan, D., Holt, R., Huang, W., Islam-Faridi, N., Jones, S., Jones-Rhoades, M., Jorgensen, R., Joshi, C., Kangasjärvi, J., Karlsson, J., Kelleher, C., Kirkpatrick, R., Kirst, M., Kohler, A., Kalluri, U., Larimer, F., Leebens-Mack, J., Leplé, J.-C., Locascio, P., Lou, Y., Lucas, S., Martin, F., Montanini, B., Napoli, C., Nelson, D.R., Nelson, C., Nieminen, K., Nilsson, O., Pereda, V., Peter, G., Philippe, R., Pilate, G., Poliakov, A., Razumovskaya, J., Richardson, P., Rinaldi, C., Ritland, K., Rouzé, P.,

Ryaboy, D., Schmutz, J., Schrader, J., Segerman, B., Shin, H., Siddiqui, A., Sterky, F., Terry, A., Tsai, C.-J., Uberbacher, E., Unneberg, P., Vahala, J., Wall, K., Wessler, S., Yang, G., Yin, T., Douglas, C., Marra, M., Sandberg, G., Peer, Y.V. de, Rokhsar, D. (2006): The genome of black cottonwood, *Populus trichocarpa* (Torr. & Gray). *Science* 313, 1596–1604.

Van de Peer, Y., Fawcett, J.A., Proost, S., Sterck, L., Vandepoele, K. (2009): The flowering world: a tale of duplications. *Trends Plant Sci.* 14, 680–688.

Vincent, J.B., Averill, B.A. (1990): An enzyme with a double identity: purple acid phosphatase and tartrate-resistant acid phosphatase. *FASEB J.* 4, 3009–3014.

Wang, L., Li, Z., Qian, W., Guo, W., Gao, X., Huang, L., Wang, H., Zhu, H., Wu, J.-W., Wang, D., Liu, D. (2011): The *Arabidopsis* purple acid phosphatase AtPAP10 is predominantly associated with the root surface and plays an important role in plant tolerance to phosphate limitation. *Plant Physiol.* 157, 1283–1299.

Wang, L., Lu, S., Zhang, Y., Li, Z., Du, X., Liu, D. (2014): Comparative genetic analysis of *Arabidopsis* purple acid phosphatases AtPAP10, AtPAP12, and AtPAP26 provides new insights into their roles in plant adaptation to phosphate deprivation: Comparative analysis of three *Arabidopsis* APases. *J. Integr. Plant Biol.* 56, 299–314.

Warnes, G.R. (2012): gplots: Various R programming tools for plotting data. R package version 2.11.0.

Wessel, D., Flügge, U.I. (1984): A method for the quantitative recovery of protein in dilute solution in the presence of detergents and lipids. *Anal. Biochem.* 138, 141–143.

Zhang, Q., Wang, C., Tian, J., Li, K., Shou, H. (2011): Identification of rice purple acid phosphatases related to phosphate starvation signalling. *Plant Biol.* 13, 7–15.

Zhang, X.M., Hong, K., Yi, Y. (2015): Effect of short-term phosphate starvation on acid phosphatase activity of *Carpinus pubescens* and *Eurycorymbus cavaleriei*. *Russ. J. Plant Physiol.* 62, 57–64.

Zhu, H., Qian, W., Lu, X., Li, D., Liu, X., Liu, K., Wang, D. (2005): Expression patterns of purple acid phosphatase genes in *Arabidopsis* organs and functional analysis of AtPAP23 predominantly transcribed in flower. *Plant Mol. Biol.* 59, 581–594.



## 4.6 Supporting information

**Table S4.1:** Proteins in the AWF of P starved poplar (on data CD)

**Additional file:** Establishment of *Arabidopsis pap*-mutant lines for functional analyses of poplar purple acid phosphatases

### Additional file: Establishment of *Arabidopsis pap*-mutant lines for functional analyses of poplar purple acid phosphatases

#### Introduction

The purple acid phosphatase PtaPAP1 was additionally secreted under low phosphate conditions by poplar (*Populus × canescens*) roots. It was found in the apoplastic washing fluid (AWF) of only P starved poplar roots and not under control conditions. Furthermore, *PtaPAP1* was highly upregulated under low P conditions and belonged to the highest regulated genes. *PtaPAP1* expression pattern was correlated with the P concentration in the plant tissues (Chapter 1). Luo et al. (2009) found *PtaPAP1*, together with four other purple acid phosphatases (*PtaPAP16*, *PtaPAP29*, *PtaPAP30*, *PtaPAP32*) downregulated in mycorrhizal poplar roots with higher phosphorus concentrations. These phosphatases were upregulated under phosphate deprivation in roots in this study.

The goal of this study was to test, whether PtaPAP1 takes part in the P acquisition under low P conditions in poplar.

The homolog of PtPAP1 in *Arabidopsis* is AtPAP10 (Table S4.1). The *atpap10*-mutant has reduced root-associated acid phosphatase activity (Wang et al., 2011), in contrast to mutants of other PAP homologs (Figure S4.1) that are also highly upregulated in poplar upon P starvation. Therefore, this mutant is a promising system to test, whether the poplar PtaPAP1 is a major root-associated PAP that is able to rescue the *atpap10*-mutant phenotype.

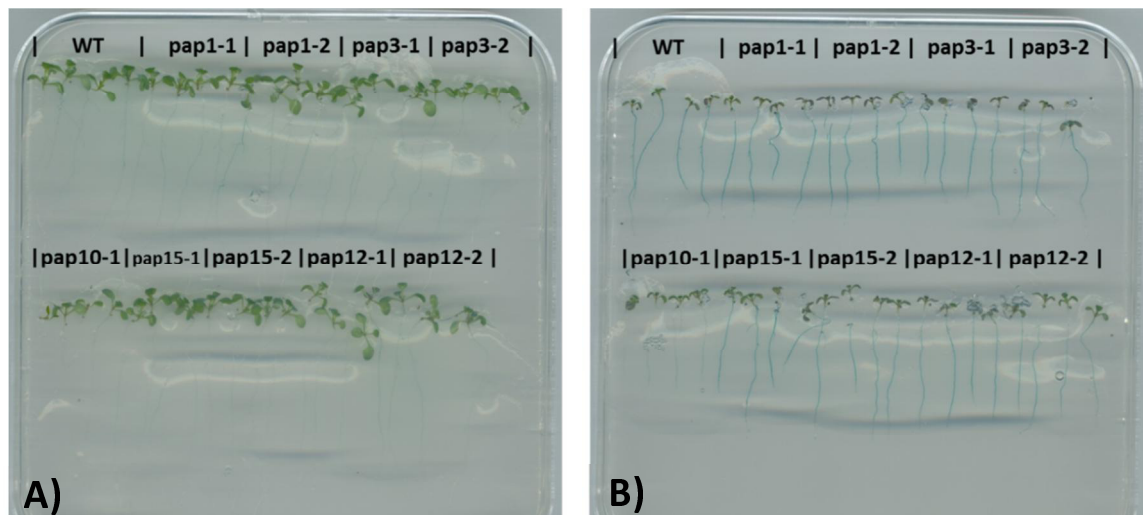


**Figure S4.1:** BCIP-staining of *Arabidopsis* roots for acid phosphatase activity. *Arabidopsis* plants (for lines refer to Table 1) were grown vertically on  $\frac{1}{2}$ MS-medium for 8 d with (A) and without (B) P, overlaid with 0.01% BCIP-0.8% Agar-medium and scanned after 17 h.

**atpap mutant lines**

The *Arabidopsis pap*-mutant lines were purchased from the European *Arabidopsis* Stock Centre (NASC). These lines are T-DNA insertion lines: A short DNA fragment (T-DNA) is inserted into the genome of *Arabidopsis*. The insertion site is random but known after sequencing. If the insert is positioned inside an important part of a gene sequence, the gene cannot be (fully) expressed.

Whether the insertion was homozygous (on both alleles), heterozygous (on one allele) or crossed out (two wild type alleles), was tested by PCR. In this PCR, one primer pair was positioned on the left and on the right side of the T-DNA insert (LP and RP primer, Figure S4.2A). The sequence between them could only be amplified without insert (wild type allele). A second primer pair consisted of the primer on the right side of the T-DNA insert (RP) and a primer binding to the T-DNA. The latter one could only bind if there was an insert present. This amplified sequence was chosen to be shorter than the previous one. The mutations were tested on leaf DNA extracts in two different PCRs or in one PCR with all three primers, resulting in exemplified gel pictures seen in Figure S4.2B for wild type (WT), heterozygous (HZ) and homozygous (HM) plants. Results of the PCRs are seen in Figure S4.3.

All selected mutations were in the Col-0 background.

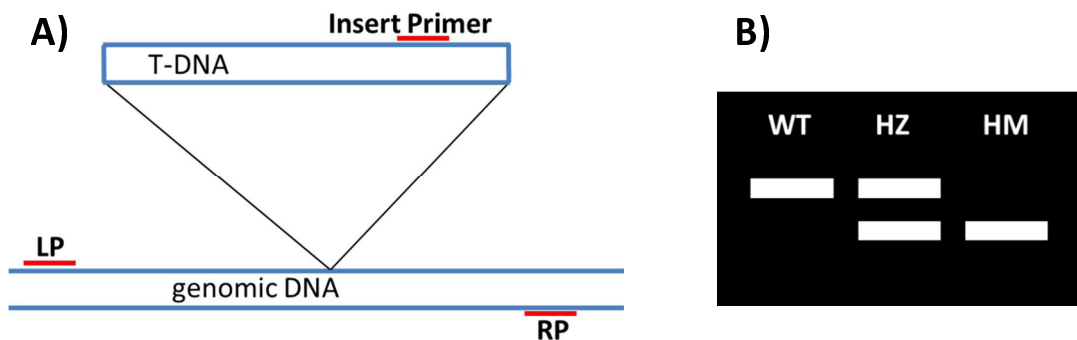


**Figure S4.2:** A) Scheme of the primer position in T-DNA insertion lines, B) schematic picture of the resulting gel after PCR with all three primers for T-DNA insertion lines (WT: wild type, HZ: heterozygous, HM: homozygous).

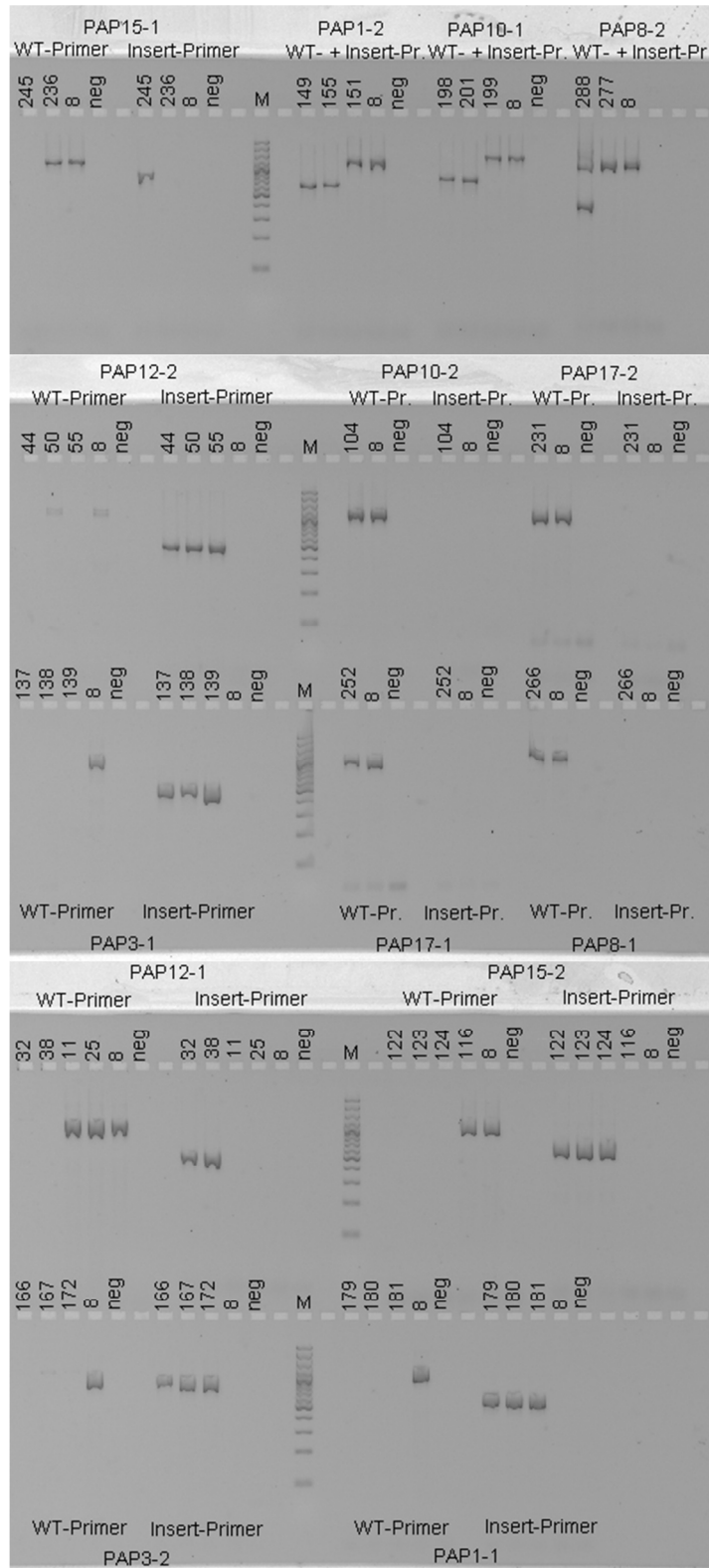


**Figure S4.3:** Results of PCR for insert testing of plants of the mutant lines. WT-Primer: LP and RP primer, Insert-Primer: Insert-primer and RP primer, M: marker (GeneRuler 100 bp Plus DNA ladder (Thermo Fisher Scientific, Waltham, MA, USA), see Figure S4.4 for DNA fragment sizes). Numbers are individual plants from the mutant lines, 8: wild type, neg: water. Colors are inverted. 1 µl PCR-product, 2 % agarose gel.

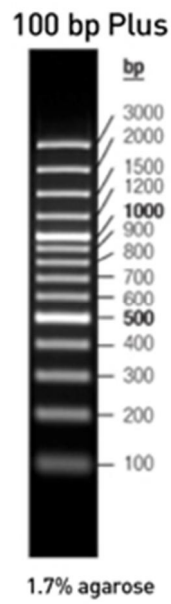


**Figure S4.4:** Fragment sizes of GeneRuler 100 bp Plus DNA ladder (Thermo Fisher Scientific, Waltham, MA, USA). Source: <https://www.thermofisher.com/us/en/home/brands/thermo-scientific/molecular-biology/thermo-scientific-nucleic-acid-electrophoresis-purification/dna-electrophoresis-thermo-scientific/dna-ladders-thermo-scientific/generuler-dna-ladders.html>

**Table S4.1:** Poplar PAP and homologous *Arabidopsis* PAP, *Arabidopsis* mutant lines with position of insert and primers used for confirmation of homozygosity of mutation.

Poplar PAP	homologous AtPAP	Ath mutant line	position of Insert	Primers	Comments
PtPAP1	AtPAP10 and AtPAP12	PAP10-1 (SALK_122362 (BV))	300-UTR5 Exon	SALK_122362_LP: CTTTTGCTTCTTGTGTCACCC SALK_122362_RP: TTTCTTGGCACTCCACAAAAC	no homozygous found
		PAP10-2 (SAIL_1234_D05)	Exon	SAIL_1234_D05_LP: ACCCTCATTGTTTCACCTTCC SAIL_1234_D05_RP: TAGCACCAAAAAGCACAAAGC	
	PAP12-1 (GK-151C09)	300-UTR5	GABI_151C09_LP: AAAGCTAGCTTCTCGAAACGC GABI_151C09_RP: ATGAGATGAATCCGGGAAAAG		
	PAP12-2 (GK-662B07)		GABI_662B07_LP2: AATGACTAAACGAATAACAAAGG GABI_662B07_RP: CTGTTGCTTCTGCTTGTTC		
PtPAP16	AtPAP1	PAP1-1 (SALK_038756C) PAP1-2 (SALK_067586C)	300-UTR5 Exon	SALK_038756_LP: AAGCTTCAAGGAACCAGTTCC SALK_038756_RP: CAAAAGCATTGACACTTTGG SALK_067586_LP: CGGTGGATAGGAAAGGAAAAG SALK_067586_RP: TCACCGTGTTCTCGGTTATTC	
PtPAP29 and PtPAP30	AtPAP17	PAP17-1 (SALK_046977 (AI))	Exon	SALK_046977_LP: GCCTACCTAGCCTGCAATAGG SALK_046977_RP: CTCGTTGCTTATCAGGTTTGG	no homozygous found
		PAP17-2 (SALK_097938)	Exon	SALK_097938_LP: GCCTACCTAGCCTGCAATAGG SALK_097938_RP: CTCGTTGCTTATCAGGTTTGG	no homozygous found

**Table S4.1** (continued)

Poplar PAP	homologous AtPAP	Ath mutant line	position of Insert	Primers	Comments
PtPAP9	AtPAP15	PAP15-1 (SALK_059899 (L))	Exon	SALK_059899_LP: CACTACAATGAAAAGCTCCGC SALK_059899_RP: AGTTTGCATAACTCACGTCGC	
		PAP15-2 (SAIL_529_D01)	300-UTR5	SAIL_529_D01_LP: GACTCAGTGAGTGCCTCAAGG SAIL_529_D01_RP: TGCTTGATATCCACTGGGTAATC	
PtPAP32	AtPAP3 and AtPAP8	PAP3-1 (SALK_109503C)	Exon	SALK_109503_LP: GATCGTGCAAGCTGGTTAAAC SALK_109503_RP: CAACAGCTAATTTTCAACCGC	
		PAP3-2 (SALK_001726C)	Exon	SALK_001726_LP: TGA CTGGAGCGGTGTATTACC SALK_001726_RP: AGCGCCTCCTTGTAAGTCTTC	
		PAP8-1 (SALK_123622 (BV))	Exon	SALK_123622_LP: GGTAACGTCTATGCGCAACTC SALK_123622_RP: CGAAATCAAACCAAATCATG	no homozygous found
		PAP8-2 (SAIL_917_D11)	Exon	SAIL_917_D11_LP: AAATTGCTAGCTGCGACAAAC SAIL_917_D11_RP: GACTACTTCTATCCACCGCCC	no homozygous found (but heterozygous)
		SALK-lines		SALK_LBb1.3: ATTTTGCCGATTTTCGGAAC	Insert primer
		SAIL-lines		SAIL_LB1: GCCTTTTCAGAAATGGATAAATAGCCTTGCTTCC	Insert primer
		GABI-KAT-lines		GABI_8474: ATAATAACGCTGCGGACATCTACATTTT	Insert primer

### The Gateway system

To try whether PtaPAP1 can functional complement the *atpap10*-mutation in *Arabidopsis*, *PtaPAP1* coding sequence was cloned into a vector containing a CamV-35S-promoter for overexpressing by using the Gateway system.

Each Gateway vector has a “death gene” (*ccdB*) between two cloning sites (*att*-sites) lethal for *E. coli*-cells. During cloning reaction, this “death gene” is substituted by the DNA-sequence of interest (Figure S4.5A). Additionally, these vectors contain an antibiotics resistance gene. After transformation into *E. coli*, during following selection, only those cells survive that were transformed with the vector with DNA-sequence of interest.

The cloning is performed in two steps: Firstly, the DNA-sequence of interest (PCR-product) is cloned into a donor vector (pDONR201) via the BP-reaction forming the entry vector. Secondly, the DNA-sequence of interest is cloned from the entry vector into the destination vector (here pGWB2) (LR-reaction). These reactions are oriented and cannot be undone in the same reaction, because the required *att*-sites are changed with each reaction (Figure S4.5B).

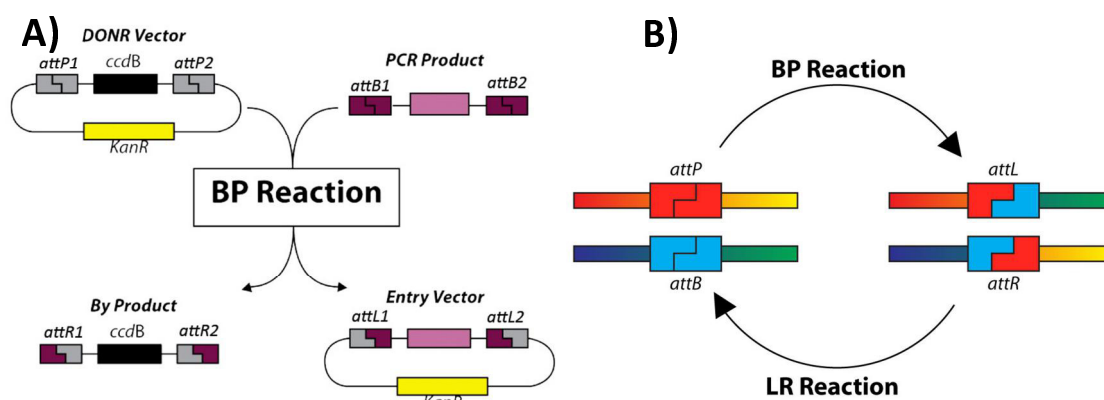


**Figure S4.5:** Scheme of cloning reactions with the Gateway system. Source: [https://www.google.de/url?sa=t&rct=j&q=&esrc=s&source=web&cd=1&ved=0ahUKEwjjvJjngc\\_MAhUhEJoKHS0DC40QFggqMAA&url=https%3A%2F%2Fsecuiqhdk.files.wordpress.com%2F2015%2F01%2Ftest2.docx&usg=AFQjCNH0a87zB0nxUVECPzhePLs2c9OILw&cad=rja](https://www.google.de/url?sa=t&rct=j&q=&esrc=s&source=web&cd=1&ved=0ahUKEwjjvJjngc_MAhUhEJoKHS0DC40QFggqMAA&url=https%3A%2F%2Fsecuiqhdk.files.wordpress.com%2F2015%2F01%2Ftest2.docx&usg=AFQjCNH0a87zB0nxUVECPzhePLs2c9OILw&cad=rja)

### Cloning-Protocol

Additionally to the poplar gene *PtaPAP1*, the *Arabidopsis* gene *AtPAP10* was used as positive control for functional complementation of the *atpap10*-mutant.

*AtPAP10* has two gene models with only one expressed gene (AT2G16430.2) (TAIR, Wang et al. 2011). The coding sequence of this gene from start until the stop codon (~1500 bp) was amplified from cDNA and simultaneously, *att*-sites for cloning were added.



*PtaPAP1* has three gene models in *P. trichocarpa* with Potri.005G233400.1 as primary transcript. The differences in the two other transcripts are: longer UTRs in Potri.005G233400.2 (no difference in coding sequence), and a shorter coding sequence for Potri.005G233400.3 at the 5'-end. For transformation, the coding sequence of Potri.005G233400.1 from start until the stop codon (~1500 bp) was amplified from cDNA of *Populus × canescens* and simultaneously, the att-sites for cloning were added. For that PCR reactions, following primers were used (black for att-site addition, red for gene):

attB1\_AtPAP10\_fw (5'-GGGGACAAGTTTGTACAAAAAAGCAGGCTTCACCATGGGTCGTGTCCGA-3')

and attB2\_At\_rev (5'-GGGGACCACTTTGTACAAGAAAGCTGGGTCTCAAGAATTACAAGAAGGAGAAATC-3')

for *AtPAP10* and attB1\_Pc005\_fw (5'-GGGGACAAGTTTGTACAAAAAAGCAGGCTTCACCATGGAAGTGAGATGGGACTC-3')

and attB2\_rev+Gen (5'-GGGGACCACTTTGTACAAGAAAGCTGGGTCTCATAACGCAGCCACGG-3') for *PtaPAP1*. The PCR settings are summarized in Table S4.2.

**Table S4.2:** PCR settings for amplification of *AtPAP10* and *PtaPAP1* coding sequence with addition of att-sites for Gateway-cloning.

Solutions	µl	Programm	Hot Start / Lid
5X Phusion Buffer	10		105°C
dNTP Mix (10 mM of each)	1	<b>Step</b>	<b>Temperature</b>
Primer fw (10 µM)	2.5	1	98°C
Primer rev (10 µM)	2.5	2	98°C
Phusion-Polymerase (2 U/µl)	0.5	3	98°C
Water (Nuklease free)	31.5	4	60°C
cDNA-Extract	2	5	72°C
<i>total volumen</i>	<i>50</i>	6	Go to 3 / Rep 35
		7	72°C
		8	Hold 4°C / Enter

After amplification, the PCR-product was purified with innuPREP PCRpure Kit (Analytik Jena, Jena, Germany) after manual instructions and eluted with 25 µl nuclease-free water. Afterwards, it was extracted from an agarose gel (1.2 % agarose, 50 ml gel volume, ~3 h, 35 mA) with the QIAquick Gel Extraction Kit (Qiagen, Hilden, Germany) after manual instructions.

The resulting DNA products (Figure S4.6) had DNA-concentrations (Biophotometer, Eppendorf, Hamburg, Germany) of 14.5 ng/µl for *Arabidopsis* gene and 19.5 ng/µl for poplar gene.

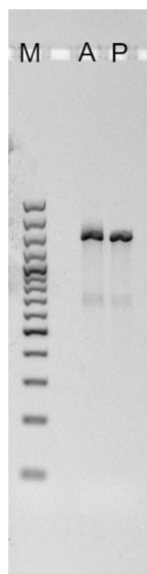


**Figure S4.6:** Purified PCR-products (M: GeneRuler 100 bp plus, see Figure S4.4), A: *Arabidopsis*, P: poplar gene. Colors are inverted. 2  $\mu$ l PCR product, 1.2 % agarose gel.

### BP-Reaction

Afterwards, the BP-reaction was set up. As donor vector, pDONR201 with kanamycin resistance (Figure 7) was used in equimolar concentration with the PCR-product (Table S4.3).

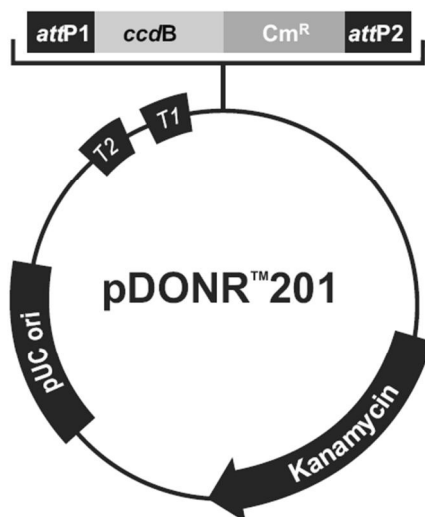


**Figure S4.7:** Map of important elements of the donor vector pDONR201. Source: <http://www.biofeng.com.img.800cdn.com/uploads/%E8%BD%BD%E4%BD%93%E5%9B%BE%E8%B0%B1/pDONR201%E8%BD%BD%E4%BD%93%E5%9B%BE%E8%B0%B1.gif>

**Table S4.3:** Settings for BP-reaction

	for Ath in $\mu\text{l}$	for Pta in $\mu\text{l}$	for positive control in $\mu\text{l}$
pDONR201 (150 ng/ $\mu\text{l}$ )	0.5	0.5	0.5
PCR-product/pos. control	1.7	1.3	1
H <sub>2</sub> O	1.8	2.2	2.5
BP-Clonase II	1	1	1
room temperature over night			
Proteinase K	0.5	0.5	0.5
37°C for 10 min			

**Transformation of *E. coli***

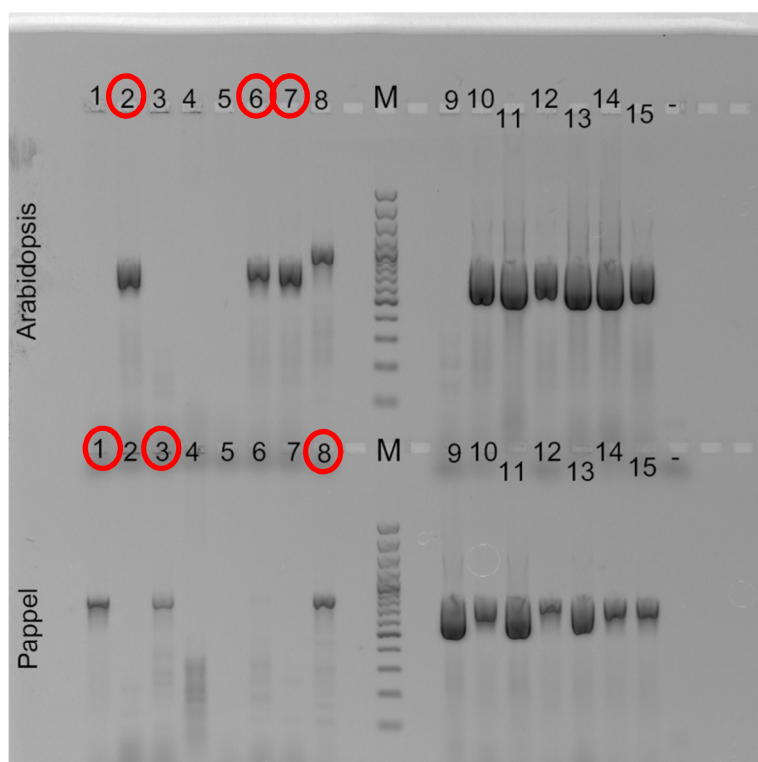
Forty  $\mu\text{l}$  of electro competent *E. coli* TOP10 cells (generated by Invitrogen but own culture) were transformed with 2  $\mu\text{l}$  of BP-reaction products by using an electro shock of 1.8 kV. Afterwards, the cells were slightly shaken for about 1.5 h at 37°C in 1 ml SOC medium.

Two hundred  $\mu\text{l}$  and 500  $\mu\text{l}$  of the cell suspension were streaked on LB-medium with kanamycin or tetracyclin (for control insert) and cultivated at 37°C overnight.

A colony PCR (PCR settings in Table S4.4) was performed to assess the success of the transformation (for the two genes). Single colonies were picked with a previously sterilized tooth stick and streaked on LB-medium with kanamycin to grow further. The tooth stick tip with the rest of the colony was swirled inside the PCR-mix. If not differently stated, nuclease free water was used for negative controls. For the *Arabidopsis* gene, pAtPAP10\_S7At\_fw (5'-CCGTTTAAGCCGTTTCACGC-3') and pDONR\_rev (5'-GTGCAATGTAACATCAGAGAT-3') were used as primers to amplify a product of about 820 bp. For the poplar gene pAtPAP10\_S7\_fw (5'-TGTCCCATATAGAGCATCAG-3') and pDONR\_rev were used to amplify a product of about 800 bp (Figure S4.8).

**Table S4.4:** Settings for PCR-reaction of colony PCR after transformation of BP-reaction

Solutions	µl	Programm	Hot Start / Lid
10x PCR Buffer (NH <sub>4</sub> ) <sub>2</sub> SO <sub>4</sub>	2.0		105°C
25 mM MgCl <sub>2</sub>	1.6	<b>Step</b>	<b>Temperature</b>
dNTP Mix (10 mM of each)	0.4	1	95°C
Primer LP (10 µM)	1.0	2	95°C
Primer RP (10µM)	1.0	3	94°C
Taq-Polymerase (5 U/µl)	0.1	4	57°C
Water (nuclease free)	12.9	5	72°C
Colony	~ 1µl	6	Go to 3 / Rep 35
<i>total volume</i>	<i>20.0</i>	7	72°C
		8	Hold 4°C / Enter

**Figure S4.8:** Results of colony PCR for transformation testing. M: marker (GeneRuler 100 bp Plus, see Figure S4.4). Numbers are individual colonies. First row: for *Arabidopsis* gene, second row: for poplar gene, -: water. Colors are inverted. 4 µl PCR-product, 1.2 % agarose gel. Red circles mark chosen colonies for next steps.**Plasmid-extraction and sequencing**

Colonies of A2, A6, A7, P1, P3 and P8 were grown in liquid LB medium and kanamycin overnight at 37°C. The plasmids were extracted as given in the manual of the innuPREP Plasmid Mini Kit (Analytik Jena, Jena, Germany) for high-copy plasmids. The DNA concentrations were determined (A2: 421 ng/µl, A6: 387 ng/µl, A7:

360 ng/μl, P1: 204 ng/μl, P3: 262 ng/μl, P8: 195 ng/μl) and a PCR conducted with the plasmids as template DNA and the same conditions as for the colony PCR (Table S4.4, results: Figure S4.9).

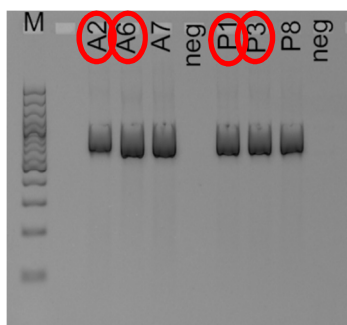


**Figure S4.9:** Results of plasmid PCR. M: marker (GeneRuler 100 bp Plus, see Figure S4.4). Numbers were individual colonies (A: for *Arabidopsis* gene, P: for poplar gene, neg: water). Colors are inverted. 1 μl PCR-product, 2 % agarose gel. Red circles mark chosen colonies for next steps.

The plasmids A2, A6, P1 and P3 were sequenced at the SeqLab Sequence Laboratories (Göttingen, Germany) with the primers pDONR\_fw (5'-TAACGCTAGCATGGATCTC-3') and pDONR\_rev (5'-GTGCAATGTAACATCAGAGAT-3') for both genes and pAtPAP10\_AtS6\_fw (5'-TCATGGGTGACACAAGAAGC-3') for *AtPAP1* and pAtPAP10\_S6\_fw (5'-TGGGCTGAAAATAGTGAGC-3') for *PtaPAP1*.

Plasmid A6 had no differences to the coding sequence at Phytozome (Figure S4.10). Plasmid P1 had one T-to-C transition at 600 bp that does not change the protein sequence. There were no further differences to the sequence at AspenDB (Xue *et al.*, 2015) or to the aligned sequence of *PtaPAP1* in the RNA sequencing results of Anna Müller (Figure S4.11).

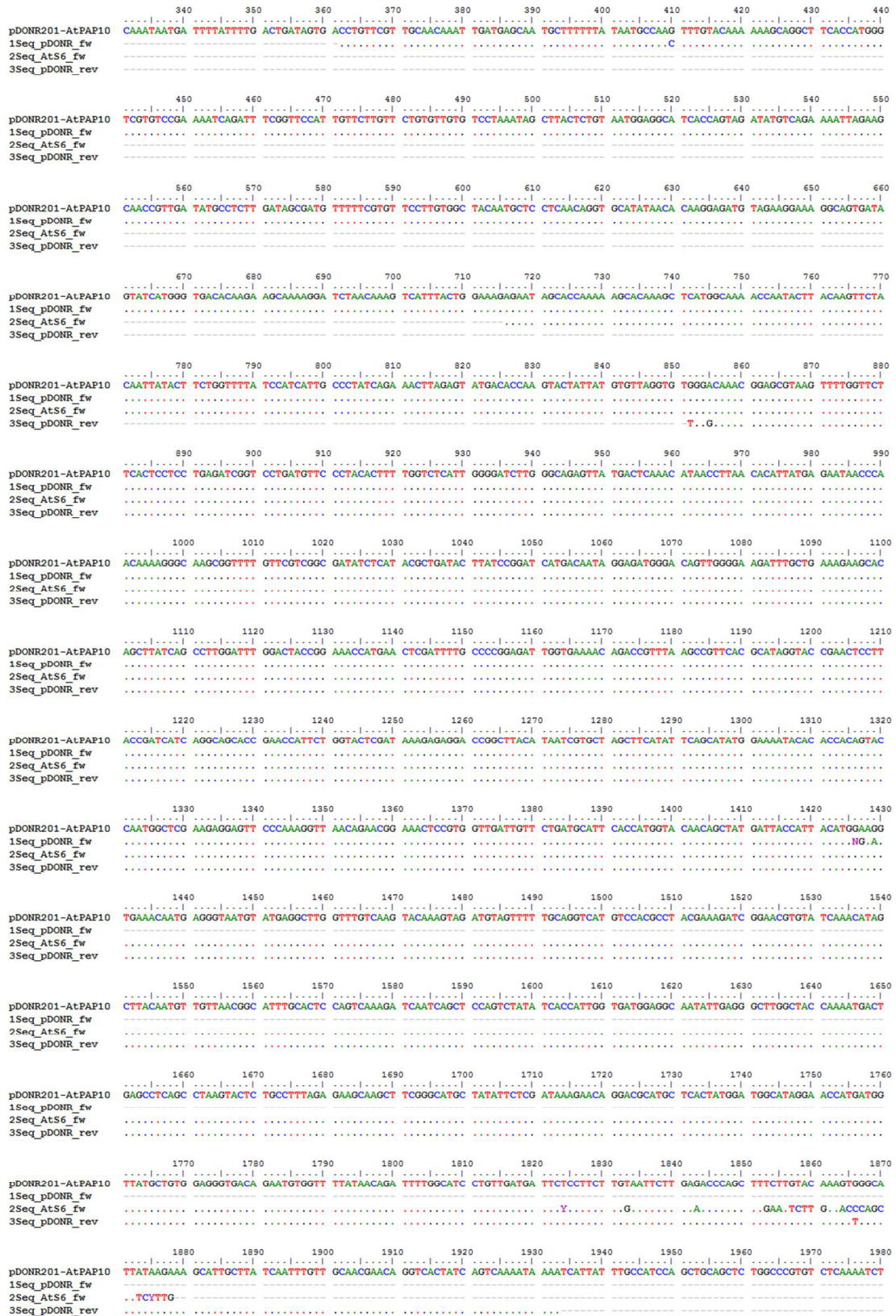


**Figure S4.10:** Alignment of the *AtPAP10* plasmid sequences (1Seq to 3Seq) with the sequence of pDONR201 with inserted *AtPAP10* coding sequence (pDONR201-*AtPAP10*).

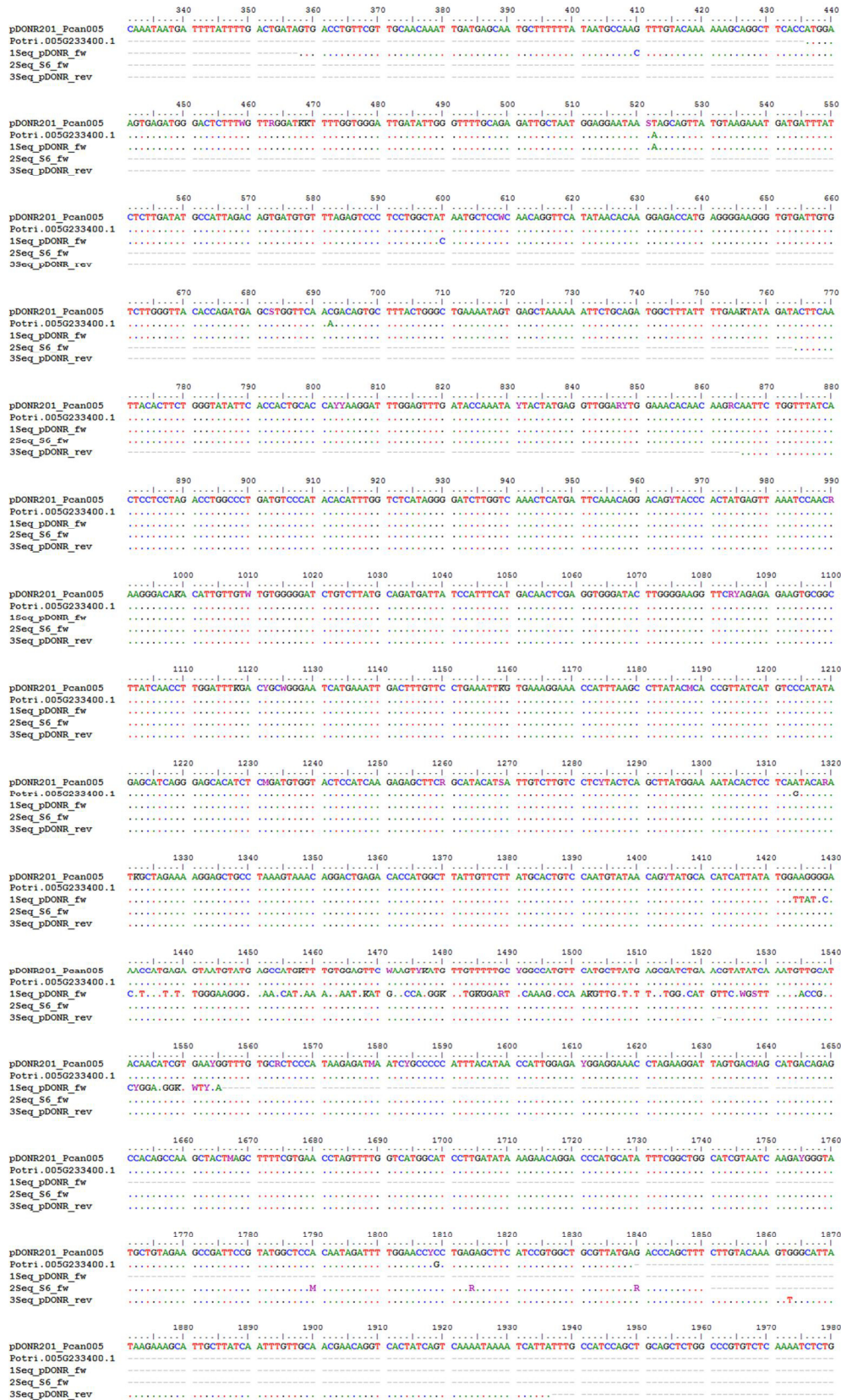


**Figure S4.11:** Alignment of the *PtaPAPI* plasmid sequences (1Seq to 3Seq) with the sequence of pDONR201 with inserted *PtaPAPI* coding sequence of Anna Müller's data (pDONR201\_Pcan005) and the data of AspenDB (Potri.005G233400.1).

**LR-Reaction**

The vector pGWB2 has the sequence of a 35S-promoter, and kanamycin and hygromycin resistance genes for bacteria and plants (Figure S4.12). Also for the LR-reaction, entry-vector and destination-vector were used in equimolar concentrations. Therefore, A6 and P1 were diluted to 11 ng/ $\mu$ l.

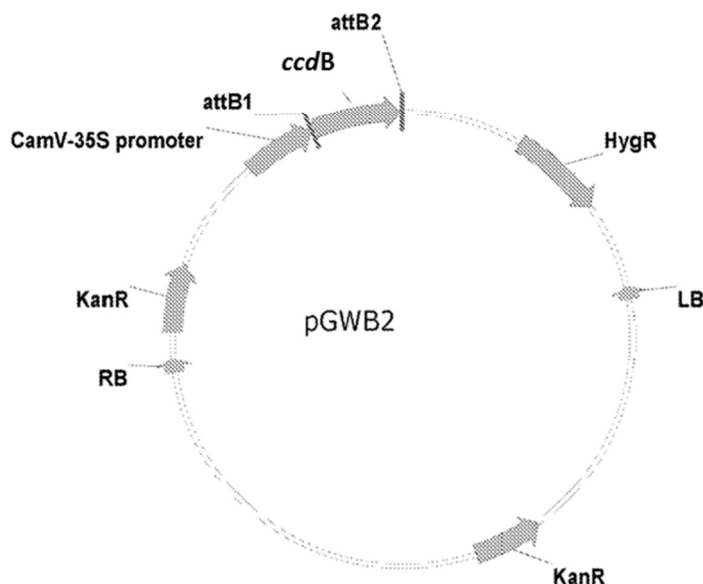


**Figure S4.12:** Map of important elements of the destination vector pGWB2. Source: [www.google.com/patents/EP2357239A1?cl=en](http://www.google.com/patents/EP2357239A1?cl=en) (mod.)

**Table 5:** Settings for LR-reaction

solution	amount in $\mu$ l
pGWB2 (50 ng/ $\mu$ l)	1
pENTR (pDONR201 with <i>AtPAP10</i> or <i>PtaPAP1</i> or pENTR-gus as positive control)	1
H <sub>2</sub> O	2
LR-Clonase II	1
room temperature over night	
Proteinase K	0.5
37°C for 10 min	

Transformation of *E. coli* TOP10 cells with the LR-reaction products was as described above for the BP-reaction products.

Selection of clones was done on LB-medium with kanamycin and hygromycin addition.

Colony-PCR for each 6 colonies for the *Arabidopsis* and poplar gene was performed with conditions described in Table S4.6 with following primers for *AtPAP10*:



SALK\_122362\_LP (5'-CTTTTGCTTCTTGTGTCACCC-3') and pGWB2\_fw (5'-catttgagagaacacggggg-3') resulting in a product of 411 bp; and primers Pc005G233400\_rev (5'-CCCAAGACACAATCACACCC-3') and pGWB2\_fw for PtaPAP1 resulting in a product of 390 bp (Figure S4.13).

**Table S4.6:** Settings for PCR-reaction of colony PCR after transformation of LR-reaction

<b>solutions</b>	<b>µl</b>			
10x PCR Puffer (NH <sub>4</sub> ) <sub>2</sub> SO <sub>4</sub>	2.0	Programm	Hot Start / Lid	
25 mM MgCl <sub>2</sub>	1.6		105°C	
dNTP Mix (10 mM of each)	0.4	<b>Step</b>	<b>Temperature</b>	<b>Time</b>
Primer LP (10 µM)	1.0	1	95°C	hold
Primer RP (10 µM)	1.0	2	95°C	60 sec
Taq-Polymerase (5 U/µl)	0.1	3	94°C	15 sec
Water (nuclease free)	12.9	4	54°C	30 sec
Colony	~ 1µl	5	72°C	30 sec
<i>total volume</i>	<i>20.0</i>	6	Go to 3 / Rep 35	
		7	72°C	5 min
		8	Hold 4°C / Enter	

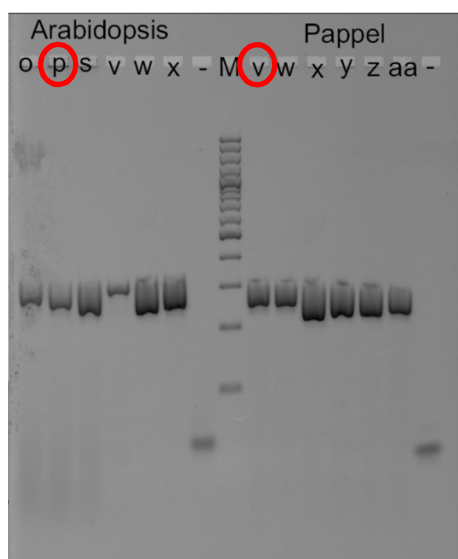


**Figure S4.13:** Results of colony PCR. M: marker (GeneRuler 100 bp Plus, see Figure S4.4). Letters were individual colonies (*Arabidopsis*: for *Arabidopsis* gene, Pappel: for poplar gene, -: water). Colors are inverted. 2 µl PCR-product, 2 % agarose gel. Red circles mark chosen colonies for next steps.

Plasmid extraction from overnight cultures of A6p and P1v was performed as described above resulting in plasmid extracts with concentrations of 18.7 ng/μl for A6p and 14.3 ng/μl for P1v.

A control-PCR of plasmids as in Table S4.6 with 1:100 dilution of plasmid extract and controls was performed (Figure 14). Enzyme digestion of the plasmids with BsrGI and NcoI in two separate reactions was performed with following conditions as control:

4 μl Plasmid

4.75 μl Water

1 μl Tango-Buffer

0.25 μl BsrGI/NcoI

37°C, 3-4 h

Expectations for BsrGI:

pGWB2 (empty): 402 bp, 1295 bp, 15539 bp

pGWB2 + Ath-Gene: 1443 bp, 15539 bp

pGWB2 + Pta-Gene: 1440 bp, 15539 bp

Expectations for NcoI:

pGWB2 (empty): 528 bp, 1310 bp, 1879 bp, 2250 bp, 3058 bp, 3398 bp, 4813 bp

pGWB2 + Ath-Gene: 528 bp, 579 bp, 959 bp, 1879 bp, 2250 bp, 2576 bp, 3405 bp, 4813 bp

pGWB2 + Pta-Gene: 90 bp, 528 bp, 579 bp, 929 bp, 1879 bp, 2250 bp, 2513 bp, 3405 bp, 4813 bp

The results of the enzyme digestions (Figure S4.14) shows that the bands 3405 bp and 4813 bp for NcoI were not divided.

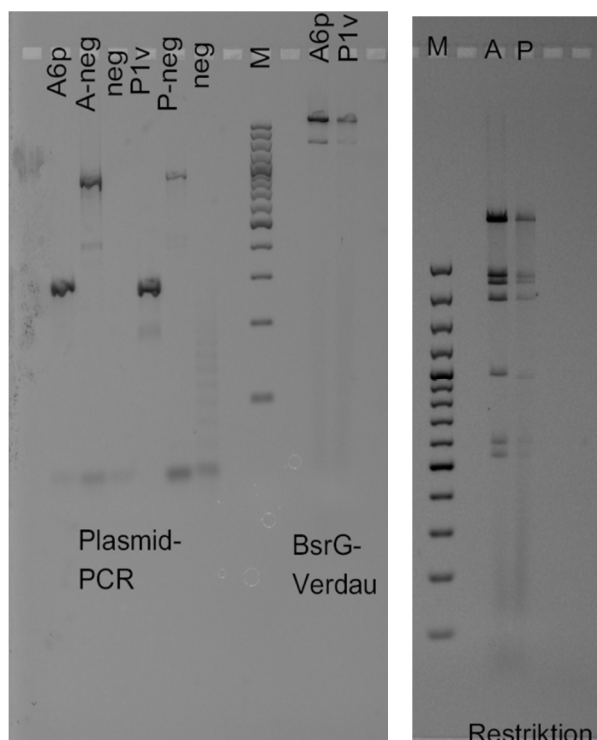


**Figure S4.14:** Results of plasmid PCR (Plasmid-PCR) and digestions with BsrGI (BsrG-Verdau) and NcoI (Restriktion). M: marker (GeneRuler 100 bp Plus, see Figure S4.4). Letters were individual colonies (A-neg/P-neg: plasmids with negative PCR results for *AtPAP10* and *PtaPAP1*, neg: water). Colors are inverted.

Plasmids of overnight cultures of A6p and P1v (-> A6p1 and P1v1) were extracted and sequenced. The sequences were identical to the sequences above (Figures S4.10 and S4.11).

These plasmids were (re)transformed into *E. coli* TOP10 cells and, after positive colony PCR (colonies number A6p1f and P1v1f) extracted by midi-plasmid extraction (Macherey-Nagel Düren, Germany) for low copy plasmids as described in the manual,, and digested with NcoI (same result as above). The concentrations were 104 ng/μl for A6p1f and 88.5 ng/μl for P1v1f.

The pGWB2-gus-plasmid was extracted from an overnight culture (Midi-Prep with column (1,2), Midi-Prep without column (3)) resulting in concentrations of 22.5 ng/μl (1, concentrated to 69 ng/μl at 50°C in SpeedVac), 10 ng/μl (2) and 1145 ng/μl (3) and digested with NcoI.

### Agrobacteria-Transformation

*Agrobacterium tumefaciens* (GV3101pMP90RK) was transformed with about 3 μg plasmid. 200 μl competent agrobacteria were mixed with the plasmid (Ath: 29 μl, Pta: 34 μl, for gus-control: 32 μl of 1) + 0,7 μl of 3)) and cooled on ice for 30 min with

occasional slight mixing, frozen for 2 min in liquid nitrogen and heated for 5 min at 37°C in a heating block. 800 µl YEB-Medium were added and the sample was slightly shaken at 28°C for about 4 h.

Two hundred and 400 µl cell suspension were streaked on YEB medium with kanamycin, hygromycin and gentamycin. After 2 d at 28°C each two colonies were grown as overnight cultures (2 d, 28°C). Glycerol stocks (A1, A2 for *AtPAP10* and P1, P2 for *PtaPAP1*) were set up and the plasmids extracted with NcoI (results as above).

#### ***Arabidopsis* transformation**

Flowering *Arabidopsis* wild type and mutants (*pap10-1*, SALK\_122362) were transformed.

Agrobacteria from stocks A1 and P1 were streaked on plates and three colonies each were used to inoculate the floral dip mix (20 ml YEB medium with kanamycin and hygromycin). Two times 400 ml YEB medium with antibiotics were inoculated with this mix and grown to an OD of 0.8. The inoculated medium was centrifuged (5000 rpm for 15 min) and the pellet resuspended in 10 to 20 ml 5 % saccharose solution, again centrifuged (5000 rpm for 15 min) and the pellet resuspended in 200 ml 5 % saccharose solution and cooled on ice. 100 µl Silwett was added and *Arabidopsis* flowers were swiveled inside for 5 to 10 sec. The *Arabidopsis* plants were left overnight in the laboratory with hood and then put again in the climate cabinet. One week later the transformation procedure was repeated.

#### ***Arabidopsis* selection**

Seeds of the transformed *Arabidopsis*-flowers were sowed on ½ MS-medium with kanamycin and hygromycin. Plants which grew longer hypocotyls (Figure S4.15) were placed on ½ MS-medium without antibiotics for about one week and then on soil.

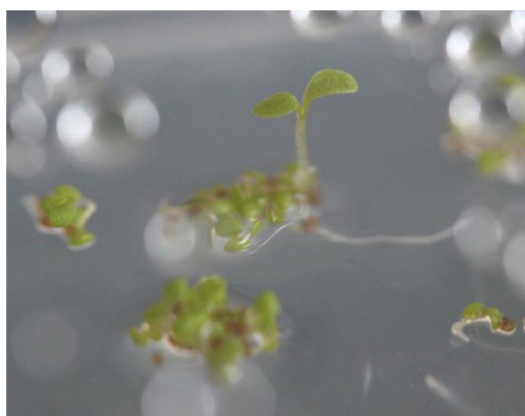


**Figure S4.15:** Germinated *Arabidopsis* seeds of plants after flower dip on selection medium. To differentiate are plants with long hypocotyl (with antibiotic resistance gene) and with short hypocotyl (transformation not successful).

A control PCR was conducted with DNA from leaves with the primers SALK\_122362\_LP or Pc005G233400\_rev or gus\_rev (5'-GATTATTGACCCACACTTTGCC-3') and pGWB2\_fw as above.

Although the successful transformation of *Arabidopsis* was demonstrated by PCR, a functional complementation could be achieved neither by the *AtPAP10* positive control nor by the *PtaPAP1* gene (Figure S4.16). Further work (semi-quantitative PCR) could not detect any expression of *PtaPAP1* in the transformed *Arabidopsis* plants and only low expression of *AtPAP10* in the *pap10*-mutant plants (also in non-transformed *pap10*-plants) (U. Lipka, personal communication).



**Figure S4.16:** BCIP-staining of *Arabidopsis* roots for acid phosphatase activity. *Arabidopsis* plants (seeds of wild type (WT), *pap10* and the plants positively tested for transformation with *AtPAP10* (A) or *PtaPAP1* (P) by PCR) were grown vertically on  $\frac{1}{2}$  MS-medium for 8 d without P, overlaid with 0.01% BCIP-0.8% Agar-medium and scanned after 4 d.

#### Possible faults and suggestions for improvement

Possible reasons for this lack of expression could be a fault of the vector (e.g. wrong labeling in the stocks that would also explain the one missing enzyme restriction site). Also gene silencing due to the 35S-promoter and possible multiple insertion sites in the genome is possible. A requirement of the UTR-sites for expression or the expression of other transcripts in wild type plants might be another possibility.

Therefore, I suggest using a different vector and a different promoter (e.g. root specific, ubiquitin promoter, *AtPAP10*-promoter, *PtaPAP1*-promoter) for future studies. Furthermore, codon optimization is a tool for improved transient expression. By using the genomic sequence or the whole transcript sequence including untranslated regions, any required additional information for expression is included.

In addition, it would be worth to transform poplar for *PtaPAP1* overexpression lines to validate PAP secretion due to PtaPAP1 under low phosphate conditions.

**Media and protocols****½ Murashige and Skoog (MS) medium for *Arabidopsis* with and without P**

<u>Macro solution</u>	<u>g/500 ml</u>
NH <sub>4</sub> NO <sub>3</sub>	8.25
KNO <sub>3</sub>	9.5
CaCl <sub>2</sub> x 2 H <sub>2</sub> O	2.2
MgSO <sub>4</sub> x 7 H <sub>2</sub> O	1.85
KCl or KH <sub>2</sub> PO <sub>4</sub>	0.465 or 0.85

<u>Micro solution</u>	<u>mg/100 ml</u>
H <sub>3</sub> BO <sub>3</sub>	620
MnSO <sub>4</sub> x H <sub>2</sub> O	1000
ZnSO <sub>2</sub> x 7 H <sub>2</sub> O	860
KJ	83
Na <sub>2</sub> MoO <sub>4</sub> x 2 H <sub>2</sub> O	25
CuSO <sub>4</sub> 5 H <sub>2</sub> O	2.5
CoCl <sub>2</sub> x 6 H <sub>2</sub> O	2.5 mg

<u>Vitamin solution</u>	<u>mg/100 ml</u>
Nicotinacid	50
Pyridoxin-HCl	50
Thiamin-HCl	10

<u>Glycin solution</u>	<u>mg/100 ml</u>
Glycin	200

<u>Inosit solution</u>	<u>g/250 ml</u>
Inosit	5

<u>Iron solution</u>	<u>g/250 ml</u>
C <sub>10</sub> H <sub>12</sub> FeN <sub>2</sub> NaO <sub>8</sub>	1.835

50 ml Macro solution, 0.5 ml Micro solution, 0.5 ml Vitamin solution, 0.5 ml Glycin solution, 2.5 ml Iron solution and 2.5 ml Inosit solution are mixed with 10 g saccharose, 0.5 g MES and 8 g Agar and water added to 1 l (pH 5.7).  
autoclaving

**LB medium**

5 g yeast extract  
10 g trypton  
10 g NaCl  
(15 g Agar)  
ad 1 l water, pH 7  
autoclaving

**YEB medium**

5 g beef extract  
1 g yeast extract  
5 g peptone  
5 g saccharose  
493 mg  $\text{MgSO}_4 \times 7 \text{H}_2\text{O}$   
(15 g Agar)  
ad 1 l water, pH 7.2  
autoclaving

**SOB medium**

20 g trypton  
5 g yeast extract  
0.6 g NaCl  
0.2 g KCl  
990 ml  $\text{H}_2\text{O}$   
autoclaving  
10 ml sterile  $\text{MgCl}_2/\text{MgSO}_4 \times 7\text{H}_2\text{O}$  solution

$\text{MgCl}_2/\text{MgSO}_4 \times 7\text{H}_2\text{O}$  solution  
20.331 g  $\text{MgCl}_2$   
24.64 g  $\text{MgSO}_4 \times 7 \text{H}_2\text{O}$   
100 ml  $\text{H}_2\text{O}$   
autoclaving

**SOC medium**

SOB medium with 20 mM glucose



**Table S4.7:** Antibiotics concentrations

Antibiotics	<i>E. coli</i> [ $\mu\text{g ml}^{-1}$ ]	<i>A. tumefaciens</i> [ $\mu\text{g ml}^{-1}$ ]	<i>A. thaliana</i> [ $\mu\text{g ml}^{-1}$ ]
Kanamycin	100	100	50
Hygromycin	50	50	25
Ampicillin	100		
Tetracyclin	20		
Streptomycin	100		
Gentamycin		25	
Rifampicin		150	

**Electrocompetent *E. coli* TOP10**

One colony of *E. coli* TOP10 cells was used to inoculate 50 ml SOB-medium with streptomycin. Five ml of this culture grown over night at 37°C was used to inoculate 500 ml SOB-medium without antibiotics and grown at 37°C until an optical density at 578 nm of 0.46-0.48. The culture was cautiously swirled on ice for 10 min, centrifuged at 5400 g for 10 min at 4°C, and the pellet two times washed with cold deionized water (about 250 ml, then about 125 ml with centrifuging as above). The pellet was resuspended in 12.5 ml 10 % glycerol (sterile, cold) and centrifuged again as above. The pellet of 500 ml culture was resuspended in 2 ml 10 % glycerol and aliquots of 40  $\mu\text{l}$  frozen in liquid nitrogen and stored at -80°C.

**Electrocompetent *A. tumefaciens* GV3101pMP90RK**

One colony of *A. tumefaciens* (GV3101pMP90RK) cells was used to inoculate 50 ml YEB-medium with gentamycin, rifampicin and kanamycin and grown for 2 days at 28°C. Two ml of this culture were used to inoculate 50 ml YEB-medium without antibiotics and grown until an optical density at 600 nm of 0.5 and centrifuged for 5 min at 4°C with 5000 rpm (Minifuge RF, Heraeus, Hanau, Germany). The pellet was resuspended in 10 ml 0.15 M NaCl (cold) and again centrifuged as above. The pellet of 50 ml culture was resuspended in 1 ml 75 mM CaCl (cold) and aliquots of 200  $\mu\text{l}$  frozen in liquid nitrogen and stored at -80°C.

**References for supplements Chapter 4**

Luo, Z.-B., Janz, D., Jiang, X., Göbel, C., Wildhagen, H., Tan, Y., Rennenberg, H., Feussner, I., Polle, A. (2009): Upgrading root physiology for stress tolerance by ectomycorrhizas: Insights from metabolite and transcriptional profiling into reprogramming for stress anticipation. *Plant Physiol.* 151, 1902–1917.

Wang, L., Li, Z., Qian, W., Guo, W., Gao, X., Huang, L., Wang, H., Zhu, H., Wu, J.-W., Wang, D., Liu, D. (2011): The *Arabidopsis* purple acid phosphatase AtPAP10 is predominantly associated with the root surface and plays an important role in plant tolerance to phosphate limitation. *Plant Physiol.* 157, 1283–1299.

Xue, L.-J., Alabady, M.S., Mohebbi, M., Tsai, C.-J. (2015): Exploiting genome variation to improve next-generation sequencing data analysis and genome editing efficiency in *Populus tremula* × *alba* 717-1B4. *Tree Genet. Genomes* 11, 82.

## 4.7 Declaration

The following data shown in this chapter have been provided:

- All laboratory steps for microarray analyses (from RNA quality determinations to raw data) were provided by the Microarray Facility (MFT Services, Tübingen, Germany).
- Proteomic analyses (from AWF to annotated proteins) were conducted by Dr. Andrzej Majcherczyk (Molecular Wood Biotechnology and Technical Mycology, Büsgen-Institute, Georg-August University of Göttingen).

## 5 Discussion

### 5.1 Discussion

Phosphorus (P) is needed in high amounts by plants but P is one of the least available nutrients in the soil. In this thesis it was studied how young poplar trees react to phosphate deprivation on transcriptional level and how these changes reflect on growth, phosphate uptake from soil and the phosphate acquisition potential from the soil.

The growth of *Populus × canescens* was decreased at P availabilities below 64  $\mu\text{M}$  similar as reported for *P. tremuloides* (Desai et al., 2014). In the present study, the phosphorus concentrations in the tissues of plants grown with P availabilities of 6.4  $\mu\text{M}$  were similar to those in poplars grown in plantations (Ge et al., 2015). Van den Burg (1985) found that foliar P concentrations between 1.7  $\text{mg g}^{-1}$  and 2.7  $\text{mg g}^{-1}$  were sufficient for growth of young *P. × canescens*. Therefore, the foliar P concentrations 1.25  $\text{mg g}^{-1}$  and 0.69  $\text{mg g}^{-1}$  dry mass in leaves of plants grown with intermediate and low P availability, respectively, seemed to suggest deficiency, whereas the P concentration for control plants (6.8  $\text{mg g}^{-1}$ ) can be considered as luxurious.

Most of the other measured nutrient concentrations in the plant tissues were also changed upon lower P availabilities, however not as strong as the P concentration. Decreased concentrations in nutrients other than P in the poplar tissues were still above the deficiency thresholds (Burg, 1985). That implies that deficiency symptoms were solely based on the decreased P concentrations or disturbed nutrient rates. Changes in nutrient concentrations were also shown in P starved *Arabidopsis* (Kellermeier et al., 2014; Misson et al., 2005; Ward et al., 2008). For example, reduced potassium, calcium and magnesium concentrations in poplar leaves were also detected in P starved *Arabidopsis* (Kellermeier et al., 2014; Misson et al., 2005; Ward et al., 2008). A reduction in manganese concentration (Kellermeier et al., 2014; Ward et al., 2008) and a strong increase in iron concentration as in P starved *Arabidopsis* leaves (Gruber et al., 2013; Hirsch et al., 2006; Kellermeier et al., 2014; Rai et al., 2015) could not be detected in P starved poplar.

Here, it was demonstrated for a tree, poplar, that a massive transcriptomic reprogramming had taken place upon P starvation. But only a small part of the regulated genes were directly correlated with the total tissue P concentrations. This observation suggests an indirect regulation by the total P concentration, by free phosphate concentrations or by co-occurring changes in e.g. other nutrient concentrations. Among the genes related to the P concentration were known P responsive genes that were also strongly regulated in *Arabidopsis* (e.g. *SPX*, *PAP*, *SQD*) (Lan *et al.*, 2015). In poplar, genes involved in membrane lipid remodeling were found in the P-responsive gene module. They were also reported in a “core gene”-set (Lan *et al.*, 2015) of P starvation response in *Arabidopsis*. This finding suggests similar transcriptional alterations in poplar and *Arabidopsis*.

Upon P starvation in leaves and roots *PtPHT1;9* and *PtPHT1;12* were upregulated in *P. × canescens* in this study. Their P responsiveness was also reported in *P. trichocarpa* roots (Loth-Pereda *et al.*, 2011). The homologous *Arabidopsis* proteins take up P in the roots (*AtPHT1;8*, *AtPHT1;9*) (Remy *et al.*, 2012) and are located in the vascular system (*AtPHT1;12*) (Mudge *et al.*, 2002). Therefore the strong induction of *PtPHT1;9* and *PtPHT1;12* gene expression suggests a role in P uptake and long-distance transport in poplar. In this study, *PtPHT1;1* and *PtPHT1;2* were highly upregulated upon P starvation specifically in roots of *P. × canescens*. High up-regulation was shown for *PtPHT1;2* also in P starved *P. simonii* roots (Zhang *et al.*, 2016). The transporters *PtPHT1;1* and *PtPHT1;2* may have functions in P uptake under low P conditions, because in *Arabidopsis*, the closely related *AtPHT1;1*, *AtPHT1;2*, *AtPHT1;3* and *AtPHT1;4* take up together more than 80 % of P from the medium (Ayadi *et al.*, 2015). In this study, *PtPHT1;3* was highly expressed in leaves and further up-regulated upon P starvation. This observation suggests an important role in P distribution inside the plant in accordance with the observed high P allocation to the young leaves in P starved poplar. The up-regulation of P transporters led to a higher uptake capacity of P starved poplars. The  $K_m$ -values for P uptake for P starved *P. × canescens* was comparable with the  $K_m$ -value for P accumulation in roots of P starved *P. deltoides* (Desai *et al.*, 2014). The present analysis showed that a minimal P concentration of 1  $\mu\text{M}$  in the growth medium was required for net P uptake. Otherwise, P uptake was prevented at very low concentrations. Since the free P concentration is low in most ecosystems (e.g. 5  $\mu\text{M}$  in

forests beneath the organic layer (*Asano et al.*, 2006; *Fitzhugh et al.*, 2001; *Ranger et al.*, 2001; *van Hees et al.*, 2003) forest trees must have evolved further mechanisms to combat P deficiency.

One of the mechanisms to cope with low P concentrations is the production and secretion of purple acid phosphatases, which make organic P sources in the soil plant available by the release of inorganic phosphate. PAPs that were upregulated in leaves and roots upon P starvation (e.g. *PtPAP1*, *PtPAP16*, *PtPAP29*, *PtPAP30*) have probably a function in internal P mobilization. The homolog of *PtPAP29* and *PtPAP30* in *Arabidopsis* is *AtPAP17*. *AtPAP17* was the first plant PAP purified and plays an role in P recycling e.g. during senescence (*Del Pozo et al.*, 1999).

In accordance with the up-regulation of PAPs in roots, the root-associated acid phosphatase activity in P starved *P. × canescens* increased. This agrees with other studies, in which an enhanced phosphatase activity was shown for other poplar species under low P conditions (*P. tremuloides*, *P. simonii*, *P. × euramericana*) (*Desai et al.*, 2014; *Gan et al.*, 2016). In *Arabidopsis*, *AtPAP10*, *AtPAP12* and *AtPAP26* are responsible for 70 % of the root-associated acid phosphatase activity under low P conditions (*Wang et al.*, 2014). In poplar, *PtPAP4* was secreted by roots under high and low P availabilities. *PtPAP1* was detected only under low P availability in the apoplastic washing fluid. Both are homologous to *AtPAP10* and *AtPAP12*. These findings suggest a conserved function for the *Arabidopsis* and poplar proteins.

Based on these results, I propose following model (Figure 5.1) for the contributions of PHTs and PAPs in P uptake and P acquisition: *PtPAP4* is secreted into the soil by poplar roots making phosphate available from organic P sources. Upon low P concentrations in the plant, *PtPAP1* is additionally secreted. Consequently, the plant root-associated phosphatase activity increases. Because of their transcriptional up-regulation, I suggest that *PtPAPs* like *PtPAP1*, *PtPAP16*, *PtPAP29* and *PtPAP30* respond to the plant P status and have a role in P acquisition in soil and P mobilization inside the plant. *PtPHT1;9* and *PtPHT1;12* take up P from the soil into the plant. With low P availability, *PtPHT1;1* and *PtPHT1;2* take part in the overall increased uptake activity. P is transported up to the leaves and re-allocated by *PtPHT1;3*, *PtPHT1;9* and *PtPHT1;12* inside the plant.

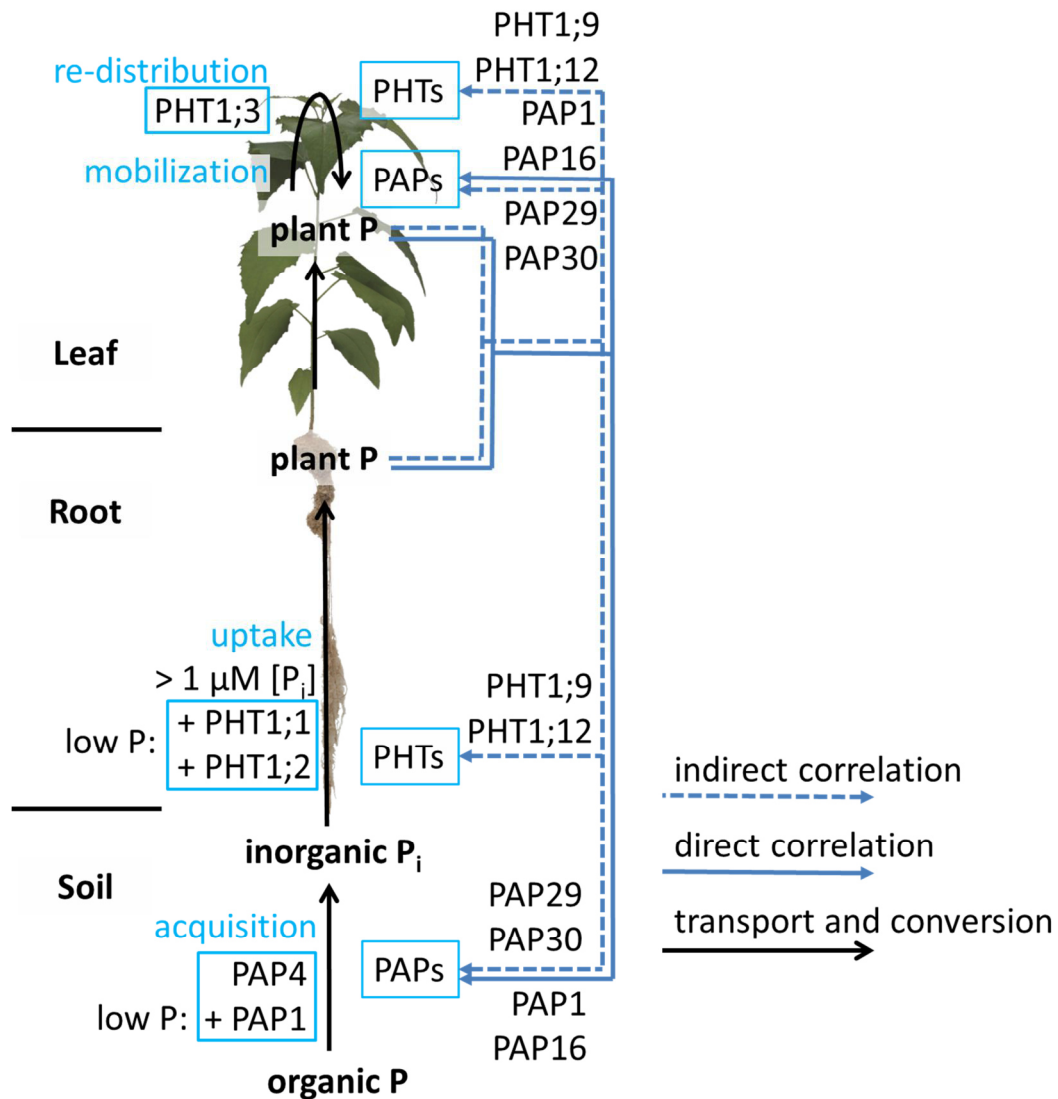


**Figure 5.1. Model for the possible contributions of PAs and PHTs in P acquisition and P uptake in poplar (*P. x canescens*).**

## 5.2 Outlook

Here, PtPHT1;1 and PtPHT1;2 were proposed to contribute to the P uptake in P starved poplar, but what amount of P they transport into the poplar and the contributions of other transporters to the enhanced P uptake efficiency remains open. Also, whether PtPAP1 is not only secreted but also cell-wall associated in poplar roots remains open. Further tests have to reveal the organic phosphate source preferences of poplars.

Under natural conditions, poplar roots are colonized by mycorrhizal fungi with different abilities for P acquisition (*Baum and Makeschin, 2000; Danielsen et al., 2013, 2012; Gehring et al., 2006; Seven and Polle, 2014*). Ectomycorrhiza reduce the  $K_m$  for plant P uptake, P accumulation (*Cress et al., 1979; Desai et al., 2014; Van Tichelen and Colpaert, 2000*) and the threshold concentration for P uptake (*Van Tichelen and Colpaert, 2000*). Loth-Pereda et al. (2011) studied the transcriptional regulation of phosphate transporters in mycorrhizal and non-mycorrhizal *P. × canescens* roots and found especially *PtPHT1;9* and *PtPHT1;12* to be upregulated upon colonization with ectomycorrhizal and arbuscular mycorrhizal fungi. But the regulation of P transporters in P starved mycorrhizal poplar roots and which fungal species are the most useful for enhanced P nutrition remains to be studied for sustainable poplar plantation management.

Timonen and Sen (1998) found enhanced acid phosphatase activity in proteins of mycorrhizal compared with non-mycorrhizal roots. Courty et al. (2010) found two poplar and no *Laccaria* PAP genes induced whereas Luo et al. (2009) found decreased expression for poplar PAPs upon mycorrhization probably due to increased tissue P concentrations. Whether fungal or plant PAPs enhance the root-associated phosphatase activity in mycorrhizal plants is not known.

These considerations indicate that poplar P nutrition cannot be fully understood when the contributions of interacting organisms are not considered. Therefore, further studies should focus on the influence of microorganisms on the P nutrition of poplar, especially since the contributions and abilities of bare-rooted poplars have been unraveled in this study.



### 5.3 References

- Asano, Y., Compton, J.E., Church, M.R. (2006): Hydrologic flowpaths influence inorganic and organic nutrient leaching in a forest soil. *Biogeochemistry* 81, 191–204.
- Ayadi, A., David, P., Arrighi, J.-F., Chiarenza, S., Thibaud, M.-C., Nussaume, L., Marin, E. (2015): Reducing the genetic redundancy of *Arabidopsis* PHOSPHATE TRANSPORTER1 transporters to study phosphate uptake and signaling. *Plant Physiol.* 167, 1511–1526.
- Baum, C., Makeschin, F. (2000): Effects of nitrogen and phosphorus fertilization on mycorrhizal formation of two poplar clones (*Populus trichocarpa* and *P. tremula* x *tremuloides*). *J. Plant Nutr. Soil Sci.* 163, 491–497.
- Burg, J. van den (1985): Foliar analysis for determination of tree nutrient status- a compilation of literature data. *Rapp. Rijksinst. Voor Onderz. Bos- En Landschapsbouw Dorschkamp Neth.*
- Courty, P.E., Labbé, J., Kohler, A., Marçais, B., Bastien, C., Churin, J.L., Garbaye, J., Tacon, F.L. (2010): Effect of poplar genotypes on mycorrhizal infection and secreted enzyme activities in mycorrhizal and non-mycorrhizal roots. *J. Exp. Bot.* 62, 249-260.
- Cress, W.A., Throneberry, G.O., Lindsey, D.L. (1979): Kinetics of phosphorus absorption by mycorrhizal and nonmycorrhizal tomato roots. *Plant Physiol.* 64, 484–487.
- Danielsen, L., Lohaus, G., Sirrenberg, A., Karlovsky, P., Bastien, C., Pilate, G., Polle, A. (2013): Ectomycorrhizal colonization and diversity in relation to tree biomass and nutrition in a plantation of transgenic poplars with modified lignin biosynthesis. *PLOS ONE* 8, e59207.
- Danielsen, L., Thürmer, A., Meinicke, P., Buée, M., Morin, E., Martin, F., Pilate, G., Daniel, R., Polle, A., Reich, M. (2012): Fungal soil communities in a young transgenic poplar plantation form a rich reservoir for fungal root communities. *Ecol. Evol.* 2, 1935–1948.
- Del Pozo, J.C., Allona, I., Rubio, V., Leyva, A., De La Peña, A., Aragoncillo, C., Paz-Ares, J. (1999): A type 5 acid phosphatase gene from *Arabidopsis thaliana* is induced by phosphate starvation and by some other types of phosphate mobilising/oxidative stress conditions. *Plant J.* 19, 579–589.
- Desai, S., Naik, D., Cumming, J.R. (2014): The influence of phosphorus availability and *Laccaria bicolor* symbiosis on phosphate acquisition, antioxidant enzyme activity, and rhizospheric carbon flux in *Populus tremuloides*. *Mycorrhiza* 24, 369–382.

Fitzhugh, R.D., Driscoll, C.T., Groffman, P.M., Tierney, G.L., Fahey, T.J., Hardy, J.P. (2001): Effects of soil freezing disturbance on soil solution nitrogen, phosphorus, and carbon chemistry in a northern hardwood ecosystem. *Biogeochemistry* 56, 215–238.

Gan, H., Jiao, Y., Jia, J., Wang, X., Li, H., Shi, W., Peng, C., Polle, A., Luo, Z.-B. (2016): Phosphorus and nitrogen physiology of two contrasting poplar genotypes when exposed to phosphorus and/or nitrogen starvation. *Tree Physiol.* 36, 22–38.

Ge, X., Tian, Y., Tang, L. (2015): Nutrient distribution indicated whole-tree harvesting as a possible factor restricting the sustainable productivity of a poplar plantation system in China. *PLOS ONE* 10, e0125303.

Gehring, C.A., Mueller, R.C., Whitham, T.G. (2006): Environmental and genetic effects on the formation of ectomycorrhizal and arbuscular mycorrhizal associations in cottonwoods. *Oecologia* 149, 158–164.

Gruber, B.D., Giehl, R.F.H., Friedel, S., Wirén, N. von (2013): Plasticity of the *Arabidopsis* root system under nutrient deficiencies. *Plant Physiol.* 163, 161–179.

Hirsch, J., Marin, E., Floriani, M., Chiarenza, S., Richaud, P., Nussaume, L., Thibaud, M.C. (2006): Phosphate deficiency promotes modification of iron distribution in *Arabidopsis* plants. *Biochimie* 88, 1767–1771.

Kellermeier, F., Armengaud, P., Seditas, T.J., Danku, J., Salt, D.E., Amtmann, A. (2014): Analysis of the root system architecture of *Arabidopsis* provides a quantitative readout of crosstalk between nutritional signals. *Plant Cell* 26, 1480–1496.

Lan, P., Li, W., Schmidt, W. (2015): “Omics” approaches towards understanding plant phosphorus acquisition and use, in: Plaxton, W.C., Lambers, H. (eds.): Annual Plant Reviews Volume 48. John Wiley & Sons, Inc., Hoboken, NJ, USA, pp. 65–97.

Loth-Pereda, V., Orsini, E., Courty, P.-E., Lota, F., Kohler, A., Diss, L., Blaudez, D., Chalot, M., Nehls, U., Bucher, M., Martin, F. (2011): Structure and expression profile of the phosphate Pht1 transporter gene family in mycorrhizal *Populus trichocarpa*. *Plant Physiol.* 156, 2141–2154.

Luo, Z.-B., Janz, D., Jiang, X., Göbel, C., Wildhagen, H., Tan, Y., Rennenberg, H., Feussner, I., Polle, A. (2009): Upgrading root physiology for stress tolerance by ectomycorrhizas: Insights from metabolite and transcriptional profiling into reprogramming for stress anticipation. *Plant Physiol.* 151, 1902–1917.

Misson, J., Raghothama, K.G., Jain, A., Jouhet, J., Block, M.A., Bligny, R., Ortet, P., Creff, A., Somerville, S., Rolland, N., Doumas, P., Nacry, P., Herrerra-Estrella, L., Nussaume, L., Thibaud, M.-C. (2005): A genome-wide transcriptional analysis using *Arabidopsis thaliana* Affymetrix gene chips determined plant responses to phosphate deprivation. *Proc. Natl. Acad. Sci. U. S. A.* 102, 11934–11939.

Mudge, S.R., Rae, A.L., Diatloff, E., Smith, F.W. (2002): Expression analysis suggests novel roles for members of the Pht1 family of phosphate transporters in *Arabidopsis*. *Plant J.* 31, 341–353.

Rai, V., Sanagala, R., Sinilal, B., Yadav, S., Sarkar, A.K., Dantu, P.K., Jain, A. (2015): Iron availability affects phosphate deficiency-mediated responses, and evidence of cross-talk with auxin and zinc in *Arabidopsis*. *Plant Cell Physiol.* 56, 1107–1123.

Ranger, J., Marques, R., Jussy, J.-H. (2001): Forest soil dynamics during stand development assessed by lysimeter and centrifuge solutions. *For. Ecol. Manag.* 144, 129–145.

Remy, E., Cabrito, T.R., Batista, R.A., Teixeira, M.C., Sá-Correia, I., Duque, P. (2012): The Pht1;9 and Pht1;8 transporters mediate inorganic phosphate acquisition by the *Arabidopsis thaliana* root during phosphorus starvation. *New Phytol.* 195, 356–371.

Seven, J., Polle, A. (2014): Subcellular nutrient element localization and enrichment in ecto- and arbuscular mycorrhizas of field-grown beech and ash trees indicate functional differences. *PLOS ONE* 9, e114672.

Timonen, S., Sen, R. (1998): Heterogeneity of fungal and plant enzyme expression in intact Scots pine–*Suillus bovinus* and –*Paxillus involutus* mycorrhizospheres developed in natural forest humus. *New Phytol.* 138, 355–366.

van Hees, P.A.W., Vinogradoff, S.I., Edwards, A.C., Godbold, D.L., Jones, D.L. (2003): Low molecular weight organic acid adsorption in forest soils: effects on soil solution concentrations and biodegradation rates. *Soil Biol. Biochem.* 35, 1015–1026.

Van Tichelen, K.K., Colpaert, J.V. (2000): Kinetics of phosphate absorption by mycorrhizal and non-mycorrhizal Scots pine seedlings. *Physiol. Plant.* 110, 96–103.

Wang, L., Lu, S., Zhang, Y., Li, Z., Du, X., Liu, D. (2014): Comparative genetic analysis of *Arabidopsis* purple acid phosphatases AtPAP10, AtPAP12, and AtPAP26 provides new insights into their roles in plant adaptation to phosphate deprivation: Comparative analysis of three *Arabidopsis* APases. *J. Integr. Plant Biol.* 56, 299–314.

Ward, J.T., Lahner, B., Yakubova, E., Salt, D.E., Raghothama, K.G. (2008): The effect of iron on the primary root elongation of *Arabidopsis* during phosphate deficiency. *PLANT Physiol.* 147, 1181–1191.

Zhang, C., Meng, S., Li, M., Zhao, Z. (2016): Genomic identification and expression analysis of the phosphate transporter gene family in poplar. *Front. Plant Sci.* 7, 1398.

## Acknowledgements

This work was done in the Department of Forest Botany and Tree Physiology and the associated Laboratory for Radio-Isotopes (LARI) and I would like to express my gratitude to many people for their help and support.

I am grateful to my supervisor Prof. Dr. Andrea Polle, for the possibility to work on this interesting project, for her support, suggestions and ideas during experiments, analysis and writing.

I thank Prof. Dr. Elvira Hörandl for being in my thesis committee and being the co-referee, and Prof. Dr. Ivo Feußner, PD Dr. Thomas Teichmann, Prof. Dr. Konstantin Krutovsky and Prof. Dr. Christian Ammer for being part of the examination committee. I also thank the University of Göttingen/LARI for funding my position and the Deutsche Forschungsgemeinschaft (DFG), Priority Program SPP 1685 “Ecosystem Nutrition” for financial support for this research project under grant number Po362/22-2.

I would like to thank Dr. Andrzej Majcherczyk from the Department of Molecular Wood Biotechnology and Technical Mycology for the proteomic analysis and his explanations and the late Karin Lange for her help during protein analysis. I thank Dr. Merlin Muhr from the Department of Plant Cell Biology for the vectors and experience in working with Gateway systems.

Thanks to all the LARI members for their great help, especially Gabriele Lehmann for helping me during all experiments involving radioactivity and for producing the phosphoimager pictures, Thomas Klein for his advice regarding molecular work, and Bernd Kopka who shared his enthusiasm for radioactivity, fixed every computer problem, and gave encouragement.

I would like to thank the people of the Forest Botany: all technicians for their help during harvests and laboratory experiments, especially Christine Kettner, who provided micropropagated poplars whenever needed and did the pressure extraction for element

## Acknowledgements

---

analysis, Marianne Smiatacz, and Gisbert Langer-Kettner, who measured C/N for me. I give many thanks to Dr. Dennis Janz who showed me how to analyze my data in R and gave many recommendations. I thank Prof. Dr. Henning Wildhagen for his suggestions especially regarding array analyses and Dr. Stephanie Werner for help with *Arabidopsis*, cloning and transformation.

Furthermore, I thank my former and current colleagues for the nice working atmosphere, inspiring discussions and becoming friends. I like to thank especially Dr. Anna Schmidt, Dr. Kristina Schröter, Dr. Bettina Otto, Lisa Kins, Gerrit-Jan Strijkstra, Shanty Paul, and Dade Yu. Finally, I especially thank my family and friends for their support and encouragement.

## **Eidesstattliche Erklärung**

Hiermit erkläre ich, dass ich die vorliegende Arbeit selbständig und ohne unzulässige Hilfe oder Benutzung anderer als der angegebenen Quellen und Hilfsmittel angefertigt habe. Es wurden alle Personen genannt, die direkt und indirekt an der Entstehung der vorliegenden Arbeit beteiligt waren. Alle Textstellen, die wörtlich oder sinngemäß aus veröffentlichten oder nichtveröffentlichten Schriften entnommen sind, wurden als solche kenntlich gemacht.

Die vorgelegte Arbeit wurde weder im Inland noch im Ausland in gleicher oder ähnlicher Form einer anderen Prüfungsbehörde zum Zweck einer Promotion oder eines anderen Prüfungsverfahrens vorgelegt.

Göttingen, Oktober 2016

## Curriculum vitae

### Persönliche Daten

Name	Mareike Jana Kavka
Geburtsdatum	10.01.1988
Geburtsort	Hamburg
Nationalität	deutsch

### Ausbildung und wissenschaftlicher Werdegang

10/2012-03/2016	Wissenschaftliche Mitarbeiterin zur Promotion Georg-August Universität Göttingen Abteilung Forstbotanik und Pflanzenphysiologie, Labor für Radioisotope Titel der Dissertation: „Phosphorus nutrition of poplar“
10/2010-09/2012	Studium MSc. Diversität und Evolution Universität Rostock Titel der Masterarbeit: „Diatomeenentwicklung vs. Klima- schwankungen der letzten ca. 80 Jahre - Untersuchungen an laminierten Sedimenten des Woseriner Sees in Mecklenburg- Vorpommern“
10/2007-09/2010	Studium BSc. Biowissenschaften Universität Rostock Titel der Bachelorarbeit: „Erarbeitung einer Artenliste pro- und eukaryonter Algen in Gewässern des Botanischen Gartens Rostock im Frühjahr 2010“
1998-2007	Gymnasium Glinde
1994-1998	Grundschule Willinghusen